LIQUID MOTION INDUCED BY ELECTROSTATIC DEFORMATION OF FLUIDIC INTERFACES

by

JANUK SWARUP AGGARWAL

B.Sc., University of British Columbia, 2001

A THESIS SUBMITTED IN PARTIAL FULFILLMENT OF

THE REQUIREMENTS FOR THE DEGREE OF

MASTER OF SCIENCE

in

THE FACULTY OF GRADUATE STUDIES

(Department of Physics and Astronomy)

We accept this thesis as conforming
to the required standard

THE UNIVERSITY OF BRITISH COLUMBIA

OCTOBER 2004

Library Authorization

In presenting this thesis in partial fulfillment of the requirements for an advanced degree at the University of British Columbia, I agree that the Library shall make it freely available for reference and study. I further agree that permission for extensive copying of this thesis for scholarly purposes may be granted by the head of my department or by his or her representatives. It is understood that copying or publication of this thesis for financial gain shall not be allowed without my written permission.

Janak Swarup Aggarwal
Name of Author *(please print)*

Oct. 7, 2004
Date (dd/mm/yyyy)

Title of Thesis: Liquid Motion Induced by Electrostatic Deformation of Fluidic Interfaces

Degree: Master of Science Year: 2004

Department of Physics and Astronomy
The University of British Columbia
Vancouver, BC Canada

Abstract

This thesis introduces a novel method for deforming fluidic interfaces while minimizing the friction and hysteresis typically associated with conventional electrowetting systems. The technique uses thin solid surfaces that are patterned so that the contact angle of a liquid drop placed on the surface depends on location. With an appropriate pattern, the contact line between the fluid interface and the solid surface is immobilized to a degree which in turn constrains the drop shape in useful ways. With suitable surfaces and liquids, the position of the contact line is stable for a range of drop shapes. The drop can be deformed by applying an inhomogeneous electric field to the fluid interface. Since the contact lines are stable, movement of the liquid in the drop is induced while no contact lines are formed or moved, thus minimizing friction and eliminating hysteresis. This technique is examined in the context of two different example applications; one is a potential reflective information display and the other is a fluidic pump for enhanced surface heat transfer. With the reflective display, the deformation moves a coloured liquid drop through a thin, reflective solid substrate. The apparent reflectivity is modulated by changing the amount of coloured liquid that is between the reflective solid and the viewer. In the fluidic pump, the induced flow is along the surface of a solid substrate, in order to transfer heat along the surface at a rate that substantially exceeds that of an equivalent copper plate.

Initial prototypes for the two applications were designed, tested and compared to simple models. These results demonstrate the basic feasibility of such systems and suggest that further research in this area is warranted.

Table of Contents

List of Tables

List of Figures

Acknowledgements

My sincere thanks go to my supervisor, Lorne Whitehead, for the freedom to pursue this work and for his many ideas, suggestions and guidance. His creativity and enthusiasm are greatly admired.

I would also like to thank Andrzej Kotlicki, who also provided me with many helpful suggestions and ideas. His advice regarding the electrical and electronic aspects of this research is particularly appreciated.

Many thanks go to the many members of the Structured Surface Physics Lab, both past and present, for putting up with my barrage of jokes and for supplying a few of their own. Our discussions and the insights that emerged from those conversations are greatly appreciated.

Finally, I would like to express my gratitude to my family, particularly my parents, for their support and patience during the course of this research.

Chapter 1 – Introduction

The manipulation of liquids on size scales where surface tension forces dominate is of great interest for many fields, including optical and chemical applications. At these size scales, fluid interfaces can be deformed using electrostatic forces. Such deformations can cause a significant redistribution of the bulk liquid. The change in shape can be used directly to control optical properties of the system in question, or it can be used in more complicated systems to pump the liquid. There is a large range of potential applications for such deformation of fluid interfaces.

A common method of deforming fluid interfaces takes advantage of the phenomenon known as electrowetting. One difficulty with typical electrowetting techniques is that they involve movement of the intersection between a fluid interface and a solid surface (sometimes known as the contact line). Friction and hysteresis are often associated with motion of this contact line, leading to inefficiency and other limitations.

Presented in this thesis is a novel technique that avoids the hysteresis and friction associated with the motion of the bulk liquid by restricting the contact lines so they cannot move along the surface. This approach is examined in the context of two distinct applications; a proposed reflective information display and a new type of fluidic pump for use in surface heat transfer.

In both applications, the contact line (or lines) of a liquid drop is restricted to form a specific shape on the solid surface. The position of this contact line is kept stable on the

solid surface even as the bulk liquid is deformed. This is accomplished using a solid with a surface that is patterned so the drop has different wetting behaviours in different regions. With an appropriate pattern on the surface, the contact lines are pinned at the border of a region where the liquid wets the surface with a region where it does not. This pinning is effective for a range of angles of contact between the fluid interface and the solid surface. Thus, even if the fluid interface undergoes substantial deformation, the contact lines and amount of contact area remain constant on the solid surface. The deformation can be induced by applying an inhomogeneous electric field. Since the contact lines are fixed, the hysteresis and friction effects associated with contact line motion are eliminated.

For the information display application, a coloured liquid drop is moved through a thin, reflective solid substrate. The two surfaces of the substrate are patterned and small holes pass through the substrate to allow fluid transfer from one side to the other. With an appropriate pattern, a single drop can be stable on both sides of the substrate simultaneously. The apparent reflectivity of the substrate is modulated by changing the amount of liquid on the side intended for viewing. This technique for changing reflectivity allows for continuous modulation between white and dark states. In other words, grey-scale control is easily achieved by controlling the magnitude of the field applied. The bulk liquid is moved to one side of the substrate by applying an electric field to the fluid interface on one side of the solid. The system can be made using either a water based drop in air or oil, or it can be made with an oil based drop in water.

For the fluidic pump application, the fluid in an oil drop, in a water background, is moved along the surface of a solid substrate. The solid substrate is patterned so that the drop is confined to tracks which form simple closed loops. The oil is deformed by applying a patterned electric field along the track. In turn, moving this pattern causes fluid motion - the oil is squeezed out of high field regions and a net flow is produced by stepping the field pattern along the track. Such flow of liquid can be used to transport heat along a surface, potentially at rates greater than conventional solid thermal conductors.

Chapter 2 provides background and introduces the basic concepts used to move the fluids as desired. Chapter 3 describes specific details for both applications, including application specific models, the construction, measurements and analysis of the results. Chapter 4 presents overall conclusions and suggestions for future work based on the concepts presented.

While the work presented in this thesis is preliminary, the results are encouraging and suggest that further research in this area is warranted.

Chapter 2 – Background Physics

2.1 – Fluid Interfaces

The work presented involved systems in which two distinct and immiscible fluids were in contact with each other on one or more solid substrates. For convenience, the term *phase* is used to describe a continuous agglomeration of an individual material. So the systems described involved two fluid phases on a substrate made of one or more solid phases.

The systems described throughout this thesis used materials that were all immiscible with each other, so each phase had a distinct, well defined border between itself and the other phases. Any of these borders could be called either an interface or a surface, since the terms are completely equivalent. For convenience, when referring specifically to a solid boundary, the term *surface* is used, and when referring specifically to a boundary between phases, the term *interface* is used. This distinction is somewhat arbitrary as evidenced by well known terms such as *surface tension* or *surface free energy*, which exist for either type of boundary. The stated distinction is necessary because many of the systems presented involve a single solid plane with multiple solid-fluid boundaries.

It should be noted that the following discussion assumes that the effect of gravity on the shapes of the boundaries is negligible. This assumption is acceptable for sufficiently small systems or for larger systems when the system has two fluid phases with similar densities.

2.1.1 – Surface Tension

An interface between two immiscible materials has an associated free energy per unit area, measured in J/m^2. This free energy, called the *surface free energy*, is defined as the work necessary to increase the size of the interface by a unit of area. The units of the surface free energy can be expressed as a force per unit length, in which case, the free energy is called *surface tension*, γ. The free energy definition is useful for describing fundamental properties of the interface, like the shape that an interface will tend to assume: In the absence of other forces, the material will tend to assume a spherical shape, which minimizes the surface area, and therefore also minimizes the surface free energy.

Alternatively, surface tension can be viewed as arising from the short-range interactions between the molecules within each of the materials. In the bulk, a given molecule has, on average, equal interactions with molecules in all directions, and so it experiences no net forces. At an interface, the molecule is not surrounded isotropically by molecules of its own type, so there is a net attraction towards the bulk.[1]

While the ideas of surface free energy and surface tension are really equivalent, in some cases, one of these descriptions may seem more intuitively clear. For example, when describing properties like the contact angle, it is easiest to speak of surface tension.

2.1.1.1 – Contact Angle

The concept of contact angle is often used to describe the intersection of interfaces between three or more phases. The systems discussed here involve a fluid-fluid interface intersecting a relatively smooth and planar solid surface. For simplicity, the initial discussion below considers the case where the chemistry of the solid surface is spatially uniform. This type of surface is called *homogeneous*, because the surface tension between at the interface of the solid and a fluid is constant everywhere on the solid surface.

When a liquid drop is placed on such a surface in a background fluid, the drop will tend to assume a shape that minimizes the total surface energy. There are three interfaces, and so three surface tensions, to be considered. As can be seen in Figure 2.1, the three boundaries are the solid-liquid drop interface, the solid-background fluid interface and the liquid drop-background fluid interface. The intersection of the three interfaces is called the contact line. The angle at which the fluid-fluid interface intersects the solid surface is called the contact angle, θ, and is usually measured in the denser of the two fluid phases. For the work presented, the background fluid can have a higher density than the liquid drop, so it is more convenient to always measure the contact angle inside the drop.

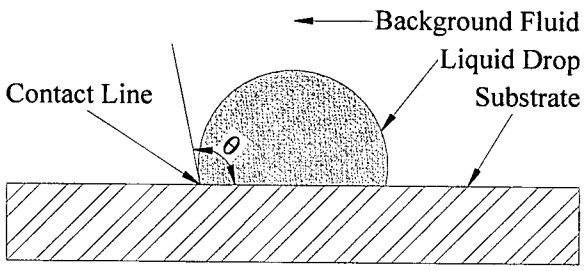

Figure 2.1 – Cross-section showing wetting behaviour on a homogeneous solid surface.

In the absence of external forces, including friction, the drop will tend to assume a spherical cap-like shape[2] and will have a well defined contact angle. The contact angle is described by Young's equation,[3] equation (2.1), which is the result of balancing the components of the surface tensions parallel to the solid's surface.

$$\gamma_{SD} + \gamma_{DB}\cos\theta - \gamma_{SB} = 0 \qquad \textbf{(2.1)}$$

where, γ_{SD} is the solid-liquid drop equilibrium surface tension, γ_{DB} is the liquid-background fluid equilibrium surface tension, γ_{SB} is the solid-background fluid surface tension and θ is the contact angle as is shown in Figure 2.1.

In real systems, the solid surface is not typically perfectly smooth and homogeneous. Porosity, impurities and other microscopic structure in the solid surface can affect the contact angle, can cause friction when moving a contact line and can cause an effect known as contact angle hysteresis.

An example of this is the observation that the contact angle will typically be larger when the contact line is advancing than when it is receding.[4] This hysteresis can be a problem for systems which need to move the contact line both efficiently and reversibly.[5] As described in more detail throughout this thesis, this issue was avoided by using a heterogeneous solid surface to 'pin' the contact line so it would not move.

Heterogeneous surfaces were made by combining two homogeneous solid surfaces. The materials were selected such that the liquid drop would have different contact angles on each of the surfaces alone. Before describing the combinations of such surfaces, it is useful to define some terminology to help describe the wetting behaviour of the liquid drop.

2.1.1.2 – Material Nomenclature

All the systems investigated included a conductive liquid phase. In the work presented, that conductive liquid was either water or an aqueous solution of simple solutes, like dyes. Since these solutes were used only to modify properties unrelated to the wetting behaviour, all aqueous phases, including solutions, are referred to as *water* for convenience. Similarly, many systems involved a non-aqueous liquid phase. The term *oil* is used to refer to any liquid that is electrically insulating and immiscible with water. This designation is purely for convenience since liquids that do not traditionally fall into the oil category can meet these requirements.

In addition to terms used for the liquid phases, it was necessary to find terms for the solid phases that would also simplify the discussion. The terms *hydrophilic*, *hydrophobic*, *lyophilic* and *lyophobic* are used, though, as described below, in many of the systems presented here their meaning is somewhat subtle. The slight definition difficulty arises from the fact that most investigations of the wetting behaviour of a drop on a solid surface are done in air. In these cases, terminology describing the solid is clear. If water beads up so it has a high contact angle, the surface is *hydrophobic*. If water wets out and thus has a low contact angle, the surface is *hydrophilic*. But in the presence of multiple liquid phases, the wetting behaviour of a water drop on the solid may be different than it had been in air. In this work, the terms need to be applied somewhat more broadly since many of the systems presented use two liquid phases. To that end, for multiple liquid phase systems, the term *hydrophobic* is used to describe a solid that attracts the oil more than it attracts water, and *hydrophilic* is used to describe one that attracts water more than the oil. Therefore on such a hydrophobic surface, a water drop in a non-aqueous background fluid on the hydrophobic surface will have a large contact angle. An oil drop, under water, on the surface will have a small contact angle. Correspondingly, according to this approach, the cases are reversed for a hydrophilic surface; the water drop would have a small contact angle and the oil drop would have a large contact angle. The behaviour of an oil drop on each type of surface is shown schematically in Figure 2.2.

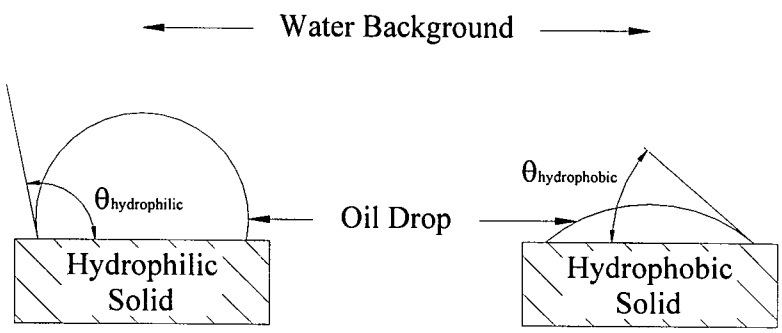

Figure 2.2 – Wetting behaviour of an oil drop in a water background

The hydrophilic and hydrophobic classifications are convenient when talking about a specific system where the drop is known to be one material, e.g. oil, and the background fluid is known to be another, e.g. water. However, the terms are too specific for discussions about general wetting behaviour where the drop could be either water or oil, but where the desired or observed wetting behaviour of the drop is the same. The confusion is evident in Table 2-1 where the ranges of contact angles used to classify materials as either hydrophobic or hydrophilic are specified.

Table 2-1 – Contact angle ranges for drops on hydrophobic and hydrophilic surfaces

Drop Material	Contact Angle of Drop	
	Hydrophobic	Hydrophilic
Oil	< ~15°	> ~90°
Water	> ~90°	< ~15°

It should be noted that for both a water drop and an oil drop, there is a range of contact angles for which the solid surfaces were not classified into the two groups. The surfaces of materials with contact angles in this range were not generally useful for the systems discussed and are therefore not included in the classification.

As can be seen, when talking about a region where the drop wets out, the term changes depending on whether the drop is water or oil. When the drop can be either material but the wetting behaviour is the same, the terms *lyophilic* and *lyophobic* are used for convenience.

The term *lyophilic* (liquid-loving) is used to describe a material on which a liquid has a small contact angle. The term *lyophobic* (liquid-hating) is used to describe a material on which a liquid has a large contact angle. When there are multiple liquid phases, these terms are normally only used to describe colloidal systems.[6] However, for the work presented, it is assumed that lyophilic and lyophobic are relative terms which describe the wetting behaviour of the drop on the solid surface in the background fluid. Table 2-2 shows the ranges of contact angles used to classify materials as either lyophobic or lyophilic.

Table 2-2 – Contact angle ranges for drops on lyophobic and lyophilic surfaces

Drop Material	Contact Angle of Drop	
	Lyophobic	Lyophilic
Oil	> ~90°	< ~15°
Water	> ~90°	< ~15°

Since the actual solids used to form a lyophobic or lyophilic region depend on the liquid drop being used, these terms can be confusing for specific systems and so they are only used in generalized discussions such as the behaviour of a drop on a heterogeneous solid surface.

2.1.1.3 – Liquid Drop on a Heterogeneous Solid Surface

With the terminology defined, the behaviour of a liquid drop on a more complex surface can be considered. For the following discussion, the solid surface is again assumed to be planar and relatively smooth.

The surface can be patterned so there are regions of lyophobic material and regions of lyophilic material. This type of patterned surface is referred to as a *heterogeneous* surface since the surface tension of a solid-liquid interface would depend on its position on the surface. Typically the patterned features are on the same size scale as the size of the liquid drop. If the regions are much larger than the drop, the wetting behaviour of the drop would tend to be just that which would be observed on a homogeneous surface. As mentioned above, a liquid drop wets a lyophilic surface since the equilibrium contact angle, $\theta_{lyophilic}$, is small. In the lyophobic regions, the equilibrium contact angle, $\theta_{lyophobic}$, is large. When a drop is placed at the border of a lyophilic and a lyophobic region, it stands to reason that the drop will tend to move towards the lyophilic region.

When the size scale of a lyophilic region is similar to the drop size, the liquid in the drop will completely cover the lyophilic region. The volume of the liquid can be increased without moving the contact line because the contact line of the drop will tend to stay *pinned* at the border of the two regions. This contact line pinning occurs so long as the contact angle is between the contact angle of the drop on the lyophilic and the contact angle of the drop on the lyophobic regions.

$$\theta_{lyophilic} < \theta < \theta_{lyophobic} \tag{2.2}$$

Since there are a range of θ values that satisfy equation (2.2), there will be a range of stable configurations as is shown in Figure 2.3. It should be noted that a phenomenon known as wetting hysteresis tends to enlarge this range since in the stable configurations, the lyophobic surface is dry and the lyophilic surface is wetted. (In a hysteretic system, when the contact line is advancing over a dry surface, the contact angle tends to increase, and when the line is receding over a wetted surface, the contact angle tends to decrease.)[7] Both situations help keep the contact line pinned at the border between the lyophilic and lyophobic regions.

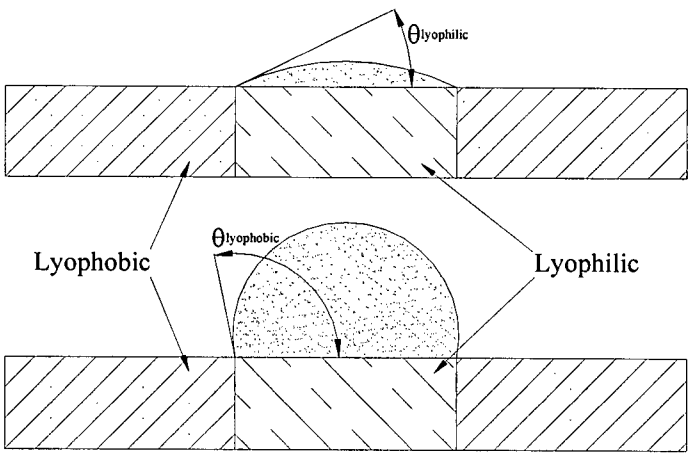

Figure 2.3 – Stable configurations of a drop on a heterogeneous surface

As drawn in Figure 2.3, the different configurations of the drop each have a different volume. The devices presented below take advantage of the multiple stable configurations by moving excess liquid to or from some connected location. To do so,

the deforming force needs to overcome an overpressure within the drop due to the curved interface, as considered in the next section.

2.1.2 – Pressure Due to Surface Tension

Surface tension on a curved interface results in a net force towards the concave side of the interface. In equilibrium, this means that there is a difference in pressure across the interface, with the pressure on the concave side being higher. This pressure difference, P, depends on the curvature of the interface. For a general curved surface, the degree of curvature can be described fully by specifying two so-called principal radii, r_1 and r_2. At any point on the surface, the curvature can be described by two radii of curvature in orthogonal directions. In general, there is an infinite number of such pairs of radii, but the principal radii of curvature, r_1 and r_2, are defined to be the pair which includes both the minimum and maximum possible radii. The relationship of curvature to pressure is described by the Young-Laplace equation,[8]

$$P = \gamma\left(\frac{1}{r_1} + \frac{1}{r_2}\right) \tag{2.3}$$

Here, γ is the surface tension of the drop-background fluid interface, and r_1 and r_2 are the principal radii of curvature of the drop.

On a perfectly smooth, frictionless and homogeneous surface, the drop would assume the shape of a spherical cap. In this configuration the contact line forms a circle on the solid

surface. It also means that the radius of curvature is the same in all directions, so equation (2.3) becomes,

$$P = \frac{2\gamma}{r} \tag{2.4}$$

where r is the radius of the sphere that makes the spherical cap.

In general, the two principal radii of curvature would be different when the base of the drop is non-circular. On a perfectly smooth, frictionless and homogeneous surface, any shape other than a perfectly spherical cap would be unstable and the contact line would tend to move until it did form a spherical cap. Wetting hysteresis and friction can act to stabilize a distorted shape when a drop is placed on a real surface that has impurities or some surface structure.

Wetting hysteresis and friction are generally not easy to control for the purposes of specifying a predefined non-circular shape. However, the drop can be forced to have a nearly arbitrary base shape by using a heterogeneous surface as is described in section 2.1.1.3. For example, the pump application discussed in section 3.2 uses long, constant width hydrophobic regions to define the shape of the base of an oil drop. In such systems, the drop is very long in one direction, so the maximum radius of curvature becomes very large compared to the minimum one. In other words, the drop shape can be approximated by a cylindrical cap. In this case, equation (2.3) becomes,

$$P = \frac{\gamma}{r} \tag{2.5}$$

where r is the minimum radius of curvature. This radius is determined by the width of the hydrophobic region and by the contact angle of the drop at the border between the hydrophilic and hydrophobic regions, as shown in Appendix A.

2.1.3 – Interface Deformation using Electrostatic Pressure

The discussion above described behaviour in the absence of deforming forces, such as gravity or electric fields. In the applications presented, a liquid-fluid interface was deformed by applying an inhomogeneous electric field in a substantially non-conductive fluid. The systems were made by placing the substantially non-conductive fluid between two conductive phases. A water phase formed one conductor and a solid material was the other conductor. Before discussing electric fields in the multi-fluid systems, it is useful to briefly review electric fields and conventional capacitors.

In a conventional capacitor, two conductors are separated by some largely non-conductive material, e.g. a dielectric material. Although each of the conductors could have an arbitrary shape, it is convenient to further simplify the discussion by considering parallel-plate capacitors, where two planar, conductive surfaces are separated by a distance, d. If a net positive charge is put on one conductor and a negative charge on the other, a well defined voltage difference, V, and an electric field, $\vec{E}$, will be established in the non-conductive material. The electric field is constant everywhere in the gap, and

its magnitude, E, can be written in terms of the voltage difference and the plate separation,

$$E = \frac{V}{d} \tag{2.6}$$

For a parallel plate capacitor, the charge put on each conductor will spread out evenly over the conductor's surface. In other words, the conductors each have a uniform surface charge. In the presence of an electric field, a surface charge will experience a force per unit area, i.e. a pressure. This pressure, P_E, is termed the *electrostatic pressure.* It is straightforward to show that in terms of the electric field just outside the conductor surface, the pressure is,[9]

$$P = \frac{\varepsilon\varepsilon_0}{2} E^2 \tag{2.7}$$

This pressure tends to attract the conductors into the field region. In the parallel plate capacitor example, the electric field is constant everywhere in the gap, and so the pressure can be written in terms of the applied voltage and plate separation,

$$P = \frac{\varepsilon\varepsilon_0 V^2}{2d^2} \tag{2.8}$$

In the applications presented, the systems for deforming the liquid drop can also be viewed as capacitors; the water phase and a solid act as the conductors with the non-conducting fluid in between. Figure 2.4-(a) shows an example of such an arrangement. The solid conductor has finite size so that an inhomogeneous field can be applied. With such a field, the electrostatic pressure will also vary depending on location. The solid conductor cannot typically be deformed by this variation in pressure. However, since the insulating material and the other conductor are both fluids, this variation in pressure will tend to deform the fluid interface such that the water is drawn into the high field region and the other fluid is pushed out. An example of this is sketched in Figure 2.4-(b).

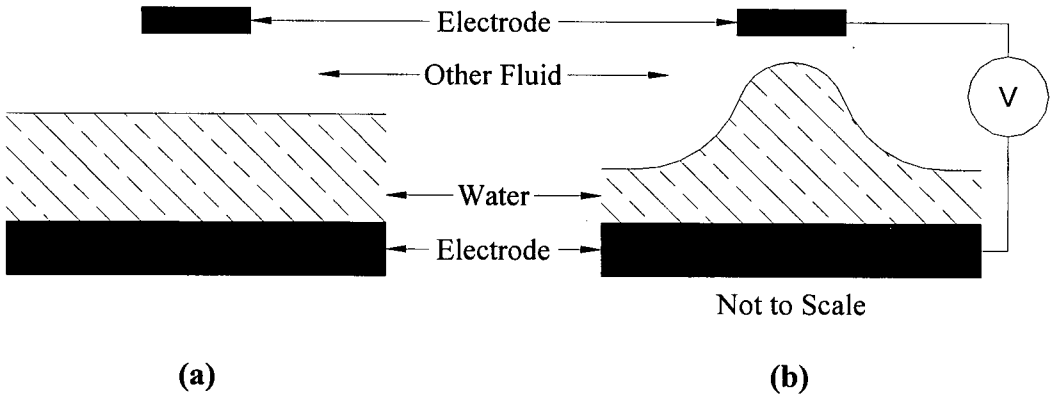

Figure 2.4 – Principle of fluid interface deformation using electric fields

As discussed in the previous section, a curved interface with a non-zero surface tension will give rise to an over-pressure between the two phases. With an applied electric field, the total overpressure can be written,

$$P = \frac{\gamma}{2}\left(\frac{1}{r_1} + \frac{1}{r_2}\right) + \frac{\varepsilon\varepsilon_0}{2}E^2 \qquad (2.9)$$

where the curvature and electric field are measured at any point on the interface. As with regular capacitors, the field can only be non-zero in the non-conductive fluid, so the field is measured in that phase. Equation (2.9) is exact for any liquid interface where other forces, like gravity, can be ignored.

Deformation of the fluid interface will only occur if the electrostatic pressure and the surface tension over-pressure are similar in magnitude. In determining if this deformation technique is practical, it was assumed that the applied electric field could be approximated by that in a similar sized parallel plate capacitor. As described throughout this thesis, the liquid drops examined quite clearly do not follow this geometry. However, this approximation is useful for estimating what magnitude of deformation is expected. For a system with oil drops in water, the drops would have a radius of curvature around 2mm and therefore a surface tension overpressure on the order of 50 Pa. By comparison, a 3×10^6 V m^{-1} field would typically result in an electrostatic pressure on the order of 70 Pa. Therefore it was reasonable to assume that using electric fields to cause bulk motion of a liquid drop would be feasible.

2.2 – Bulk Motion of Fluid

As discussed above, a liquid drop on a solid surface can be forced into a specified shape by the appropriate patterning of lyophilic and lyophobic surfaces. When this is done, there exists a range of contact angles for which the drop's base area tends not to change,

so the liquid can be constrained to move in a predefined manner when deforming forces are applied. In the work presented, the deforming force is applied by an inhomogeneous electric field. This technique for deforming a liquid drop is used in the applications presented to cause flow of the liquid in the drop.

As stated, the drop is constrained by using a relatively smooth, planar solid surface that is patterned with lyophilic and lyophobic regions. The contact line(s) of the oil drop was immobilized (*pinned*) at the border between the two types of solids for a range of contact angles. The minimum pinning angle is determined by the extent to which the liquid drop wets the lyophilic material. With an appropriate choice of solid materials and liquids, this minimum contact angle can be close to zero. In this case, the drop will tend to wet the lyophilic regions even when there is a vanishingly small volume of liquid. Even when the drop is deformed, a microscopically thin layer of the liquid will remain wetted on the lyophilic region. This wetting behaviour of the deformed drop is the underlying principle that allows fluid flow to be induced while minimizing friction and eliminating hysteresis.

Throughout this thesis, systems are described which make use of this effect for both water and oil drops. So while the discussion above applies for either type of drop, it is convenient to illustrate the effect in terms of an oil drop in a water background, as shown in Figure 2.5. When an inhomogeneous field is applied in the oil drop, the water tends to move into the high field regions, thus squeezing the oil out. However, a microscopically thin layer of oil remains wetted on the lyophilic surface in the high field region.

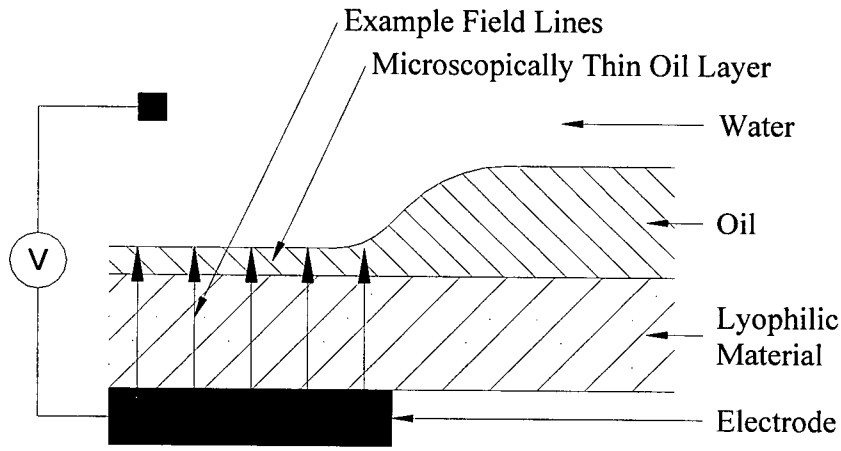

Figure 2.5 – Sketch of liquid wetting when liquid drop is deformed

Note that the sketched field line magnitudes and directions are for illustrative purposes only.

The thin layer of liquid which remains wetted on the lyophilic surface means that no new contact lines are formed or moved when the drop is deformed, and so friction and hysteresis associated with their movement are eliminated.

Using the technique described above, fluid flow can be induced along the surface of a solid substrate, or through holes in a solid substrate. Although the basic underlying principles for the two types of motion are the same, the structures needed to produce the desired motion were different. Two applications were investigated, each using one of the types of motion. The applications were sufficiently different that the focus when studying each type of fluid motion was unique for each case. The principles used specifically for fluid flow along the surface are detailed in section 2.2.1 and those used specifically for fluid motion through the substrate are detailed in section 2.2.2.

2.2.1 – Fluid Flow along Surface

There are many ways of getting a liquid drop to move along a surface using various electrowetting systems.[10,11,12] Typically these experiments move small, discrete drops and involve movement of a contact line which leaves them susceptible to wetting angle hysteresis.[13] In the system described below, a relatively large oil drop is moved along the surface without moving a contact line, and the system can be configured so that the liquid is moved over arbitrarily long distances. In the work that is presented in this thesis, such flow was examined in the context of a fluidic pump where the net flow of the bulk fluid is the most important feature.

An oil drop, placed in water, can be moved along a thin, solid hydrophilic surface using a combination of an appropriately shaped hydrophobic region and an appropriate pattern of electrodes under the substrate. The patterned electrodes can be used with the water background to apply an electric field at localized points along the hydrophobic region and therefore cause localized deformations to the oil-water interface. The oil can be forced to flow in a specified direction by applying an appropriate sequence of localized deformations.

With the oil flowing along a surface, the pump can potentially be used to transport heat along the surface at a rate higher than is possible with conventional conductors. The pump was examined primarily in this context, so while other applications are possible, some design elements were optimized primarily for heat transport.

2.2.1.1 – Component Geometry

As mentioned above, the fluidic pump was used to induce flow in an oil drop, surrounded by a water background, along a solid substrate surface. The substrates examined had a single, planar, heterogeneous surface. The entire pump structure can be separated into three basic layers; a liquid layer, a thin solid substrate layer and an electrode layer.

The solid substrate layer is placed between the other two layers and provides both electrical insulation between the other two layers, and the heterogeneous surface. The surface which contacts the liquid layer is patterned such that it has a hydrophobic region surrounded by hydrophilic material. In this work, the hydrophobic regions formed long, narrow and constant width tracks which were curved to form closed simple loops, such as the one shown in Figure 2.6.

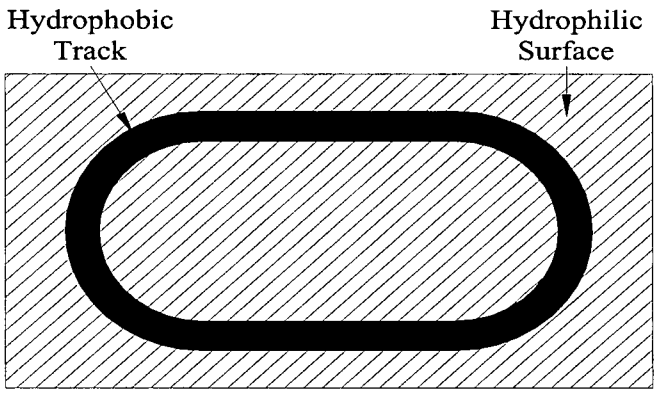

Figure 2.6 – Example of simple closed-loop track

The electrode layer consists of distinct electrodes placed under the hydrophobic region. In the case of the pump, the electrodes are placed sequentially along the length of the track. Specific details of the electrode design and control for the pump are discussed in section 3.2.1.3.

The liquid layer is composed of a water background with a drop of oil. In the absence of fields, the oil drop spreads evenly over the length of the hydrophobic track, as shown in Figure 2.7-a. The shape of the drop as seen in a cross-section across the width of the path is described below in section 2.2.1.2.

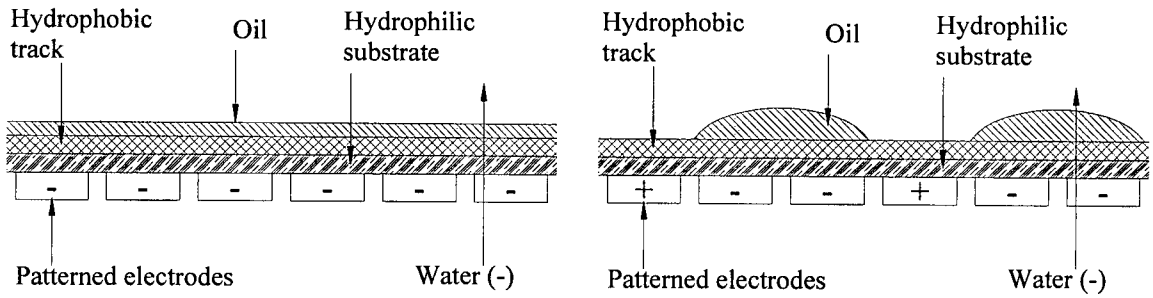

(a) (b)

Figure 2.7 – Cross-sectional view of fluidic pump along the length of a track with (a) no field applied and (b) voltage applied to every third electrode. (Not to scale)

The oil can be deformed by applying a voltage between the aqueous background and some of the patterned electrodes (see section 3.2.1.3). The oil drop is pinched out of the high field regions, as shown in Figure 2.7-b. Since the contact lines are pinned, the oil tends to be forced to move in the directions which keep it on the track. If the hydrophobic material and the oil are chosen so that their contact angle is sufficiently

small, then a thin layer of oil remains wetted on the hydrophobic region at all times, even when the field is applied. In this way, the fluid can move without creating or moving contact lines.

2.2.1.2 – Drop Geometry and Surface Tension Pressure

As mentioned above, with no fields applied, the oil drop will spread evenly across the length of the track in the fluidic pump. Taking a cross-section across the width of a track, the drop shape tends to be a circular cap, as shown in Figure 2.8.

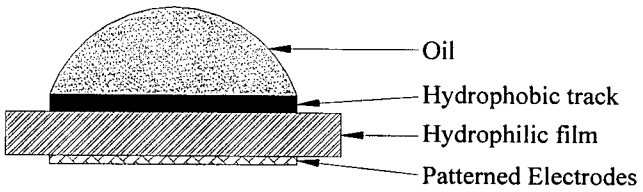

Figure 2.8 – Cross-sectional view across width of one track of pump

The tracks are long and straight enough that the maximum radius of curvature, r_2, of the oil-water interface does not significantly contribute to the over-pressure in the drop due to surface tension. This can be shown using equation (2.3). In the pump, the hydrophobic track does have some curvature to form a closed loop; however, this curvature was typically an order of magnitude smaller than the curvature of the circular cap in the work presented. The overall shape of the drop can therefore be approximated as a cylindrical cap.[14]

With this shape, the Young-Laplace equation is given by equation (2.5) with the minimum radius of curvature, r, being the radius of the cylindrical cap. This radius can be written in terms of the track width, w, and the contact angle, θ. The radius of curvature is therefore given by,

$$r = \frac{w}{2\sin\theta} \tag{2.10}$$

Using equation (2.5), the pressure due to curvature of the surface, P_S, can be written,

$$P_S = \frac{2\gamma\sin\theta}{w} \tag{2.11}$$

This is approximately the pressure that must be overcome to cause a deformation to the drop. Typical systems had a contact angle of 45° and a track width of 2 mm. So, using a typical oil-water surface tension of 50 mJ m^{-2}, typical surface tension pressures for this system would be on the order of 35 Pa.

The pressure due to surface tension can be used as a first order approximation when estimating the expected maximum flow rate of the oil, as discussed below.

2.2.1.3 – Fluid Flow Rate

When a real liquid is restricted to flow through a pipe of a given size, the flow rate will be limited by the viscosity of the fluid, the length of the pipe, and pressure difference between the ends of the pipe. The Hagen-Poiseuille equation,[15] equation (2.12), gives this flow rate for laminar fluid flow through a circular tube. For the fluidic pump application, the pumping pressure is applied using a patterned electric field, but sustained flow is generated by stepping the pattern along a hydrophobic track. This means that in this pump, the overall flow rate and pumping pressure are somewhat independent. The Hagen-Poiseuille flow rate can be used to estimate an upper bound on the flow rates that are expected to be achievable when using the presented pump.

$$v_{linear} = \frac{r^2 \Delta P}{8 l \rho \nu} \tag{2.12}$$

Here, v_{linear} is the linear velocity of the fluid, r is the tube radius, ΔP is the pressure difference between the ends of the tube, ν is the kinematic viscosity, ρ is the density and l is the length of the tube. For the presented pump, the pressure difference, the tube radius and the tube length need to be defined. The length of tube is the path length over which the oil travels, so in this pump, it depends on the field patterns that are applied. Appropriate field patterns and the electrode designs needed to generate them are described in section 3.2.

For the purposes of this estimate, equation (2.12) is generalized to an arbitrary tube cross-section by replacing the circular area with an arbitrary area, A_{XS}.

$$v_{linear} = \frac{A_{XS}\Delta P}{8\pi l \rho \nu} \tag{2.13}$$

For the presented pump, there is no well defined pipe, so the pipe cross-section is not well-defined. However, using the drop cross-section allows a first-order estimate to be made. With no field, the drop tends to form a cylindrical cap shape giving a cross-sectional area of,

$$A_{XS} = \frac{w^2}{4}\left(\theta \csc^2\theta - \cot\theta\right) \tag{2.14}$$

Using equation (2.14) as a first order approximation to the average cross-sectional area of the flowing drop, equation (2.13) becomes,

$$v_{linear} = \frac{w^2 \Delta P}{32\pi l \rho \nu}\left(\theta \csc^2\theta - \cot\theta\right) \tag{2.15}$$

In this estimate, the pressure used to pump the fluid can be estimated using pressure due to the curved surface. This pressure is convenient to use because it is expected to be the minimum pressure needed to deform the drop. Substituting in equation (2.11), equation (2.15) becomes,

$$v_{linear} = \frac{w\gamma}{16\pi l\rho\nu}(\theta \csc\theta - \cos\theta) \tag{2.16}$$

For typical pump designs tested, this model suggests that flow rates of up to 60 cm/s should be achievable with the materials tested.

As stated above, the fluid flow in this pump is generated by stepping a patterned electric field along a hydrophobic track. Since these are discrete steps, the actual flow rate of a given volume of fluid varies with time. The actual flow rate must be time averaged since the fluid will tend to flow very quickly after the field pattern changes to reach a stable shape until the pattern changes again. In addition to time averaging the motion, the flow rate must be averaged over the total path traveled in case the length of the electrodes varies locally. This variation usually depends on the geometry of the track and alters the local flow rate since the oil has to flow different distances to get out of the high field region. The overall average flow rate can be calculated using,

$$\langle v_{driven} \rangle = f_{switch} \langle l \rangle \tag{2.17}$$

where, $\langle v_{driven} \rangle$ is the average flow rate at which the oil is being driven, f_{switch} is the frequency at which the field is stepped along the path, and $\langle l \rangle$ is the average length over which the fluid must flow. When the electrodes are sufficiently close together, $\langle l \rangle$ is taken to be the center to center distance between electrodes.

2.2.2 – Fluid Flow through a Surface

As described throughout this thesis, the technique for inducing fluid flow using patterned electric fields was examined in the context of two potential applications. The fluidic pump described above, in which fluid flow is induced along a substrate, and a proposed reflective information display. For the information display application, a coloured liquid drop is moved through a thin, reflective solid substrate. The information display application is described in detail in section 3.1; fluid flow through a surface is described below.

A liquid drop can be moved through a thin, solid substrate that has small holes that pass through it, and patterned heterogeneous surfaces on both sides. With an appropriate pattern of holes and heterogeneous surfaces, a single liquid drop can be forced to be on both sides of the substrate simultaneously. A homogeneous electric field, and therefore the electrostatic pressure, is applied to one side. The drop-background fluid interfaces deform to balance this pressure, inducing fluid flow from one side to the other. Both water drops and oil drops can be made to move in this manner. The details of the substrate design are different in the two cases, but the desired wetting behaviour for the liquid drop is the same.

2.2.2.1 – Drop Geometry and Surface Tension Pressure

As stated above, a liquid drop can be moved through a solid by using a thin, solid with heterogeneous surfaces and small holes through it. The surfaces are prepared such that there are islands of lyophilic material completely surrounded by lyophobic material. The contact line of a drop placed on this island is pinned at the border between the two regions and so the shape of the drop's base area is determined by the shape of the lyophilic island.

An island from one side is connected to an island on the other side through a small hole in the substrate. This means that drops on the lyophilic islands on either side are connected forming one drop. A cross-section of the basic arrangement is sketched in Figure 2.9. Since there is a range of contact angles for which each contact line is stable, the bulk fluid in the drop can move between the two sides without moving the contact line on either side.

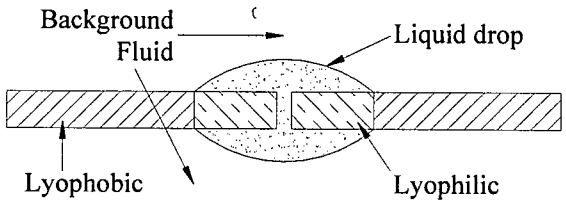

Figure 2.9 – Cross-section of a liquid drop and substrate for motion through a surface

Figure 2.9 shows a cross-section of a drop where the bases of the drop on both sides of the solid are the same size and the lyophilic regions on both sides are perfectly aligned. Neither of these conditions is necessary. The alignment is only restricted in the sense that

the two lyophilic regions must completely surround the hole, but the hole does not have to be in the center of either region. The lyophilic regions can be different shapes and sizes, although the shapes and sizes of the islands do affect the overall equilibrium shape of the final drop.

Each of the two curved drop-background fluid interfaces has a pressure associated that can be described by equation (2.3). The pressure within the drop must be constant, so in the absence of external fields, the over-pressure due to the curvature of each of the two sides must be equal. Therefore the interfaces tend to assume shapes such that,

$$\underbrace{\gamma\left(\frac{1}{r_{1,A}}+\frac{1}{r_{2,A}}\right)}_{\text{Pressure from Side A}}=\underbrace{\gamma\left(\frac{1}{r_{1,B}}+\frac{1}{r_{2,B}}\right)}_{\text{Pressure from Side B}} \tag{2.18}$$

where $r_{1,A}$ and $r_{2,A}$ are the principal radii of curvature of the interface on side A and $r_{1,B}$ and $r_{2,B}$ are the principal radii of curvature of the interface on side B. The shape of the lyophilic islands can be optimized for the particular application, and so the four principal radii of curvature could, in principle, all be different.

It is convenient to consider the case where the lyophilic islands are circular, with radii a_A and a_B, on both sides. When the drop is placed on such a substrate, the drop will tend to move until the drop-fluid interfaces on both sides are shaped like spherical caps. Thus the curvature of each interface can be completely described by a single radius. In

equilibrium, the over-pressure associated with the surface tension of each interface must be the same. This means that in the absence of external forces, the curvature of each of the two interfaces must also be equal.

Since in the absence of external forces, both interfaces have the same curvature, and both form spherical caps, a convenient way to describe the drop shape is by considering the height of each interface. For convenience, the height a drop-fluid interface is defined as the maximum elevation between that interface and the solid surface. For the spherical caps, this height is given by,

$$h_i = r - \sqrt{r^2 - a_i^2} \tag{2.19}$$

where r is the radius of curvature of the interface and a_i is the radius of the circular base. So in the absence of external fields, the equilibrium shape and position of the drop is determined by the sizes of the lyophilic islands.

2.2.2.2 – Component Geometry and Electrostatic Pressure

Both water drops and oil drops can be deformed by electrostatic pressure to cause fluid flow through a thin solid substrate. In both cases, a non-conductive fluid phase and a water phase are present. The deformation is induced by applying an electric field across the non-conducting fluid on one side of the substrate, thus attracting the water phase into the high field region. Since in one case the drop makes up the water phase, and in the

other the background fluid is water, the structures needed to apply these fields are different in the two cases, and are discussed below. It should be noted that, as discussed above, the desired wetting behaviour of both the oil drops and water drops is the same.

2.2.2.2.a – Water Drop

As described above, a water drop surrounded by a non-conductive background fluid can be made to flow through a thin substrate by applying an electric field across the background fluid on one side of the substrate. For this type of flow, the water is deformed by applying a potential to the water and a conductive plane some distance, d, away as shown in Figure 2.10. Since the drop is water based, and therefore conductive, when an electric field is applied, the electrostatic pressure tends to attract the drop into the high field region. This means that the liquid in the drop tends to flow to the side with the field applied. This is sketched in Figure 2.10-b.

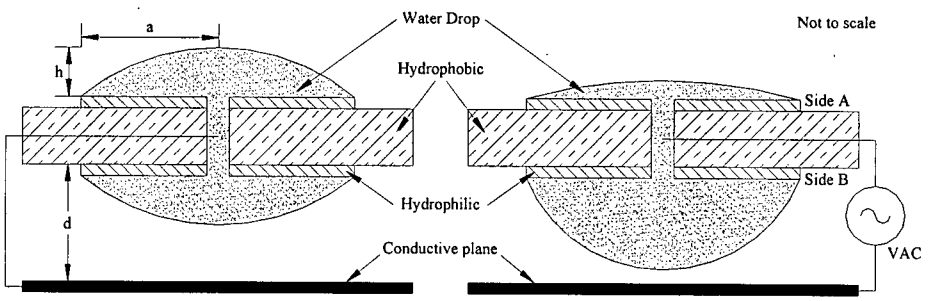

(a) Equilibrium state – no E-field **(b) Deformed state – E-field applied**

Figure 2.10 – Cross-section of water drop system

As can be seen in Figure 2.10, the gap distance is considered to be the separation between the substrate and the external conductive plane for convenience. It should also be noted that as the drop is deformed, the radius of curvature of the water-background fluid interface decreases in the high field region and increases in the no-field region. This means that the pressure due to the surface tension increases in the high field region, thus providing a restoring force which prevents the water from completely flowing onto the high field side. The amount of liquid that does flow into the field depends on the magnitude of the electric field applied and is discussed below in section 2.2.2.3. For the reflective information display application, this can be used to provide grey-scale control. The water remaining on the no-field side remains completely wetted on the hydrophilic region, so when the electric field is removed, the drop can flow back to its equilibrium position without contact angle hysteresis.

It should also be noted that the background fluid could be a gas, like air, or a liquid, like oil. The basic structures required and the underlying principles of the induced flow are the same in both cases, though using an oil background can have practical advantages over air. Two major disadvantages of using air as a background fluid are; the water drop itself must be limited in size to minimize the effect of gravity on the shape, and the drop tends to evaporate unless a sealed cell around the drop is used. When using an oil background, evaporation of the water drop can be effectively eliminated without the necessity of sealed cell systems. Also, the density of the oil is closer to that of water, so larger drops can be used as the influence of gravitational forces becomes negligible. In addition to these primary benefits, with an appropriate choice of oil, this background can

support larger electric fields than air. Using air as a background fluid is convenient when doing measurements, as described in section 3.1.1

2.2.2.2.b – Oil Drop

The water drop systems have the fundamental drawback that the conducting plane and the substrate must be relatively far apart. This is because the minimum gap between them is limited by the size of the water drop used and the amount of movement desired. This means that relatively large voltages are required to produce an electric field of the desired magnitude.

A thin gap for any size drop can be obtained when using an oil drop with water as the background fluid. An electric field can be applied across a thin, insulating film which provides the desired wetting behaviour for the oil drop. The film can be made almost arbitrarily thin without affecting the surface properties, so large fields can be produced with relatively small voltages. In typical systems examined, the gap for water drops was on the order of 0.5 to 1 mm, while the films used for the oil drops were on the order of 10-100 μm. Using the parallel plate capacitor approximation, this means that the voltages could be two orders of magnitude smaller for the oil drop systems than those for the water drops.

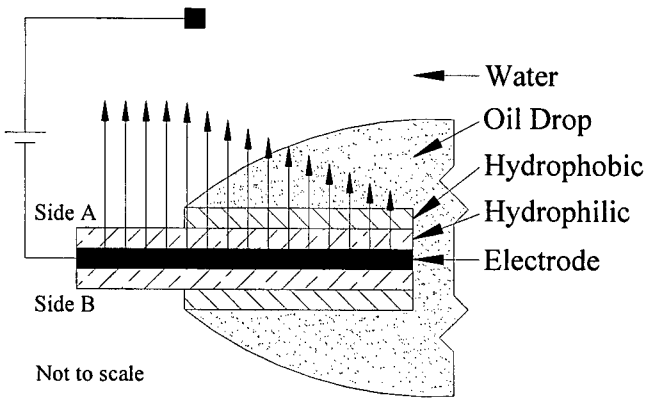

Figure 2.11 – Cross-section of front side of oil drop with example electric field lines sketched

The electric field is applied to the system on one side of the substrate, as is shown in Figure 2.11. As it is sketched, near the edges of the oil drop, the oil is thin and the field is relatively large. The water exerts a large force at the edge of the drop, tending to push the oil out of this region, but as more oil is pushed out, the "thin" region increases, so more oil can be pushed out. In this manner, the oil drop tends to get pushed to the other side of the substrate. As the volume of oil on the no-field side of the substrate increases, the curvature of the corresponding oil-water interface increases. This is because, as discussed above, the contact angle of the oil on the hydrophobic islands is sufficiently low that the contact lines are pinned at the edges of the islands even when very little oil remains. This means that the thin layer of oil remains wetted on the high field side, and no contact lines are moved and no new ones are formed. So long as the angle of contact is less than 90°, increased volume means decreased radii of curvature and therefore increased pressure.[16] The pressure due to the curved interface on the no-field side of the substrate provides a restoring force which prevents the oil from completely moving over. This also means that when the electric field is removed, the drop can flow back to its equilibrium position without hysteresis.

Inducing motion through the substrate requires that a field is applied to one side, thus causing a net pressure difference between the two sides of the substrate. For the oil drop, this is accomplished by inserting an electrode layer into the substrate, shown schematically in Figure 2.11. As stated above, the oil drop must be surrounded by water on both sides to exert the electrostatic pressure on the drop. In the discussion above, it is implicitly assumed that the hydrostatic pressure of the water is constant and equal on both sides at all times. In order to avoid any additional perturbations due to a gradient in the hydrostatic pressure, the experimental apparatus had pressure balancing channels so that the water from both sides could mix. This ensures that the water on both sides is always at the same pressure, but has the consequence that the water on both sides has the same electric potential. With this restriction, the system in Figure 2.11 does not have the requisite inhomogeneity in the field and so there would be no net movement of the oil.

For the oil drop to exhibit net motion from one side to the other, the field must be inhomogeneous. One way this can be done is by making the hydrophilic layer much thicker on one side than the other. In the parallel plate capacitor approximation, the electric field is inversely proportional to thickness. Given that the pressure is proportional to the square of the fields, a ten times difference in thickness of the two hydrophilic layers results in a hundred times difference in the electrostatic pressure on each side. This means that there is a significant net pressure difference and so the interface will tend to deform pushing the bulk of the oil drop towards the side with the thick hydrophilic layer. This structure is sketched in Figure 2.12.

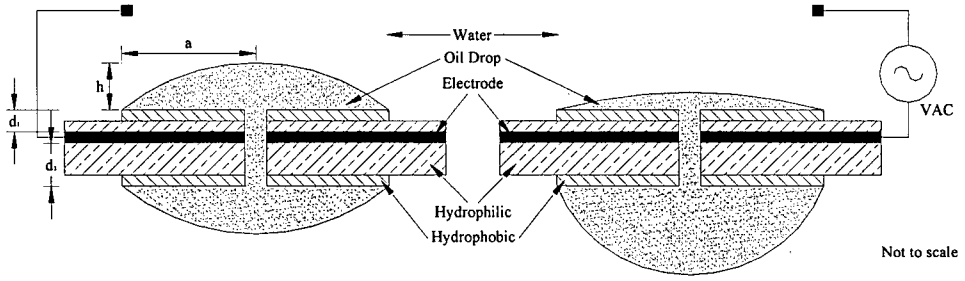

(a) No Field (b) Field Applied

Figure 2.12 – Cross-section of oil drop system with asymmetric hydrophilic layers

By building the asymmetry into the substrate, the drop can only be forced in one direction. When the field is removed, the motion of the drop as it moves back to the original position is determined by the curvature of the oil-water interfaces.

In cases where it is desirable to be able to choose which direction the oil should flow, an alternate configuration, such as that shown in Figure 2.13, can be used to produce the asymmetric fields. The method illustrated uses two conductive layers separated by an insulating layer within the substrate. The hydrophilic layers can then be the same thickness on both sides. The asymmetric electric field is produced by keeping one conductive layer and the water at a reference potential and applying a high potential to the other conductive layer. With this method, the drop can be forced in either direction by simply switching which layer is shorted with the water.

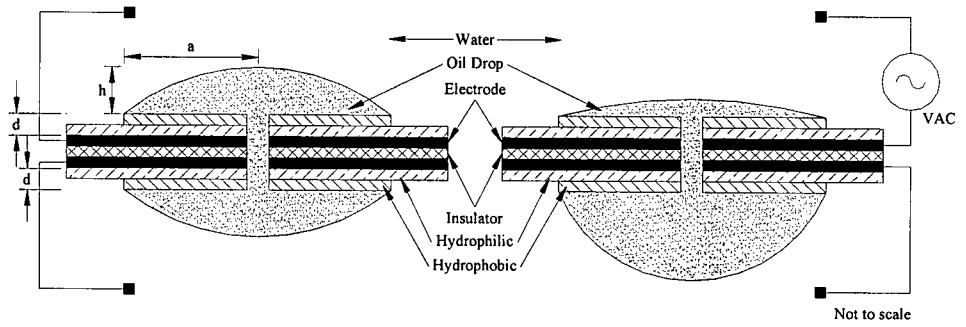

(a) No Field (b) Field Applied

Figure 2.13 – Cross-section of oil drop system with two conductive layers

Though the symmetric substrate design can be useful in general, the asymmetric substrate was easier to manufacture for the initial tests presented. For the reflective information display application, it may be sufficient to have forced movement only in one direction, so the asymmetric substrate could be used. However, the symmetric substrate design could be used to increase the contrast between white and dark states, or to improve the switching speed from the white to dark state.

2.2.2.3 – Drop Height Change

With the proposed information display, the apparent reflectivity of a substrate is modulated by changing the amount of coloured liquid between the viewer and the reflective surface. This is done by deforming a liquid drop such that it moves through the surface, as described above. Since the drop is coloured, more liquid will absorb more light, and thus reduce the apparent reflectivity. This means that the change in height of the drop, on the side of the substrate intended for viewing, can be used to determine the contrast ratio between the white and dark states. As described above, the height of the

drop, h, is defined as the maximum distance between a drop-background fluid interface from the solid surface.

To estimate the expected change in height, it is illuminating to consider a simple energy perturbation argument using the energy in the applied electric field, W_E, and the free energy of the drop-fluid interfaces, W_S. The change in curvature of the drop depends on the amount of energy that the electric field adds to the system. For simplicity in this estimate, it is assumed that the structures used to apply the electric field to the drop can be approximated as parallel plate capacitors. This means that the energy in the electric field is simply,

$$W_E = \frac{\varepsilon\varepsilon_0}{2} E^2 A d \qquad \textbf{(2.20)}$$

where A is the area of the drop-fluid interface, d is the capacitor gap and ε is the dielectric constant of the insulating fluid. As discussed above, the capacitor gap is the distance between the substrate and the conductive plane for water drop systems, and it is the thickness of the thin hydrophilic film in the oil drop systems.

With no electric fields, the free energy associated with the two drop-fluid interfaces is given by the surface free energy (equivalently, the surface tension) multiplied by the area of the two interfaces. As discussed above, if the lyophilic regions on both sides of the substrate have the same dimensions, then in equilibrium, the two interfaces have equal surface areas, and so the free energy is given by,

$$W_S = 2\gamma A \tag{2.21}$$

The perturbation argument is that the change in energy of the system, the energy of the electric field, is approximately proportional to the change in the radius of curvature of the drop, Δr. Specifically, the change in energy, W_E, divided by the unperturbed energy, W_S, is approximately equal to the change in radius of curvature, Δr, divided by the unperturbed radius of curvature, r. So the expected change in radius of curvature of the drop-fluid interfaces is approximately,

$$\Delta r = \frac{Ad\,\varepsilon\varepsilon_0 E^2/2}{2\gamma A} r \tag{2.22}$$

Using equation (2.19), the change in height of the interface is the same as the change in the radius of curvature to first order. So equation (2.22) can be rewritten in terms of the change in height,

$$\Delta h = \frac{\varepsilon\varepsilon_0 r}{4\gamma} \frac{V^2}{d} \tag{2.23}$$

Recognizing the expressions for electrostatic pressure, equation (2.8), and the surface tension pressure, equation (2.4), equation (2.23) can be simplified to,

$$\Delta h = \frac{P_E}{P_S} \times d \tag{2.24}$$

where Δh is the change in height, d is the gap thickness, P_E is the electrostatic pressure in equation (2.8) and P_s is the pressure from the curvature of the interface from equation (2.4).

Chapter 3 – Applications

During the course of this work, the fluid deformation described in the previous chapter was examined in the context of two example applications, a proposed reflective information display and a fluidic pump for surface heat transport. The reflective display application, discussed in section 3.1, was based on moving a liquid drop through a thin, reflective solid substrate. The fluidic pump was based inducing flow of an oil drop along the substrate surface and is discussed in section 3.2. As discussed in Chapter 2, the underlying principles used for both types of fluid flow are the same, though the structures and control systems needed to induce the desired flow were slightly different in each case.

3.1 – Reflective Information Display

There are two basic types of information displays available, emissive and reflective displays. Emissive displays are ones that modulate emitted light; for example CRTs, plasma screens, backlit LCDs, and LED arrays. Reflective displays modulate reflected environmental light to display their information. Examples of common reflective displays are LCDs in calculators, printed material, etc.

Other fluidic reflective display technologies have been demonstrated, and are typically based on traditional electrowetting.[17,18] Electrowetting reflective displays in which a contact line moves can require mechanisms to overcome hysteretic effects due to the movement of a contact line on the substrate surface.[19]

In the method for deforming fluid interfaces presented in this thesis, hysteresis was avoided by immobilizing the contact lines of the liquid drop on the solid substrate for a range of angles of contact. The proposed display presented uses the motion of a coloured liquid drop through a substrate, as described in section 2.2.2, to modulate the apparent reflectivity of the substrate's surface. In the work presented, a single drop formed a single pixel.

When the drop is in its dark state, shown in Figure 3.1-a, there is a relatively thick layer of absorptive material between the viewer and the reflector so incident light will be largely absorbed. When the drop is deformed so it moves primarily to the back side, shown in Figure 3.1-b, then there is a relatively thin layer of liquid on the side intended for viewing. In this configuration, incident light will be largely reflected, giving a white state. The extent to which the drop can be displaced depends on the magnitude of the field applied, as estimated using equation (2.24), so grey-scale can be achieved by straight forward control of the applied potential. In a display, the drop would be coloured with some predetermined concentration of dye, so the height of the drop would determine the amount of light absorbed. Thus the change in height would determine the contrast between the white and dark states. In principle, colour information could be displayed using multiple drops to form a single pixel, and some sort of colour filter. The colour filter could be as simple as using a different dye in each drop of the pixel, or it could be integrated into the reflective surface.

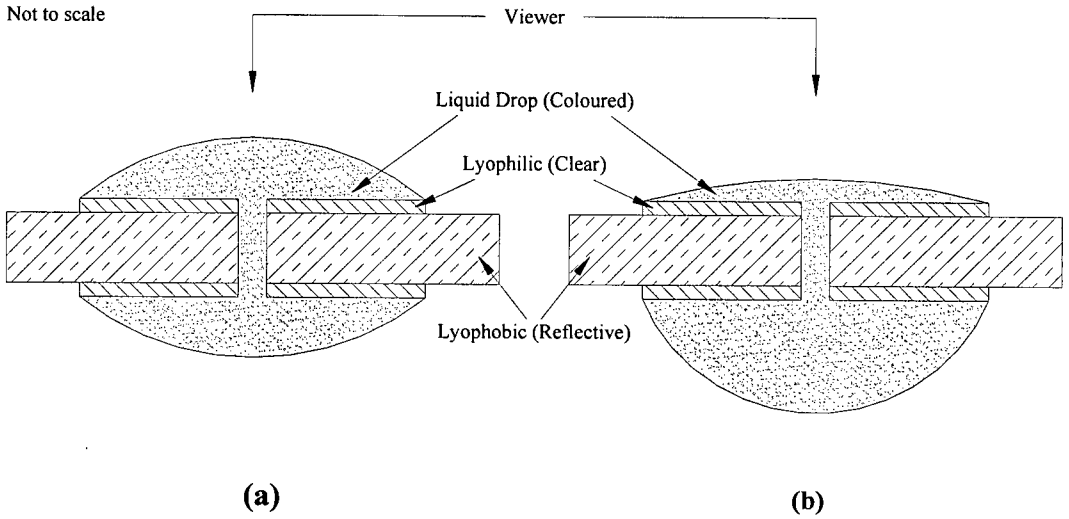

Figure 3.1 – Schematic cross-section of a pixel while in (a) dark and (b) white states

With an appropriate choice of materials, the system can be made with an oil drop or a water drop as is described in section 2.2.2. For convenience, the lyophilic regions in all systems were made to be the same size and circular on both sides of the substrate. This meant that when no fields were applied, only one radius of curvature was needed to describe the curvature of both interfaces.

3.1.1 – Water Drop in Insulating Fluid

One version of the device used a water drop in an insulating fluid background, such as air or oil. Although aqueous solutions of ionic dyes were used in the results presented below, the drop is referred to as a water drop. Within the water drop pixels, there were two systems demonstrated, one with an oil as the background fluid and the other with air as the background fluid. The two systems required different substrates and coating materials to get the right wetting behaviour. However, in both systems, the water was

deformed by applying a potential to the water and a conductive plane some distance away as shown in Figure 2.10.

The water drop in air system was a convenient system to study because of ease of construction and the accessibility of the drop to measurement devices. In a system that was open to air, evaporation of the drop was a major drawback. However, evaporative losses from the water drop could have been effectively eliminated by using sealed cells. When using a sealed cell, the volume of air would be fixed, and an equilibrium between the liquid and its vapour could be reached. It has been shown, by V. Kwong,[20] that because the drops contained an ionic solute, water condensation would tend to take place into the original drop rather than on other surfaces in the sealed system. It should be noted that it is assumed that such a sealed system would be designed so the air pressure is always equal on both sides of the drop.

As an alternative to making sealed cells for the water drops, evaporative losses from the drop were avoided by using oil as the background fluid. The oil also offered the advantage that it could support larger fields and had the potential to be density matched with the water drop. The materials used for demonstrations of the water drop in oil systems made construction, assembly and measurement of the device more difficult than for the water drop in air systems. Materials found for the pump application in section 3.2 could help ease these problems, but they were not used in the presented results due to time constraints.

In both the air and oil systems, electric fields with magnitudes on the order of 10^6 V m^{-1} were required to get significant movement. To achieve these fields, an adjustable amplitude power supply was built. AC voltage was used to avoid charge build-up effects that tend to occur when using DC voltages.[21] V. Kwong showed that in traditional electrowetting experiments, using a DC electric field could lead to reduced drop deformation as charge would build up around the contact line of the drop. He also showed that using an AC electric field would effectively eliminate the issue. The voltage supply that was built can produce a 60 Hz sine wave with amplitude from 0 V to about 10 kV. Typical root mean square (rms) voltages used were about 800 V_{rms}.

3.1.1.1 – Water drop in air

The water drop in air pixel was demonstrated with simple materials and construction techniques. Methods for creating a system which demonstrated significant movement of the drop proved to be reliable and reproducible, thus the water drop in air system was deemed a convenient system on which to perform the measurements.

A pixel of the proposed information display containing a single drop was built using copper shim stock as the reflective, hydrophobic substrate, Rain-X anti-fog treatment as the hydrophilic coating and a solution of naphthol blue black dye in deionized water for the drops.

The copper shim stock served multiple purposes in the pixel. It was found that in air, the water drops had a contact angle of 90° ± 10° when placed on the copper substrate. This

contact angle was found to be sufficiently large that the copper could be used as the hydrophobic substrate. The copper shim stock is sufficiently reflective that no other reflective material was needed for the purposes of this work. Since copper is conductive, the substrate was used to connect the water drop to the power supply with no need for a layered substrate or additional wires. Touching the drop with a wire would have added contact lines where the wire intersected the drop-fluid interface. Such contact lines could have been required to move in order to get the desired range of motion of the drop. This could have resulted in effects such as hysteresis and friction to the motion, both of which are fundamentally undesirable.

The hydrophilic regions were created by treating the copper surface with Rain-X anti-fog treatment. The treatment was applied as a liquid and dried to form a clear coating on which the water drops had a wetting angle close to 0°. The coating was patterned manually by applying the Rain-X liquid directly on the desired locations. Together, the copper and Rain-X had natural contact angles that were sufficient to pin the drop's contact lines for the range of motion observed.

The water drop was coloured with an ionic dye, naphthol blue black[22]. This dye dissolved readily in water and did not significantly alter the wetting behaviour of water on the substrate surfaces. The drops were made from a solution of 3.5 mM (millimoles/liter) naphthol blue black. Using drops with this concentration of naphthol blue black allowed a visible reflectivity change to be demonstrated when the bulk of the liquid was moved through the substrate, as shown in Figure 3.2. Further optimization of

the concentration of the solution and the volume of the drop could yield improved contrast, though this was not explored in this work due to time constraints.

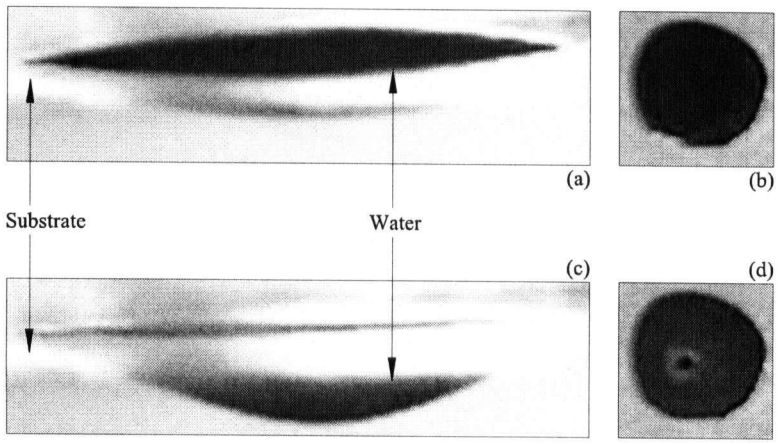

Figure 3.2 – Photos of water drop in air system.

With no voltage applied, the drop is in a dark state, (a) cross-sectional view & (b) viewing surface.

With a voltage applied, the drop is in a white state, (c) cross-sectional view & (d) viewing surface.

The change in height, Δh, of the drop with electric field was measured using an optical distance probe[23] placed above the viewing surface, as shown in Figure 3.3. The probe used a near-infrared light source to measure the distance of a surface from the probe tip. It was found that naphthol blue black is not absorptive to near-infrared light, so what was measured was a combination of the top surface reflection of the water-air interface and reflection off the copper substrate. The two reflections resulted in a distance measurement that was a combination of a moving signal and a constant signal. To compensate for this, a rough calibration was done by placing the probe a known distance from a copper plate flooded with a layer of the naphthol blue black solution. The area of the layer was well-known and restricted so the thickness of the layer could be controlled

by adding a known volume of solution. It was found that the change in height measured by the instrument was approximately a third as large as the actual change in height of the drop. Using this factor of 3, the measured height changes were simply rescaled to get the actual height change of the drop. This simple calibration is not ideal for the system, but was used to confirm that order of magnitude estimates of the expected drop movement were reasonable.

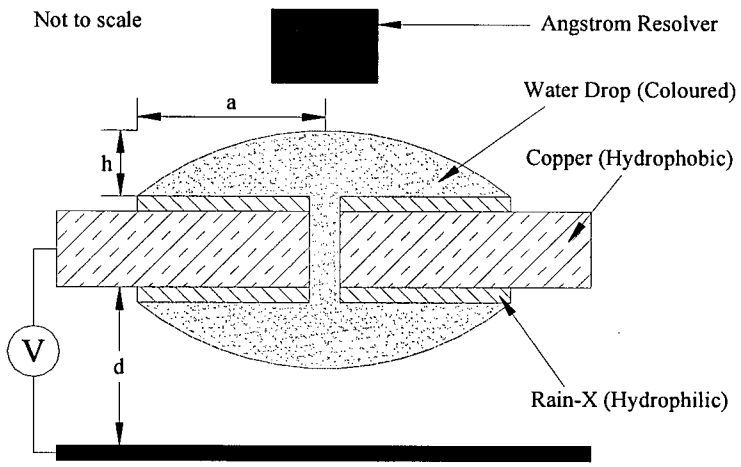

Figure 3.3 – Water drop in air configuration with distance probe

Table 3-1 shows the height change of a water drop and the expected change as calculated using equation (2.23). The dielectric constant of air, ε, was taken to be 1. The surface tension of pure water at 25 degrees is 72 mN/m.[24] Though the presence of dye is expected to reduce the actual surface tension of the drop's fluid interface, the difference is expected to be far smaller than other errors in this estimate. So for the surface tension of the fluid interfaces, the surface tension of pure water was used. The volume of the drop was adjusted so that the liquid-air interfaces had radii of curvature around 6 mm. The gap between the copper substrate and the conductive plane was set at 750 μm.

Table 3-1 – Change in height of front-side of drop in response to voltage with 750 μm gap

Voltage (V)	Rescaled Change in Height (μm)	Expected Change in Height (μm)
199	29	39
251	39	63
301	65	90
375	73	140
450	77	202

From these results, it can be seen that the model gives reasonable order of magnitude estimates for the lower voltages. Further investigation into the model at higher voltages was not pursued in the interest of investigating systems that eliminated evaporative losses from the drop and used lower voltages.

While the water drop in air pixels were convenient systems to perform measurements on, the drops tended to completely evaporate on relatively short time scales, i.e. about 15-20 minutes. In principle, this could be avoided by sealing the drop and air in a closed cell. In such a cell, the vapour phase and the liquid phase would come into equilibrium. As Kwong has shown,[25] condensation from the vapour would tend to occur in the existing liquid phase (the drop) rather than forming new droplets of pure water on other surfaces in the cell. This occurs because the drop contained an ionic solute, and therefore the equilibrium vapour pressure of the drop would be less than that of pure water.

3.1.1.2 – Water drop in oil

As discussed above, the water drop in open air systems were not ideal because the water drops would evaporate. This could be avoided by enclosing the pixel in a closed cell, or by using an oil as the background fluid. Using oil as the background fluid is convenient since the density of the oil is closer to water than air. With the right choice of oils, it should be possible to get density matching between the drop and the background. This means that gravity can be ignored for relatively large drops. Oils which would sustain larger electric fields than air can also be used.

For the pixels examined, type B immersion oil[26] was used. The use of this oil required the substrate materials to be changed from those used in the water drop in air pixels. The Rain-X anti-fog treatment did not remain bonded to the copper surface when put in the immersion oil. For this system, glass cover slips[27] were used as the hydrophilic surface with conductive ink[28] painted onto the surface to form a hydrophobic coating. It should be noted that although this arrangement was a little different than the arrangements discussed throughout this thesis (in this case, the lyophobic material formed the coating), the difference was found to be irrelevant in any practical sense.

Since the glass cover slips are clear, the substrate was made reflective by sandwiching a diffuse, white reflective material[29] between two glass cover slips. A cross-sectional view of the resulting structure is shown schematically in Figure 3.4.

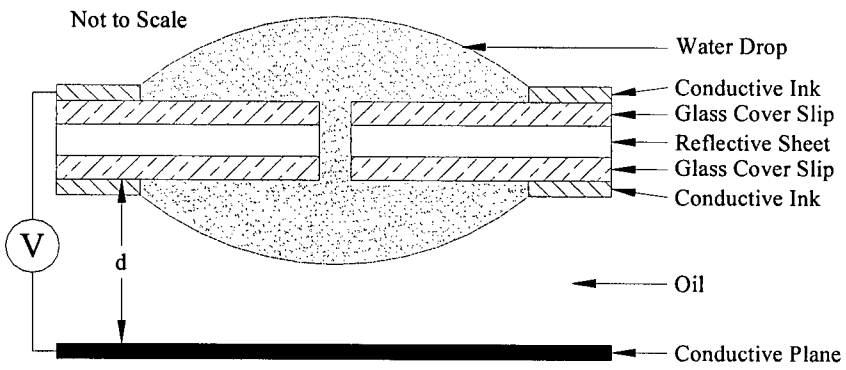

Figure 3.4 – Water drop in oil configuration

As discussed above, connecting the drop to the voltage source without creating any movable contact lines was a concern. In these pixels, the conductive ink layer was used to connect the water drop to the power supply. While this was suitable for this work because of the materials and liquids used, a more general structure could incorporate a conductive layer in the core of the substrate, i.e. between one of the glass and EDR layers.

Motion was shown in this system as proof of concept, but was not measured since the water drop in air was much more easily manipulated for measurement purposes. Figure 3.5 shows photos from a demonstration using a gap distance, d, of 500 μm. The drop is shown in cross-section. In Figure 3.5-a, the drop is shown with no field applied, and in Figure 3.5-b, the drop is shown with a field applied to the bottom side of the drop.

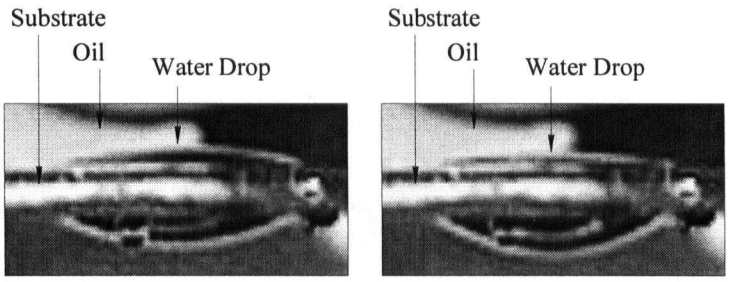

Figure 3.5 – Photos of water drop in oil in (a) dark state and (b) white state

Measurements and optimization of the dye for the water drop in oil system were not investigated in order to focus on the oil drop in water system (described in the next section). The water drop systems required large voltages (~800 V_{rms}) to produce the fields (~10^6 V m^{-1}) necessary to cause movement. This is a fundamental problem with the water drop system since the gap distance, d, is limited by the size of the drop and the desired range of motion. If the gap was too small, the water drop could come into contact with the conductive plane. This is an irreversible event and so the gap thickness was made relatively large to avoid such contact.

3.1.1.3 – Conclusions

Two versions of a water drop based, reflective, information display pixel were built as proof-of-concept demonstrations. The water drop in air system was measured to have movement roughly in agreement with what was an expected based on the estimate of the electrostatic and surface tension pressures. Typical drop height changes were on the order of more than 30 μm. Using this system, a visible reflectance change was demonstrated using drops made with an aqueous solution of naphthol blue black.

The water drop in oil pixel was constructed and movement was shown. The oil was used so that evaporation from the drop and gravity could be ignored, even for a pixel that was not sealed.

3.1.2 – Insulating Drop in Water

As described in section 2.2.2, large voltages are needed to get a significant deformation of the water drop in an insulating fluid. This is simply because the gap between the surface and the conductive plane must be relatively large, and so the electric field generated by a given voltage tends to be small. The minimum gap thickness is limited by the size of the drop and deformation desired. If the gap is too small, the drop could come into contact with the back electrode, which is an irreversible event. Since the electric field is established in the non-conductive fluid, it is possible to get smaller effective gap thicknesses by using an oil drop in a water background. As described in the previous chapter, the field is established in the oil and a thin non-conductive film. This means that the effective gap is limited by the thickness of the oil, which is very thin, especially at the edges of the drop. While this type of pixel is very simple in principle, the major challenge was finding the right combination of materials and construction techniques.

When assembling the various components of a pixel, several different sets of techniques were used depending on the solid materials being tested. For example, when using polyethylene terephthalate (PET) plastic film and wax, the wax could first be printed on the plastic surface of an aluminized PET plastic film. In this example, the solid layers

could be laminated together using solid adhesive sheeting. Other materials, such as glass, could not be processed in exactly the same manner in the lab, so techniques more suited to the particular material were used.

Once the substrate was assembled, a container for the background water was built around the substrate. The design of the water container is considerably more important for the oil drop pixels than it is for the water drop pixels. In the water drop pixels, the only conductive fluid is in the drop itself, so the only way a short can develop is if the water drop contacts the conductive plane. This occurs even if all parts of the pixel are submerged in oil. Since a single body of background fluid could completely surround the pixel, the hydrostatic pressure of the background could be completely ignored.

In the oil drop system, the water background was conductive, so special care had to be taken to prevent shorts, especially at the edges of the substrate where the conductive layer could be exposed. To this end, separate water baths were placed on each side of the substrate so the water could not seep under the electrically insulating layers of the substrate at the edges of the sample. The two water baths were connected so that the hydrostatic pressure could be kept constant on both sides when the drop was deformed. To simplify construction, the substrate and drop were oriented such that the water baths on both sides were open to air. Figure 3.6 shows a sketch of the system as viewed from above.

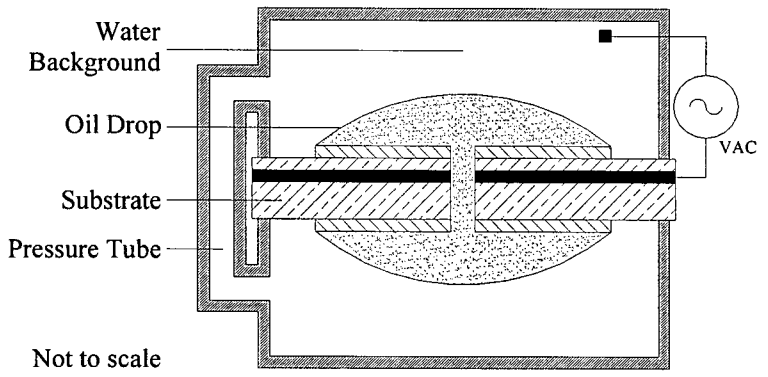

Figure 3.6 – Cross-section of oil drop in water pixel with water container (Top View)

In spite of these precautions, many of the oil drop pixels examined shorted at the hole that connects the oil on the two surfaces. It was not clear if these shorts were due to faults in the materials (e.g. electrical breakdown) or in the construction techniques (e.g. perhaps a small crack formed while drilling the hole). The testing of materials was separated from testing of the construction methods by evaluating candidate materials in an apparatus that induced flow along the surface. As described below, the apparatus was designed so that the risk of a short circuit was eliminated. Using this apparatus, liquids for the oil drop, and solids for the hydrophilic surface and hydrophobic surface were accepted or rejected for further evaluation based on visual assessment of key characteristics. These included; wetting angles of the drop on each of the two solids, response of the drop to an applied field, apparent swelling behaviour and solubility of the solids in the presence of the liquids (oil and water), and the adhesion between the two solids. Swelling and solubility were assessed based on secondary effects. For example, one of the solids may have an increased brittleness such that it would break under minor mechanical stress, or perhaps the adhesion between the hydrophobic and hydrophilic

solids in a heterogeneous solid might change so the solids separate with little or no mechanical stress. Occasionally, the secondary effect would appear in the liquid phases, there might be a change in volume or wetting angle of the drop, the viscosity of the oil might become dramatically larger, even gel-like, or there might be a change in turbidity or colour of one of the liquids. With this apparatus, it was possible to simultaneously observe the wetting angles of the drop on both the hydrophobic and hydrophilic surfaces, the response of the drop to an applied electric field, the swelling behaviour of the solids in the presence of the liquids (described above), and changes to the properties of any of the materials.

The material evaluation apparatus had a single long, narrow electrode under a water bath. A 5 mm wide electrode was placed along the width of a clear plastic water bath, and covered with a 65 μm thick layer of Mylar. In this way, the electrode was completely electrically insulated from the water. An electric field could then be applied in a sample (described below) that was in contact with the Mylar and placed over the electrode. A sample was a thin film, typically less than 100 μm thick, with a single heterogeneous surface (made from the hydrophobic and hydrophilic solids of interest). The surface was patterned so that it had a relatively long and narrow track of the hydrophobic material completely surrounded by the hydrophilic material. Typical tracks were 10-20 mm long and 5 mm wide. The samples were held in contact with the Mylar at the bottom of the water tank so there was effectively no water between the sample and the Mylar. The samples were aligned such that one end of the track was lying above the electrode, as shown in Figure 3.7.

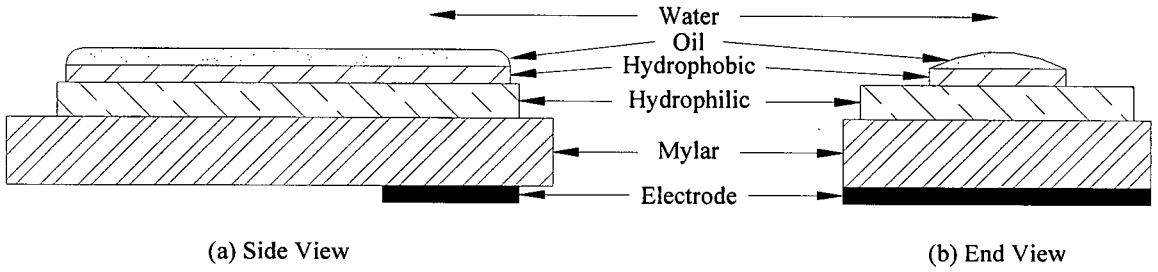

Figure 3.7 – Materials test apparatus cross-sectional view

In this arrangement, a patterned electric field could be applied in the oil by applying an electric potential between the water and the electrode to push the oil drop out of the field region. When there was good contact line pinning, the displaced oil drops tended to remain on the hydrophobic track.

While the materials evaluation was underway, it was realized that the test apparatus could be modified to pump the oil along the surface. This was explored in the context of a surface heat transfer device and is discussed in Section 3.2. As evidenced by the materials test apparatus, the material requirements for the proposed oil drop-based information display application are very similar to those of the fluidic pump application. During the course of investigation of the pump, materials and assembly techniques were found that may be appropriate for the display application. The requirements and descriptions of the materials are discussed in section 3.2.1.1.

A working demonstration of an asymmetric substrate was produced using a layer of PET plastic film[30] (12 μm thick, aluminized on one side), double-sided solid adhesive[31] (135

μm thick) and a relatively thick layer of Mylar (65 μm thick). The PET and Mylar films were used as the hydrophilic surfaces. A hydrophobic layer of printed wax (~10 μm thick, Xerox ColorStix printer wax) was patterned (using a Xerox Phaser 8200DP solid ink printer) directly onto each of the plastic films. The two films were then laminated together with the adhesive. A hole connecting the two hydrophobic regions was drilled into the substrate using a #64 drill bit. The resulting structure is shown in Figure 3.8. The oil used in the drop was Dow Corning® OS-30 silicone fluid, which had a contact angle of 90°±10° on the PET and Mylar films, and less than 10° on the printed wax.

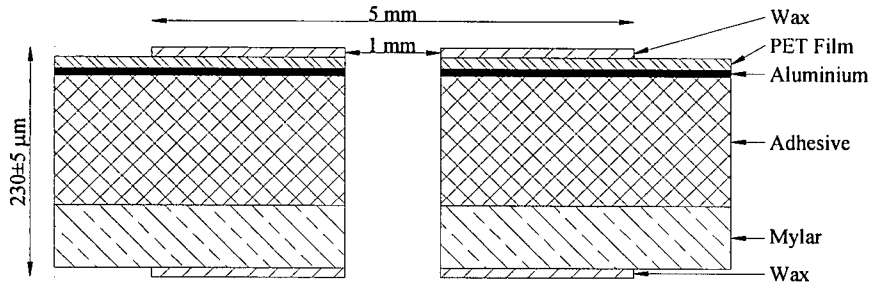

Figure 3.8 – Layering of asymmetric substrate for oil drop based display

The symmetric substrate system was also demonstrated successfully using similar techniques. The only difference between this system and the asymmetric one was that a layer of aluminized PET plastic replaced the Mylar. The resulting structure for the symmetric substrate is shown in Figure 3.9.

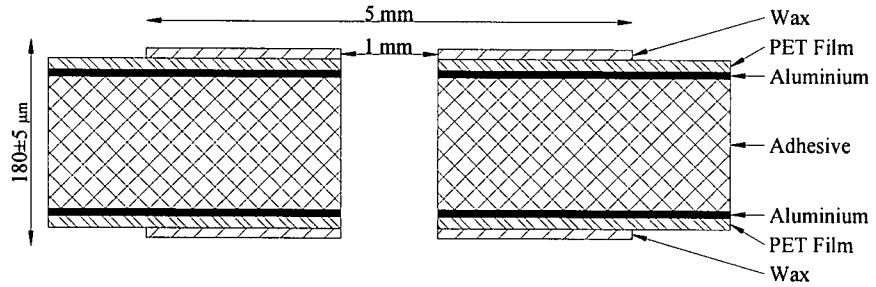

Figure 3.9 – Layering of symmetric substrate for oil drop based display

While the systems described above were built and exhibited motion successfully over a few hours, time constraints prevented further testing and development. It should be noted that during the development of the fluidic pump, it was found that the printed wax does not adhere very well to Mylar. In the devices studied, this lack of bonding causes the wax layer to be fragile, and in some instances the wax will spontaneously separate from the plastic surface in the presence of the OS-30 silicone fluid. For the pump, this issue was found to happen primarily for long tracks, though no mechanism for area or length scale-dependent behaviour was found. This means that the printed wax and PET film combination may not be ideal, but for the purposes of the demonstrations discussed above, this combination could be used. For the pump, the wax was found to adhere well to an optical filter film (discussed in section 3.2.1.1). A demonstration of the proposed pixels was not attempted with the optical filter film due to time constraints.

3.1.2.1 – Conclusions

Motion of an oil drop in water through a solid surface was demonstrated successfully using both a symmetric and asymmetric substrate. The work presented was limited by

time constraints, so a demonstration of visible reflectivity change was not attempted. There are many avenues of future work that could be pursued; the materials need to be further optimized to get a visible reflectivity change, a suitable dye needs to be found so that the silicone oil can be absorbing instead of clear and colourless and the colour of the wax-based hydrophobic coating needs to be chosen optimally. The wax that was used contains absorbing dyes that could be used for colour filtering in a colour display; however a pure black and white pixel would require finding a clear material for the hydrophobic coating.

3.1.3 – Conclusions

Individual pixels of a proposed novel reflective information display were demonstrated in three distinct systems; a water drop in air, a water drop in oil and an oil drop in water. Motion of a drop was demonstrated for all three systems, a visible change in the apparent reflectance of the substrate was demonstrated using the water drop in air system, and the magnitude of induced motion was shown to have order of magnitude agreement with the simple perturbation model.

3.2 – Fluidic Pump for Surface Heat Transfer

During the course of the oil drop in water display investigation, a material evaluation apparatus was constructed. With some modification, the apparatus can be used to have sustained pumping of liquid along a surface, as described in section 2.2.1. This surface

flow can then be used to transport heat along the surface at a rate that substantially exceeds that of an equivalent copper plate, which may be desirable in many situations.

In many situations, it would be desirable to transport heat along a surface at a rate higher than is possible with conventional conductors. In principle, active transport of heat, such as forced convection, can transport heat at higher rates than passive mechanisms, like conduction, for similar sized systems. The work presented below introduces a novel fluidic pump and examines it in the context of actively transporting heat along a surface.

3.2.1 – Fluidic Pump Design

As discussed below, there were several design elements involved in making and testing a pump for the surface heat transport application. For this application, the pump needed both to be simple to manufacture, and to operate stably over long periods of time, since it is compared to a simple, solid piece of copper.

As described throughout this thesis, the fluidic pump is based on placing an oil drop, in a water background, on a heterogeneous solid where the contact lines are immobilized for a range of angles of contact. The drop is deformed by applying an inhomogeneous electric field, and pumping is induced by sequentially stepping this field along the drop. It was important to find materials for both the liquids and the heterogeneous surface which would have the appropriate physical properties. It was also important that the materials for the surface had the potential to be patterned in a relatively simple and automated manner. Designs of the electrode systems, used to apply the inhomogeneous field, that

would allow effective fluid pumping, minimize thermal resistance and minimize the complexity of the overall electrical system, are also discussed below

3.2.1.1 – Materials

As it was for the oil drop based reflective display, a big challenge for this system was finding materials that satisfied the requirements for the pump. When determining the types of liquids to use, several restrictions were used to select the candidate materials. The most important conditions were that the two liquids must be non-toxic, non-corrosive, immiscible and low viscosity fluids. The first two requirements were primarily to alleviate safety concerns, the low viscosity requirement was so the viscosity-limited flow rate could be maximized (see section 2.2.1.3) and the requirement of immiscible fluids ensured that there were two distinct liquid phases.

The materials used for the hydrophilic and hydrophobic surfaces also had several conditions upon them. The materials needed to be electrically insulating and it was crucial that the oil have a low contact angle with the hydrophobic material, and a high contact angle with the hydrophilic material. It was required that these solids be impermeable to the liquids, insoluble in the liquids and could not show significant swelling due to the liquids. The heterogeneous surface also needed to be made so that the solids would adhere well to each other and the patterning could be done using some easily automated technique, like printing.

Many material combinations were evaluated and several systems which fulfilled most of the conditions above were demonstrated. A system that satisfied all the conditions above used Dow Corning® OS-30 silicone fluid drop in distilled water. The hydrophilic substrate was made from Lee Filters lighting filters[32] and the hydrophobic regions were made from a wax-based ink[33] used in Xerox® Phaser™ solid ink printers.

Water was used for the electrically conductive liquid because it satisfied all the requirements, and preparation of the material was straightforward. A simple purification apparatus[34] first deionized then distilled water for use in the pump. It was found that the purified water was sufficiently conductive that good deformation of the oil-water interface could be induced without requiring enhancement of the electrical conductivity of the water. Attempts at enhancing the conductivity using simple ionic solutes (i.e. NaCl salt) failed to show any significant benefit, and perhaps more significantly, when the salt was present, the wetting properties and the amount of deformation that could be induced were found to degrade quickly over time.

Several candidate materials for the non-conductive fluid were tested, though Dow Corning® OS-30 silicone fluid[35] was selected for having an excellent combination of characteristics for the work presented. This liquid is rated by the manufacturer to have a low health hazard risk level,[36] density[37] of 850 kg m^{-3}, viscosity[38] of 1.5 cSt and heat capacity[39] of 1.72 J g^{-1} K^{-1}. The viscosity of the OS-30 was reasonably close to that of water, [40,41] which is 0.89 cSt. Under distilled water, OS-30 was found to have a receding

contact angle on the printed wax of 0-10°. In the same conditions, the oil was found to have a contact angle on the optical filter material of 110-120°.

The wax material was printed onto the optical filter material using a Xerox® Phaser™ 8200DP solid ink printer. The surface of the filter was roughened with 120 grit sandpaper before printing the wax to improve adhesion between the two solids.

Adhesion between the coating (in this case the printed wax) and underlying substrate (in this case the filter material) was tested using a simple scratch adhesion test. A small gauge needle[42] was ground to have a blunt tip. This tip was manually raked across the coating with varying amounts of pressure, and the resulting state of the coating was observed visually. Generally, good adhesion was observed if the coating would scratch with less force (i.e. before) delaminating from the other surface. It was found the wax coating was scratched with less force than was required to delaminate it from the roughened filter. Adhesion was first tested immediately after patterning the wax onto the filter material, and before exposing either material to the liquids. To further evaluate the durability of the patterned substrate, a pump was assembled and allowed to run for several hours each day for nearly five days. A scratch adhesion test was performed at the end of the soaking period with the liquids in place, and it was found that the wax still scratched before the two solids delaminated.

In addition to the adhesion test, there was no visible change in the volume of the oil drop over the duration of this soaking period, and the wetting behaviour of the drop did not

visibly change. This indicated that any swelling or dissolution of the two solids was negligible and that the solids were impermeable to the liquids.

The colouration of the optical filter film is a result of a proprietary coating of dyestuffs and lacquers. This coating was responsible for the wetting behaviour of the OS-30 silicone fluid on this material. Since this coating is proprietary to the manufacturer, only the commercially produced film thickness of 85 μm was available for the work presented. As discussed below, in some systems it might be desirable to be able to use different thicknesses of films. Standard plastic films, such as Mylar and PET plastic films, could be readily obtained in a variety of thicknesses, though they were not quite as hydrophilic as the filter material. A drop of OS-30 placed on their surfaces had a contact angle of 70-85°. In addition, when a scratch adhesion test was performed, it was found that the wax would delaminate off of these plastic surfaces with a similar amount of force as was necessary to scratch the wax. After about an hour in contact with the liquids, the hydrophobic tracks could be delaminated from the plastic films with less force than was necessary to scratch the wax. For the long pump systems, it was found that the wax would even delaminate when the OS-30 fluid was pumped using electrostatic pressure. This "spontaneous delamination" was only consistently observed in long pumps and not for short pumps.

This meant that the Mylar and PET films were not ideal, and in some cases (long track pumps) they were not appropriate either. However, these films had sufficiently good

properties that they could be used for specialized testing, like in short track pumps or in the oil drop in water proposed information display described in section 3.1.2.

3.2.1.2 – Pump Construction

As discussed above, the oil drop was restricted to move along the surface by patterning a track of hydrophobic material on a hydrophilic surface. For the surface heat transport application, the oil was used as a carrier to transport the heat, so the track was shaped into a simple closed loop; an oval shape in the work presented. The oval shape shown in Figure 3.10 was chosen so that the curvature of the track would be sufficiently small that it would be insignificant compared to the maximum curvature of the oil-water interface. This shape also had the advantage that it was straight-forward to design patterned electrodes that could drive multiple concentric tracks. Definitions of relevant dimensions for this geometry are shown in Figure 3.10.

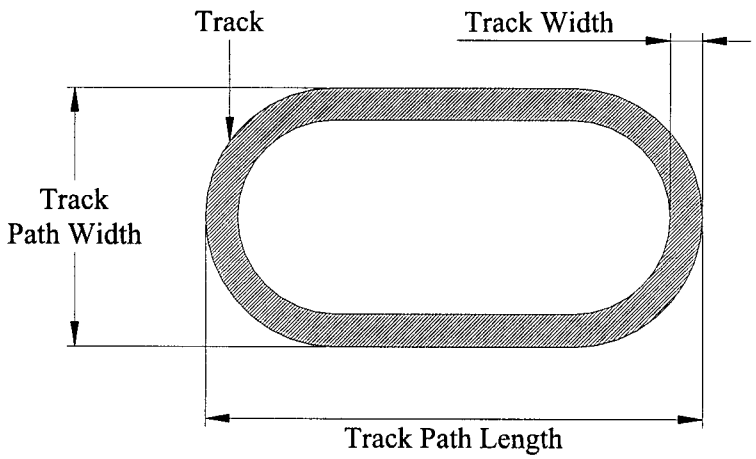

Figure 3.10 – Top-view of sample track with dimension terminology defined

The tracks were designed to have a constant track width of 2 mm around the loop. This width was chosen so that the drop was as large as possible without observing distortion due to the oil's buoyancy. As discussed in the preceding chapter, using equation (2.11), the over-pressure due to the curvature of the oil-water interface was estimated to be typically on the order of 50 Pa. This estimation ignores the curvature of the track and assumes that the drop has a cylindrical cap shape. This assumption is reasonable because the typical radius of the cylindrical cap was more than an order of magnitude smaller than the radius of curvature of the curved track segments.

In the work presented, there were two sizes of pumps examined, a short track pump and a long track pump. Both pumps had a track path width of 2 cm wide. The difference between the two was the track path length, which was 3.6 cm long for short tracks and 23.2 cm long for long tracks. As discussed below, these two length tracks were chosen for convenience. In principle, the track paths could be nearly arbitrarily long or wide. In a device which had multiple concentric tracks, the track path widths and lengths were different for each track, so it is convenient to refer to the dimensions of the outermost track when discussing multiple concentric track systems.

One major concern in the assembly of the pump systems was avoiding "bulges" in the oil. For the tracks described above, the oil drop spreads evenly along the length of the tracks when there are no fields applied. A bulge was defined to be when excess liquid accumulated along a section the track. Because the contact lines were immobilized, a

bulge would tend to remain confined on the track, though the angle of contact in the bulging region would increase as the volume of oil in the region increased.

Bulges were undesirable since the bulge increased the effective gap and therefore decreased the field across the bulging region. This reduced the force exerted by the water in the bulge regions, and so the oil tended not to be pushed out of these regions. In some cases a bulge would reach a state where the amount of liquid pumped in would be equal to or less than the amount of liquid pumped out. These bulges tended to be transient and not considered a problem. Bulges in which more liquid was pumped in than out were observed more frequently. When they became sufficiently large, one of two failure modes would tend to occur. If the angle of contact exceeded the natural contact angle of the oil on the hydrophilic surface, the oil would tend to spread onto the hydrophilic surface. Once this occurred, wetting angle hysteresis on the hydrophilic surface prevented restoring the pump to the original condition without removing a relatively large fraction of the oil from the device.

The OS-30 oil in water had a sufficiently high contact angle on the optical filter material that this spreading of the bulges of oil onto the hydrophilic material tended not to be the major failure mode. Instead, when the volume in a bulge became too large, a drop of oil would detach from the bulge and float to the surface of the water, leaving the track still wetted with oil. In this case, getting the system back to original conditions simply required adding more oil on the track to replace the volume which was lost.

Bulges in the oil drop could be formed a number of ways, though in most cases it was because of variations in the electric field applied by the driving electrodes. As discussed below, this variation was due to irregularities of the lamination of the substrate film to the electrodes. In principle, it should be possible to eliminate any significant variation of the gap thickness between the electrodes and the heterogeneous solid surface using a variety of methods. One such method could involve metallizing and printing the electrodes directly on the back of the substrate film. This method was not practical for the preliminary design work presented here since both the electrode design and the substrate materials were variable. Instead, a more modular design was used to facilitate development. The electrodes were printed on single-sided circuit boards or metallized plastic films that could be reused with many substrate samples. The design of the electrode systems is discussed in section 3.2.1.3.

Because of this modular design, a thin adhesive layer was used to laminate the substrate to the electrodes. For short tracks, a thin layer of olive oil had a sufficiently high surface tension to act as the adhesive and keep the gap between the water and electrodes constant. For long systems, the surface tension of olive oil was not sufficient, so a polymer based spray adhesive[43] was used.

The spray adhesive was applied to the electrodes as an aerosol spray. The spray deposited a relatively uniform layer of polymer droplets on the electrode surface. The patterned substrate film was then aligned and placed on top, bonding it weakly to the electrodes. The spray adhesive was useful because the bond was sufficiently weak that

the film and the electrodes could be peeled apart with minimal force, yet it was sufficiently strong that the layers did not slide relative to one another. Despite these advantages, this choice of adhesives was not ideal. While the overall uniformity of the adhesive layer was reasonably good, occasionally a relatively large polymer droplet would be deposited which would increase the gap thickness at that point. For testing purposes, most of such droplets were removed manually from the layer. That left relatively uniform thickness layers that were about 100 microns thick, but the fractional area covered by polymer tended to be low, about 20% polymer. This meant there was a large fraction, about 80%, of the layer which was air; resulting in a very low thermal conductance for the layer.

It is likely that the issue of low thermal conductance could have been avoided by using an adhesive that was applied as a liquid, such as an epoxy, or by using sheets of solid adhesive. It is also expected that these adhesives would allow the production of a more uniform thickness adhesive layer than is possible with the spray adhesive. However, both the liquid adhesive and the solid adhesive sheets had associated challenges that had to be overcome to make them practical for the prototyping work presented. Thus, time constraints prevented significant exploration of either option.

3.2.1.3 – Electrode Design, Control and Manufacture

As described throughout this thesis, an oil drop in a water background was pumped along a heterogeneous surface using a patterned set of electrodes to apply a time-varying inhomogeneous electric field. The water displaces the oil in the high field regions, so by

stepping these high field regions along the surface, the oil can be pumped in specified direction. As described above, the magnitude of the fields needs to be the same in these high field regions to avoid formation of bulges in the oil while the pump is running. It should be noted that since it is the magnitude of the field which determines the amount of deformation, the gap thickness between the electrodes and the heterogeneous surface could, in principle, be different over each electrode. All that would be needed is that different voltages were applied to each electrode to compensate for these gap variations.

An easier solution is to keep the gap between the electrodes and the heterogeneous surface the same for all of the electrodes. In this case, a potential difference, V, between the water and an electrode always gives the same magnitude field regardless of which electrode is considered. Obtaining a uniform gap was simplified by keeping the electrode sets in a single, planar layer of conductive material. This also helped simplify production of the electrodes and the power supply needed to use them, as described below.

In addition to this single-layer constraint, there were many features that were required from the electrode systems. The electrode systems were designed to provide reliable pumping on multiple concentric tracks. The electrodes themselves and the power supply driving them were created to demonstrate that the overall cost and complexity of the system had the potential to be kept minimal. The actual power supply built was more complex than absolutely necessary; it used a microprocessor based controller to regulate the timing and sequence in which the field stepped along the hydrophobic tracks. This

approach of having a flexible controller was used so that the fluid flow rates used for heat transport could be specified. Since the fluidic pump was used for heat transport applications, simple manufacturing techniques were also demonstrated that could allow the electrode systems to be made with low thermal resistance.

Due to limitations of the equipment available, it was not possible to optimize both the design of the electrode set and the thermal resistance of the entire pump. As discussed below, these are not fundamental limitations, and so in principle, they could be overcome by using different equipment or techniques.

3.2.1.3.a – Electrode Design Requirements

One of the primary requirements when designing the pump for the surface heat transfer application was that the pump should have the potential to be made readily and inexpensively. To this end, all the electrode designs were made in a single layer of conductive material, such as a single-sided printed circuit board or a metallized plastic film. Besides making manufacturing the electrodes very simple, keeping all the electrodes on one layer had the benefit that the gap between the electrodes and the water could easily be made the same for all the electrodes. This provided flexibility for the design of the power supply since one voltage could be used to generate the same magnitude field regardless of which electrodes are used.

The electrodes were made so that a field applied by a single electrode would be uniform across the width of a track. This way, when the oil-water interface was deformed using

an electric field, the oil would be forced to flow along the length of the track since the contact lines were immobilized at the track edges. In principle, the liquid would be free to flow in either direction along the track, so to unambiguously pump the liquid in one direction, a minimum of three independent, adjacent electrodes are needed to step the high field regions along the track path.

Another major requirement for the pumps was that the expected achievable fluid flow rate should be maximized. Looking at the modified Hagen-Poiseuille's relation in equation (2.16), it is apparent that the flow rate can be increased by keeping the tube length short for a given pumping pressure, i.e. for a given magnitude electric field. In the pump system, the tube length is the distance over which the fluid has to travel after the electric field pattern changes. This means that the tube length is just the center to center distance between adjacent electrodes. The system can be viewed as series of tubes, each of which could have different lengths. Over a region with no electrodes, the tube length becomes long as compared to a region where the electrodes are closely packed together. These regions with few electrodes offer more resistance to flow, so by eliminating any regions with no electrodes, the longest tube length can be minimized and thus the expected upper bound on achievable flow rates can be maximized. Since the flow rate must be the same around the track for stable fluid flow, viscosity limits would be imposed by the longest tube length. This can be minimized by keeping the center to center distances between electrodes relatively uniform around the track, meaning the individual electrodes should be about the same size as each other. There is some

flexibility in this restriction since some variation in the electrode size is necessary when going around curves in order to keep the electrodes as close together as possible.

Three major restrictions on the widths of the electrodes (measured along the length of the track) were found to be necessary in order to get consistent motion. One was that the width of individual electrodes had to be large compared to the separation between adjacent electrodes. At the same time, the width of the electrodes needed to be smaller than the width of the hydrophobic tracks. The minimum reproducible electrode separation that could be achieved with the production techniques used was about 250 microns. It was found that 1 mm wide electrodes were wide enough for this electrode separation to be considered small. Moving to wider electrodes resulted in longer tube lengths without any significant benefit to the pumping.

Figure 3.11 shows a track superimposed on a basic arrangement of electrodes which could support multiple concentric tracks and which satisfied the design requirements listed above.

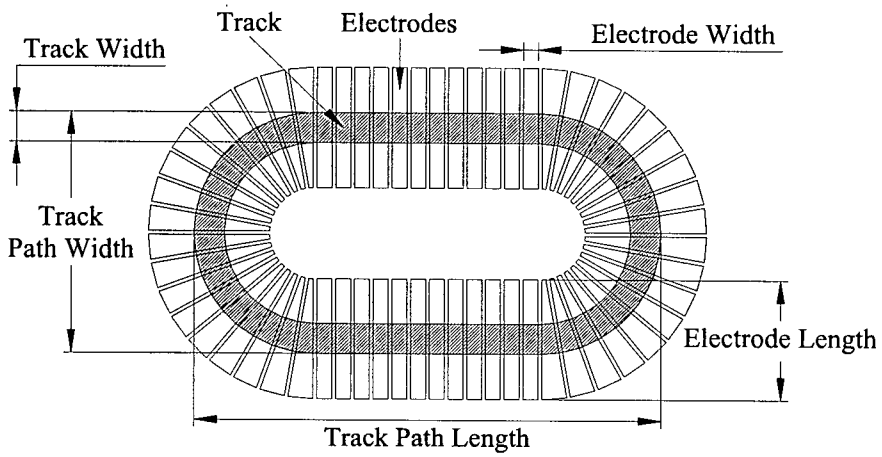

Figure 3.11 – Basic electrode layout with a track superimposed

3.2.1.3.b – Basic Electrode Design

A time-dependent, patterned electric field that moves in a distinct direction can be generated from a minimum of three independent neighbouring electrodes, designated A, B and C. As is described above, there were electrodes all along the path, but they could be just repeating sets of those three neighbouring electrodes, so long as the order, as established in Figure 3.12, is maintained.

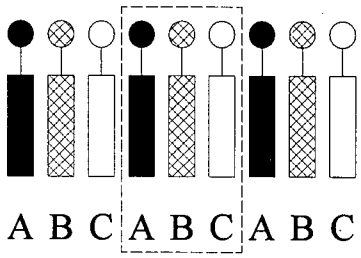

Figure 3.12 – Repeating unit for simple electrode control.
Circles above rectangular electrodes indicate connection points
for electrode systems with a single conductive layer.

By sequentially applying the field to the A, B and C electrode types and then repeating the sequence, the electric field steps unambiguously in one direction. The bulk effect is that the oil tends to be pushed in the same direction as the field sequence. Table 3-2 illustrates how the field propagates along the track in a specified direction. In the table, the water is held at a reference potential, while "~" denotes that a non-zero potential is applied to the electrode and "0" denotes that the electrode is shorted with the water.

Table 3-2 – Potential of electrodes with respect to time in ABC electrode design

	Electrode					
Step	A	B	C	A	B	C
1	~	0	0	~	0	0
2	0	~	0	0	~	0
3	0	0	~	0	0	~
4	~	0	0	~	0	0

Because the electrodes were restricted to be in a single layer, the repeating ABC design could not be printed directly. Instead, independent electrodes needed to be printed in single layer, and the electrodes of the same type could be connected externally; possibly by using soldered wires to connect them. This means that the number of connections that

need to be made after printing the electrodes is proportional to the number of electrodes desired, as can be seen in Figure 3.13. It should be noted that it is possible to connect all the electrodes of two of the electrode types within the single conductive layer. However, the electrodes of the third type all need to be connected outside the plane, thus requiring the number of external connections to be proportional to the total number of electrodes.

The electrodes shown in Figure 3.13 were the basis for several electrode systems that were demonstrated successfully. As can be seen, the electrodes in the curved portions are wedge shaped to keep the gap widths constant. This means that the electrode widths in the curves varied slightly, though on average they were the same width as in the straight sections.

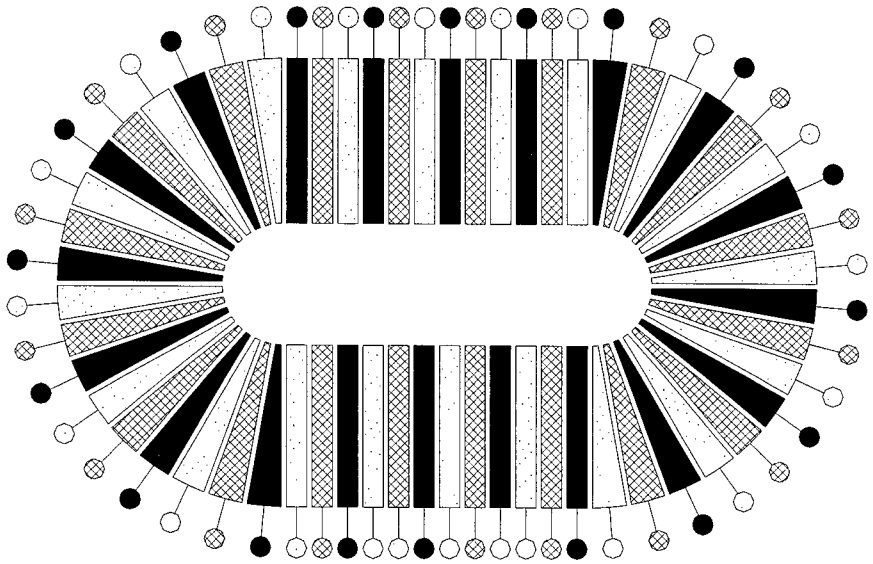

Figure 3.13 – Simple electrode design for fluidic pump

Circles indicate possible connection points for electrode systems printed in a single conductive layer. With alternate designs of the lead wires, the total number of connection points can be reduced, though in any design of the simple ABC repeating pattern, the total number of required connection points scales linearly with the number of electrodes (see text).

3.2.1.3.c – Scale-Invariant Electrode System

The ABC design is simple and can be produced using a variety of printing techniques, as discussed in the following section. However, the system can not be extended easily to an arbitrary number of electrode repeat units. In a single layer, the number of connections needed to be made outside that layer grows linearly with the number of electrodes in the system. Two types of electrodes can be interleaved on a single-sided circuit board, each with only one connection to the power supply. In that same layer, it is not possible to add a third type of electrode between the other two in a way that both maintains the ABC ordering asymmetry and only has one connection out of the layer (the one to the power

supply). The additional connections mean that the cost and complexity of increasing the total number of electrodes can become prohibitive for large systems.

If the requirement for an asymmetric, e.g. ABC, electrode ordering is relaxed, using the ABCB repeating unit offers the ability to have only one connection per electrode type for an arbitrary number of repetitions around the loop. This configuration is shown schematically in Figure 3.14. An equivalent repeat unit can be made with ABCCBA type electrodes.

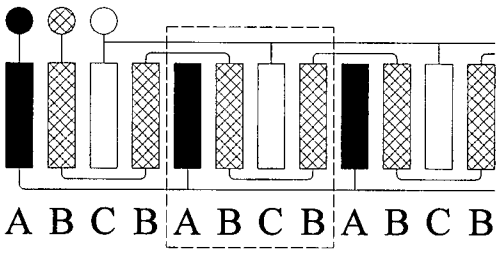

Figure 3.14 – Symmetric repeat unit for a scale-invariance
Circles indicate required connection points for electrodes printed
in a single layer of conductive material

If the electrodes are all equal width, as drawn in Figure 3.14, the repeating ABCB pattern is symmetric around the A and C electrodes. This means that there is no time-dependent pattern of voltages that would result in an unambiguous single direction for the fluid motion. An example of such a pattern is shown in Table 3-3.

Table 3-3 – Potential of electrodes with respect to time for ABCB electrode design

	Electrode								
Step	A	B	C	B	A	B	C	B	A
1	~	0	0	0	~	0	0	0	~
2	0	~	0	~	0	~	0	~	0
3	0	0	~	0	0	0	~	0	0
4	~	0	0	0	~	0	0	0	~
5	0	~	0	~	0	~	0	~	0
6	0	0	~	0	0	0	~	0	0

An asymmetry can be introduced by making the first A, B and C electrodes relatively wide and the second B electrode extremely narrow. For convenience a prime is added to the electrode type to indicate that it is a narrow electrode. The B' electrode can be made sufficiently narrow that it will not cause a significant deformation to the drop. This pattern is shown schematically in Figure 3.15. By introducing an asymmetry in the widths of the electrodes, the net effect is that the electrodes which cause a significant deformation have the simple ABC repeating pattern needed for unambiguous directional motion. At the same time, the pattern can be printed in a single layer of conductive material with only a constant number of connections to the power supply for an arbitrary total number of electrodes.

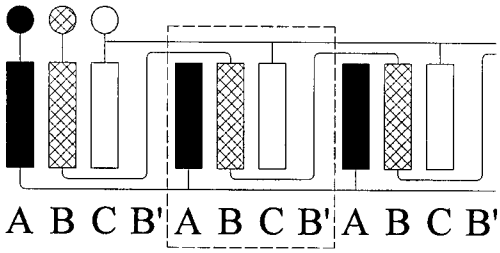

Figure 3.15 – Repeating unit for a scale-invariant electrode design

Circles indicate required connection points for electrodes printed

in a single layer of conductive material.

An example of an electrode system with the ABCB' configuration can be seen in Figure 3.16. Here the gaps between electrodes are 250 μm wide while the B' electrodes are 180 μm wide. The A, B and C electrodes are, on average, 1 mm wide. It was found that with these dimensions, there was no visible deformation of an oil-water interface due to the B' electrodes.

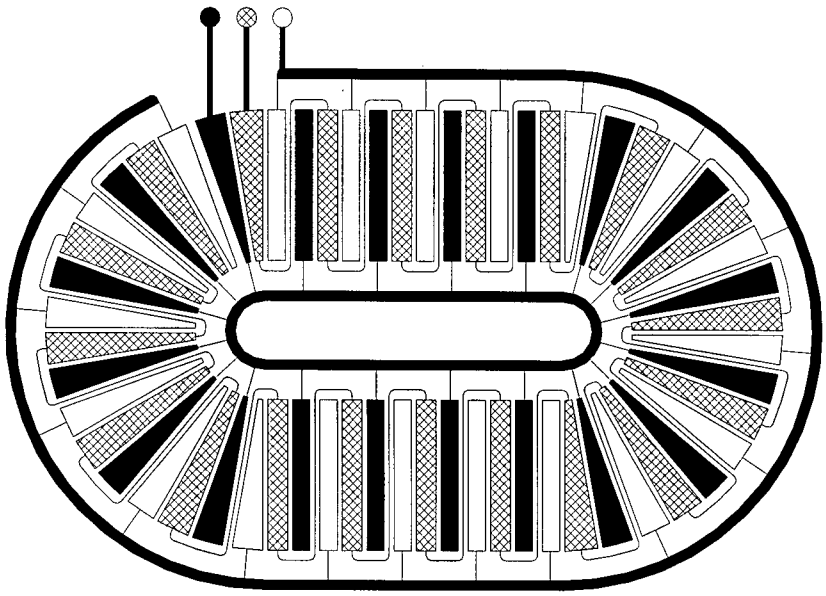

Figure 3.16 – Sample scale-invariant electrode design

Circles indicate required connection points for electrodes printed

in a single layer of conductive material.

3.2.1.3.d – Electrode System Production

The electrodes were made using automated patterning techniques like those used for standard printed circuit boards. This satisfied the requirement that the electrodes could be made quickly, inexpensively and accurately in a mass-manufacturing situation. The patterning techniques also facilitated getting an even surface for all the electrodes. Having an even surface for the electrodes was important so that when the thin substrate was laminated onto the electrodes, the gap thickness between each of the electrodes and the background water was the same for all the electrodes. With a constant gap thickness above each electrode, the magnitudes of the fields produced were similar and therefore similar deformation pressures could be induced around the loop.

Electrode systems were made using both standard copper-clad printed circuit boards (PCBs) and aluminized Mylar. In both cases, a layer of metal was supported on an insulating laminate. The PCBs had a 30 micron thick layer of copper on 1.5 mm thick glass-epoxy, while the aluminized Mylar had a layer of aluminium less than 1 micron thick on 120 micron thick Mylar. In principle, any metallized plastic film could be used, so the electrode systems could be made very thin. This means that the electrode system could have low thermal resistance. The aluminized Mylar system was produced to demonstrate the possibility of using metallized films instead of circuit boards.

The aluminized Mylar itself was produced by depositing aluminium on Mylar using standard vapour deposition techniques. The Mylar was double-metallized, which means that two layers of aluminium were deposited on top of each other to minimize microcracks and pinholes. Microcracks and pinholes can interfere with the electrical conductivity of the aluminium layer since they tend to introduce breaks in printed wires and electrodes.[44] Double-metallization also helped to increase the durability of the aluminium layer so that small scratches during the printing and etching stages were less likely to affect the electrical conductivity of the wires and electrodes in the final system.

The aluminized Mylar film was prepared for etching by printing the etch mask directly onto the aluminium surface using a Xerox® Phaser™ 8200DP solid ink printer. The printer deposited a wax image of the electrodes directly on the aluminium. The exposed aluminium was etched away with a solution[45] of phosphoric and nitric acid. After

etching, the wax mask was removed with paraffin oil leaving the aluminium electrodes on the Mylar backing. Electrode systems with 60 electrodes and the ABC electrode pattern were printed in this manner for use with the short track system.

The technique detailed above worked well for the simple ABC electrode system, though it was not possible to print the scale-invariant design with the equipment available. The 8200DP printer showed significant moiré effects when printing details smaller than about 200 μm. The B' electrodes of the scale-invariant electrodes were approximately 180 μm wide, and therefore required higher resolution printing. The etch mask could have been made using other techniques, including photolithography, to print the scale-invariant design on the aluminized Mylar, but these options were not explored due to time constraints.

Electrode systems using both the ABC and scale-invariant designs were produced using commercially available copper-clad circuit boards.[46] The boards came presensitized with a positive photoresist allowing the etch mask to be made by photolithography. To print a board, a positive image of the electrode system was printed on a transparency to act as the photomask. The transparency was placed on the presensitized board and the board was exposed under a UV light source. The exposed photoresist was then removed by placing the exposed board in a dilute NaOH developer solution, leaving an image of the electrodes in the photoresist. The bare copper was then removed using a ferric chloride etching solution. The remaining photoresist was removed using ethanol.

The photolithography method detailed above allowed higher resolution features to be printed than the wax method used for the aluminized Mylar electrodes. The choice of printers used to make the photomask transparency was less limited. Standard consumer level laser printers were found to be unable to print reliably on the aluminium surface, but could print well on a transparency. A Hewlett-Packard® 1000 Series laser printer had sufficient resolution to print a photomask for both the ABC and ABCB' electrode systems. Short track systems, with 60 electrodes each, were printed using both the simple ABC pattern and the scale-invariant design. The ABCB' design was also used to print a long track electrode system with 372 electrodes.

3.2.1.3.e – Power Supply

Both the ABC and the ABCB' electrode systems described above were designed and constructed to drive fluid flow by independently applying a voltage to each of three independent electrode types relative to the water background. AC voltages were used to avoid the charge build-up effects that have been observed in conventional electrowetting systems.[47]

It was possible to use AC fields since the deformation of the oil-water interface in the pump is independent of the polarity of the applied field, as shown in equation (2.7). Although low frequency AC fields were used, the deformation of the oil-water interface did not appear follow the sinusoidal signal. It appeared that the deformation was in response to the average applied field, i.e. the root mean square (RMS) field. It is,

therefore, reasonable to quote values for AC voltages and fields using their root mean square (RMS) values. This is the convention used below.

The state of the electrode types was specified to either be in a *high* state, where a potential difference was applied between the electrode and the water background, or a *low* state, where the electrode was at the same potential as the water. This nomenclature is convenient, even though AC potentials were used. As the nomenclature suggests, there were only two states for the electrodes, and so the state of a given type of electrode could be completely specified using a single logical bit.

Given that all the electrodes were in one layer, equal voltages were required on each electrode to produce fields with equal magnitude. Electric field magnitudes on the order of 10^6 V m^{-1} were required to fully deform the oil-water interface. With the materials used, the gap between the water and the electrodes was between 0.2 mm and 0.3 mm, so this order of magnitude field could be produced by applying a potential difference of approximately 300 V.

A power supply was built that could output up to 320 V_{rms} at 60 Hz on three output channels. A common terminal was connected to the water, and the three output channels were each connected to an electrode type. The supply was built so that the output channels could be switched between 320 V_{rms} or 0 V_{rms}, relative to the common terminal, using digital logic circuitry, i.e. using +5 V_{DC} or 0 V_{DC} respectively. Switching the outputs between states was limited to occur at the zero crossings of the AC voltage, so

the maximum switching frequency was 120 Hz. Further details of the power supply can be found in Appendix C.

The ability to switch the state of the high voltage output channels using digital logic was chosen so the field patterns and timing between stepping the patterns along the track could easily controlled. A Motorola MC9S12DP256B microprocessor was used as a basis for the controller used for testing purposes. The microprocessor allowed the pumping parameters to be adjusted quickly and safely while the pump was running. The microprocessor's timing was synchronized to the high voltage zero-crossings using a zero-crossing detection feedback circuit. The details of the peripheral circuitry and the microprocessor programming can be found in Appendix D.

3.2.2 – Heat Transfer

With the pump designed and built, it was possible to investigate heat transfer along a surface using forced convection. There are three primary mechanisms for heat transfer; conduction, convection and radiation. At temperatures around room temperature, conduction and convection are typically the most important heat transport mechanisms, and so radiation is ignored in this discussion. Conduction transfers heat by collisions, while convection transfers heat by the large-scale motion of fluid.[48] Conduction tends to be the most important mechanism for heat transport in solids, especially in metals like aluminium or copper. Convection transports heat through the bulk motion of a material, typically some fluid, and in principle, a system using forced convection could transport heat at a substantially higher rate than is possible with conventional conductors.

In the discussion below, a simple estimate of the rate of heat transport by forced convection is derived, conduction in a solid is reviewed and a metric, which is independent of the heat transfer mechanism, for comparing the capability of a device to transport heat is described.

3.2.2.1 – Rate of Heat Transfer

The fluidic pump described throughout this thesis was examined in the context of the possibility of using it to transport heat along a surface. In order to estimate if this application of the pump is reasonable, it is necessary to consider a simple model of how much heat could be transported by the moving oil. However, because heat can be transported very easily by a simple uniform plate of copper, the fluidic pump is compared to an equivalently sized, uniform plate of copper.

When discussing the rate of heat transport, there must be some sort of temperature gradient in the system in question. For this work, this temperature gradient is between two thermal reservoirs, one at temperature T_1 and the other at temperature T_2, separated by some distance, l. In the discussion here, both the fluidic pump and the plate of copper provided the only significant heat transport pathway between the two reservoirs.

To model the rate at which heat can be transported by the fluidic pump using forced convection, it was assumed that liquid near a thermal reservoir would come into thermal equilibrium with that reservoir. In this mode, the rate of heat transfer, H, is proportional

to the mass flow rate, the specific heat capacity, c, of the liquid and the difference in temperature, ΔT, between the heat source and the heat sink. This relationship is shown in equation (3.1).

$$H = (\text{mass flow rate}) \times c \times \Delta T \tag{3.1}$$

In contrast, the rate at which heat can be conducted through a particular material can be characterized by the material's thermal conductivity, K. This constant is independent of the geometry of the material and is proportional to the rate of heat transfer through a particular sample. For a uniform plate of material, the rate of heat transfer, H, via conduction is given by[49]:

$$H = KA\left|\frac{dT}{dx}\right| \tag{3.2}$$

where A is the cross-sectional area (with the normal parallel to the direction of heat flow) of the plate and $|dT/dx|$ is the temperature gradient along the plate. In the case where the ends of a uniform plate of length l are held at constant temperatures, T_1 and T_2, the gradient becomes uniform and equation (3.2) can be written,

$$H = \frac{KA}{l}\Delta T \tag{3.3}$$

To compare systems that heat transfer by either convection or conduction, it is convenient to find a quantity which is representative of the system in question, and independent of the details of the measurement setup. This can be thought of as an analogue of the thermal conductivity, K, which is characteristic of the material and independent of the sample shape. When comparing these two different heat transport mechanisms, it is not possible to ignore the geometry of the particular system in question. It is, however, possible to ignore the temperature gradient used in a particular measurement. As can be seen from equations (3.1) and (3.3), both models of the rate of heat transfer are proportional to the temperature difference between the two thermal reservoirs. This means that the constant of proportionality is a convenient measure to compare the two mechanisms. In this discussion, this constant of proportionality is termed *thermal conductance*, k, as opposed to the *thermal conductivity*, K. The thermal conductance is measured in Watts per Kelvin whereas the thermal conductivity is measured in Watts per meter per Kelvin. It should be noted that for the conduction mechanism, the constant termed thermal conductance is just the reciprocal of the more commonly defined *thermal resistance*.[50]

3.2.2.2 – Thermal Conductance Models

As discussed in the preceding section, the fluidic pump and a uniform copper plate are compared using their thermal conductances (defined above), which describes the capability of a particular system to transport heat, independently of the heat transport mechanism. From equation (3.3), the thermal conductance for conduction through a uniform plate is given by:

$$k = \frac{KA}{l} \tag{3.4}$$

Similarly, the model of forced convection in equation (3.1) yields a thermal conductance given by:

$$k_r = (\text{mass flow rate}) \times \text{c} \tag{3.5}$$

In terms of calculable or known variables, the thermal conductance due to the movement of the oil can be written,

$$k_{r,oil} = \underbrace{(v_{lin} A_{XS} \rho_{oil})}_{\text{mass flow rate}} \times c_{oil} \tag{3.6}$$

where v_{lin} is the linear velocity of the fluid from equation (2.15) or (2.17) , A_{XS} is the cross-sectional area of the drop from equation (2.14), ρ_{oil} and c_{oil} are the density and specific heat capacity of the oil respectively.

The model shown in equation (3.6) only models the conductance due to moving oil. It was observed that when the oil was being pumped, some water was entrained and so there was net flow of the water as well. The velocity at which the water moves and volume of water that moves are not known nor are they easily estimated based on the work presented in this thesis. As a result, for the purposes of this work, the volume flow

rate of water is assumed to be some fraction, f_{water}, of that of the oil. The volume flow fraction was estimated by fitting. Since the two mechanisms transport heat in parallel, their conductances add, so the total thermal conductance due to forced movement of liquid is given by,

$$k_{r,Total} = v_{lin} A_{XS} \left(\rho_{oil} c_{oil} + f_{water} \rho_{water} c_{water} \right) \tag{3.7}$$

3.2.2.3 – Input and output resistance

In the discussion above, it was implicitly assumed that heat could flow directly between the heat transfer medium (oil and water or copper), and the thermal reservoirs. This is equivalent to having the heat transport medium in direct contact with the thermal reservoirs. While this could be done practically for a plate of copper, the oil in the pump had to be separated by some material from the reservoirs.

Since the pump was being evaluated in the context of surface heat transport, it is assumed that the thermal reservoirs exist in a single plane and are relatively large. This assumption means that if the reservoirs were in contact with the oil, there would have been significant contact lines of the oil on the reservoirs' surfaces which could move. Moving contact lines could have caused additional friction and could have disrupted the oil flow. With this restriction, heat can be injected into the oil from two directions with relative ease. One is by placing the heat source and heat sink in the background water near the oil-water interface, as shown in Figure 3.17-a. The other is by placing the

thermal reservoirs under the pump substructure, which includes the electrodes and the heterogeneous substrate, as shown in Figure 3.17-b.

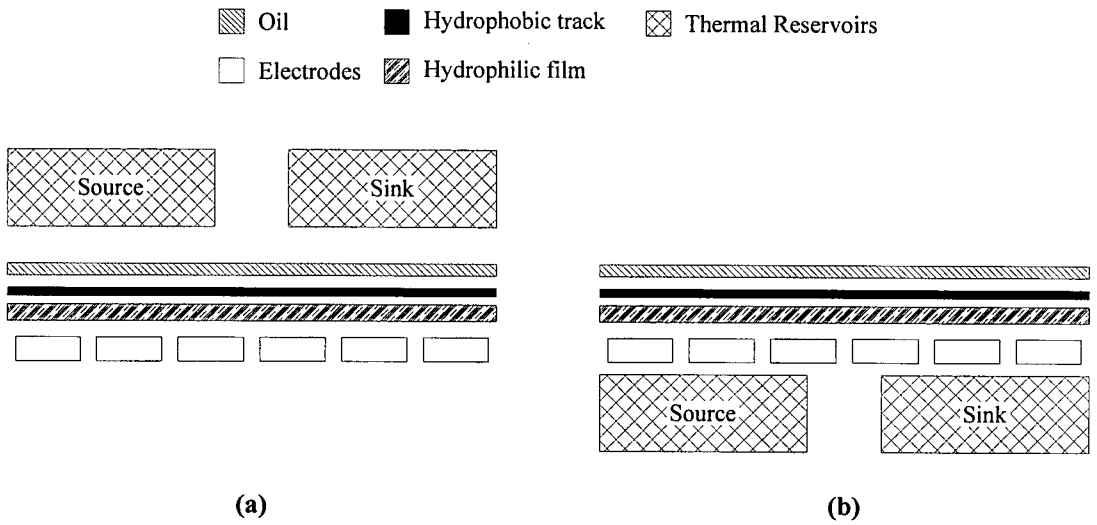

Figure 3.17 – Cross-sectional view of fluidic pump with thermal reservoirs sketched with reservoirs (a) in water and (b) below pump substructure. (Not to scale)

When the reservoirs are placed in the water, they must be kept a minimum distance away from the oil to avoid a phenomenon known as *snap-down*. Snap-down is said to have occurred when the oil-water interface spontaneously jumps onto a nearby foreign surface. In typical pump systems, snap-down tended to occur if the foreign surface was placed within about 250 to 500 μm from the oil drop. Since the reservoirs had to kept outside this range, If the reservoirs are kept far enough away from the surface so that snap-down does not occur, then there is a layer of water between the oil and the reservoir. The heat must flow through the water before being transported by the rotating oil. Assuming the water to be stationary, the thermal conductance of the moving oil pathway becomes,

$$k_{r,meas} = \left[\frac{d_{water}}{K_{water}} \left(\frac{1}{A_{source}} + \frac{1}{A_{sink}} \right) + \frac{1}{k_r} \right]^{-1} \quad \textbf{(3.8)}$$

where d_{water} is the separation between the oil-water interface and the thermal reservoirs, K_{water} is the thermal conductivity of the stationary water, A_i is the projected area of the oil onto the thermal reservoir, and k_r is the conductance of the moving oil, as given by equation (3.6).

As discussed in the previous section, some water is entrained with the moving oil. Thus there are two significant heat transfer pathways; one through the moving oil with a layer of water acting as thermal resistors in series and the other through convection of the entrained water. A model including both pathways would be overly complex and difficult to verify in this case.

The water conduction pathway can be effectively eliminated by injecting the heat through the pump substructure. A cross-section of the resulting structure is sketched in Figure 3.18.

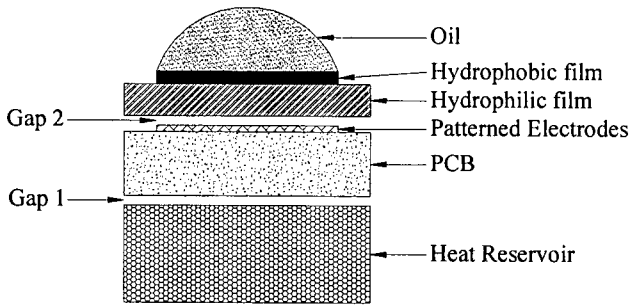

Figure 3.18 – Cross-sectional schematic of pump with heat reservoir

With this design, the heat is transferred to and from the oil through solid layers rather than through a moving liquid layer. The heat transferred due to forced convection of the entrained water is still important, but conduction through the water is no longer important and can be ignored. In this case, it is reasonable to treat the water movement pathway as being in parallel with pathway due to the oil movement, as shown in equation (3.7). It should be noted that conduction through the oil does not need to be considered for the water convection pathway. This is because the oil was squeezed out of the high field regions by the water, allowing the water to get sufficiently close to being in direct contact with the track that heat could be injected into the water convection pathway while bypassing conduction through the oil.

With the thermal reservoirs below the pump substructure, there are a number of insulating layers between the reservoirs and the liquids, as is shown in Figure 3.18. The primary mechanism for heat transfer through each of the layers is conduction, so the thermal conductance of the pump substructure is given by,

$$k_j = A_j \left(\frac{d_{Gap1}}{K_{Gap1}} + \frac{d_{PCB}}{K_{PCB}} + \frac{d_{Electrode}}{K_{Electrode}} + \frac{d_{Gap2}}{K_{Gap2}} + \frac{d_{Substrate}}{K_{Substrate}} + \frac{d_{Track}}{K_{Track}} \right)^{-1} \quad \textbf{(3.9)}$$

where the d_i and K_i are the thickness and bulk thermal conductivity of each layer respectively. Here, A_j is the area of tracks nearest to the thermal reservoirs. The subscript on the area and total thermal conductance is to distinguish the conductance over the source from that over the sink since the areas for the two could be different.

In all, the expected measurable thermal conductance of a real pump is given by,

$$k_{meas.;rot.} = \left[\frac{1}{k_{source}} + \frac{1}{k_{sink}} + \frac{1}{k_r} \right]^{-1} \quad \textbf{(3.10)}$$

where k_r is given by equation (3.7) and k_{source} and k_{sink} are from equation (3.9). The areas of the heat source and heat sink were estimated using the area of the oil immediately above the respective thermal reservoir.

As described below, the materials used for the pump substructure presented in this thesis were not optimized to maximize their thermal conductance due to time constraints. Such optimizations could be as simple as using thinner films of the same materials. This means that in order to make a reasonable comparison of forced convection and conduction, the copper was similarly placed in series with the pump substructure. Therefore, the measured copper conductance would be,

$$k_{meas.,copper} = \left[\frac{1}{k_{source}} + \frac{1}{k_{sink}} + \frac{1}{k_{Cu}} \right]^{-1} \quad \textbf{(3.11)}$$

where k_{Cu} is given by equation (3.4).

3.2.2.4 – Measurement Technique

Thermal conductance was measured by applying heat a known rate, $H_{Applied}$, to a heat source and measuring the temperature difference, ΔT, between the source and a heat sink. Once the temperature difference reached a steady-state, the total conductance of the system was given by,

$$k_{Total} = \frac{H_{Applied}}{\Delta T} \quad \textbf{(3.12)}$$

When performing a measurement of thermal conductance using a real measurement device, there are usually several parallel thermal transfer pathways besides the pathway of interest. When the rate of heat transport for each of the pathways varies linearly with temperature, thermal conductance adds for parallel pathways, as shown in equation (3.13).

$$k_{parallel} = k_1 + k_2 + k_3 + \ldots \quad \textbf{(3.13)}$$

In this case, any of systemic heat transport pathways can be treated as constant offsets to the measurement of the desired pathway. When measuring the conductance of the moving liquid, the effect of these systematic pathways could be effectively ignored by measuring the baseline conductance with the pump in place but not pumping liquid and subtracting that from the measured conductance when liquid was being pumped.

When using this linearity assumption, the actual magnitude of the temperature difference between the thermal reservoirs does not affect the measured conductance. In this case, the conductance of the pump with the oil moving and not moving can both be measured while keeping the rate at which heat is applied constant. With this method, the conductance of the moving fluid pathway is given by:

$$k_{move} = H_{applied}\left(\frac{1}{\Delta T_{move}} - \frac{1}{\Delta T_{stop}}\right) \qquad \textbf{(3.14)}$$

Although this measurement technique is relatively fast, the assumption that conductance adds for parallel pathways, equation (3.13), is only strictly true if there are no heat transport pathways whose rates of heat transport vary non-linearly with temperature. If some of the significant systematic heat transport pathways are non-linear, the pathways can be marginalized by adjusting the rate at which heat is injected into the system so that ΔT is the same for both when the liquid is being pumped and when it is not being pumped. The difference in the rates of heat injection needed to keep ΔT constant is

assumed to be the rate at which heat is transferred by the moving liquid pathway. In this case, the thermal conductance due the moving liquid pathway, k_{move}, is given by,

$$k_{move} = \frac{H_{move} - H_{stop}}{\Delta T} \tag{3.15}$$

where H_{move} and H_{stop} were the rates at which heat is applied to give a temperature difference of ΔT with the liquids moving and not moving respectively.

It was found that these two measurement methods consistently gave the results that agreed within error, suggesting that any non-linear components of the thermal pathways were small. Taking the non-linear components into account was very time intensive and somewhat sensitive to noise in the temperature and applied power measurements. For the results presented, the constant power method in equation (3.14) was used.

3.2.2.5 – Thermal Conductance Measurement Apparatus

In the actual measurements, the heat source and heat sink were part of the thermal conductance testing apparatus. There were a few major iterations of the heat flow testing apparatus, though all the systems used the same basic formation. All the heat flow testers had a heat source and a heat sink separated by a polymer spacer. The heat source was heated using a simple electrical resistor connected to a regulated DC power supply.[51] The voltage drop across the resistor was measured, so the electrical power dissipated was simply,

$$P_{heater} = \frac{V_{heater}^2}{R_{heater}} \tag{3.16}$$

where R_{heater} is the resistance of the electrical resistor. Since this resistor dissipates electrical energy as heat, the amount of electrical power dissipated by the heater was taken to be the rate at which heat was added to the system. With the analysis methods being used, any inefficiency at this point would be indistinguishable from a systemic thermal conduction pathway in parallel with the one of interest. Therefore, such inefficiencies can be ignored. The conductance of the pathway due to the moving liquid can be calculated by substituting equation (3.16) into equation (3.14),

$$k_{move} = \frac{V_{heater}^2}{R_{heater}} \left(\frac{1}{\Delta T_{move}} - \frac{1}{\Delta T_{stop}} \right) \tag{3.17}$$

As discussed in section 3.2.2.3, there were two primary directions for injecting heat into the moving oil. The heat could be injected either through the water, or through the pump substructure. Conductance measurement apparatuses were constructed for each of the two injection directions, though as discussed above, the presented results were obtained by injecting heat through the pump substructure. For convenience, a thermal conductance measurement apparatus is called a *conductance tester* or *tester* for short.

Since the application was enhanced surface heat transport, the conductance testers were designed so that the heat was transported along a smooth planar surface. One end of the

surface acted as a heat source and the other as a heat sink. The two thermal reservoirs were separated by a polymer, such as acrylic, which acted as insulation between the two. The heat source and the heat sink were made with fairly large surface areas so that the area of the oil over each was relatively large. As can be seen from equation (3.9), by increasing this overlap area, the thermal conductance of the pump substrate is increased and its effect on the measured conductance is decreased. Figure 3.19 shows a sketch of the testing surface layout with example tracks superimposed.

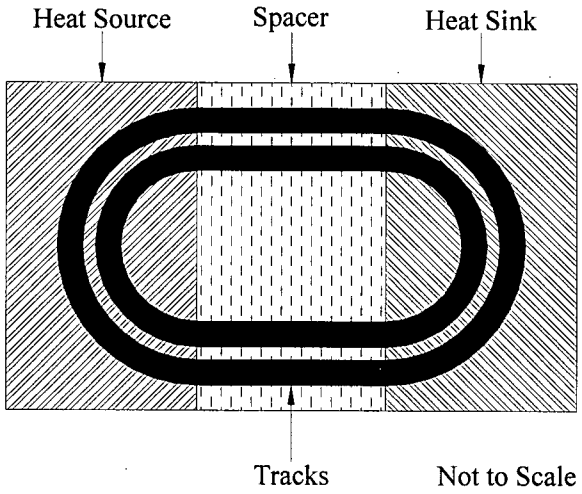

Figure 3.19 – Sketch of conductance tester surface with example tracks superimposed

A tester was built to inject the heat through the water, but was not used for the presented results. As discussed above, placing the apparatus in the water was not suitable for the measurement of the moving oil systems because the water was involved in two heat transport pathways, each of which had different heat transport mechanism. It may have been possible to determine how the two mechanisms interacted by adjusting the thickness of the water layer between the measurement apparatus and the moving oil, but it was

found to be very difficult to get a repeatable measurement. With the tester in place, the system was very fragile, so adjusting the height of the testing surface often caused the amount of oil in the system to change or caused damage to the heterogeneous surface. This tester was built for the short pump systems before the scale-invariant system was developed. The difficulty of setting up the apparatus and the inherent uncertainty associated with this method precluded testing this injection direction with the long pump.

Injecting heat through the pump substructure meant that the pumping surface did not have to be disturbed. This prevented changes in the oil volume and damage to the heterogeneous surface. Conductance testers for this *subterranean* injection direction were built for both the short track and the long track systems. It was found that for the short track system, the thermal conductance of the pump substructure was sufficiently small, and systemic conductances were sufficiently large that the conductance of the moving oil and the copper reference were difficult to distinguish within error. By using a long pump system, the systemic conductance and the conductance of the copper plate were made sufficiently small that it was possible to compare differences between the moving oil and copper. Though the subterranean conductance testers for short and long track systems had the same basic design, the discussion below focuses on the long track system.

In the subterranean design, the heat source and heat sink were made from solid copper blocks and mounted on half inch thick acrylic. A second block of acrylic was placed between the two thermal reservoirs to provide a continuous surface to support the pump.

This whole assembly was machined so that the top surface, with the source and sink, was continuous and flat. A side view of the tester is shown in Figure 3.20.

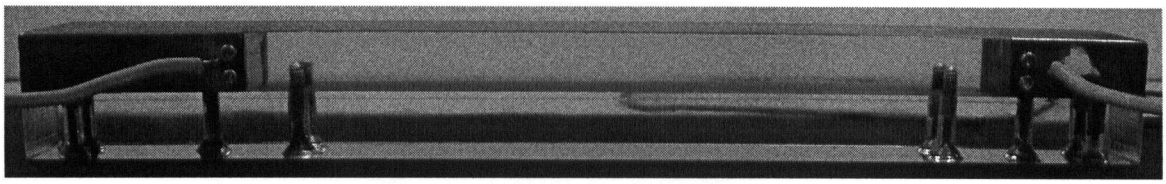

Figure 3.20 – Side view of subterranean thermal conductance measurement apparatus

With this arrangement, the pump rested on top of the conductance measurement device for thermal measurements (Figure 3.21).

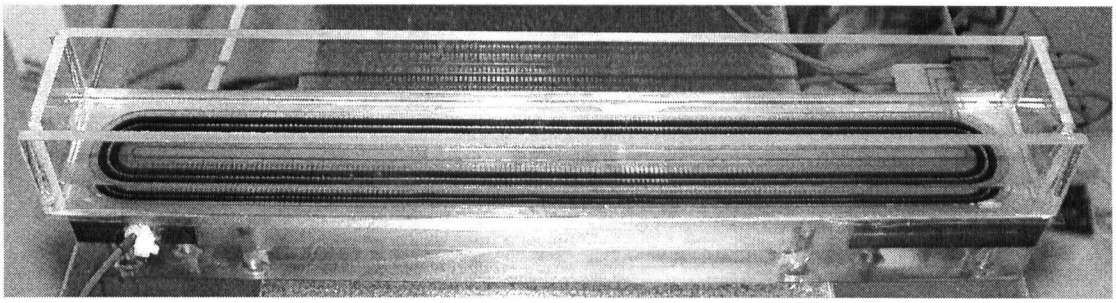

Figure 3.21 – Thermal conductance apparatus with pump in place

One of the copper blocks was made into a heat source by embedding a 3W, 100Ω resistor in a hole, drilled parallel to the top surface. The resistor was held near the center of the block using plastic clips and by filling the open ends of the hole with cotton. The cotton also acted as insulation to help maximize efficient heat transfer from the resistor to the copper. The temperature of the thermal reservoirs was measured using K-type thermocouple junctions that were held on the sides of the reservoirs near the acrylic spacer using small copper clips. Measuring the temperatures of the reservoirs at these

points meant assuming that the copper blocks were sufficiently conductive that there were no temperature gradients across a given reservoir. Figure 3.22 shows the final thermal conductance tester that was built.

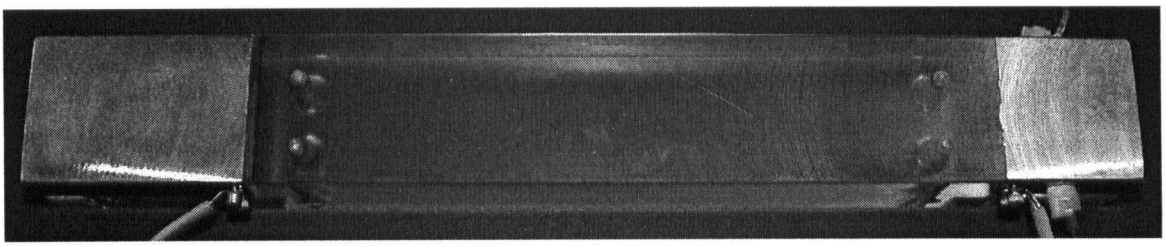

Figure 3.22 – Top view of subterranean thermal conductance measurement apparatus

3.2.3 – Results

As described above, a novel pump based on electrostatic deformation of an oil-water interface was built and used to transfer heat along a surface. The estimated maximum flow rate of the oil is calculated and compared to the achieved maximum flow rates in section 3.2.3.1. Based on the oil flow rates that could be achieved, the expected measurable thermal conductances are calculated and compared to the measured conductances in section 3.2.3.2.

3.2.3.1 – Fluid Flow

As described in section 2.2.1.3, the expected maximum flow rate based on fluid viscosity can be estimated from the modified Hagen-Poiseuille equation, (2.16). This estimate for the maximum flow rate depends on the density of the oil, ρ, the viscosity of the oil, ν, the surface tension of the oil-water interface, γ, the angle of contact of the oil drop when

the fluid is not being pumped, θ, the width of the tracks, w, and the average length of a tube, l.

The material properties of the OS-30 silicone fluid used were specified by the manufacturer, though the surface tension between the fluid and water was not known. A typical oil-water surface tension[52] of 50 mN/m was used for this order of magnitude estimate. The manufacturer's rated density is 850 kg/m^3 and the rated viscosity is 1.5 cSt.[53]

The width of the tracks, the length of the tubes and the contact angles were all controlled during the pump design and assembly. Because of the electrode designs used, there were evenly spaced, equal-sized electrodes all along the length of the tracks. This simplified the flow rate estimate since using the average center-to-center distance between electrodes gave a reasonable estimate for the distance over which the fluid had to flow between field pattern changes. With the electrode designs used, the average center-to-center distance, and therefore average tube length, was 1.25 mm. The angle of contact of the drop with no fields applied and the track width were selected to be 40°±10° and 2 mm respectively. With these values, the expected maximum flow rate was 40±20 cm/s.

The actual flow rates achieved were limited by the voltage supply used. The voltage supply was designed to switch the field patterns only at the zero crossings of a 60 Hz AC signal, resulting in a maximum switching frequency of 120 Hz. Because the electrodes used had a center-to-center separation of 1.25 mm, this meant that the maximum flow

rate that could be generated was 15 cm/s. The net movement of oil was confirmed by introducing small air bubbles, 0.5-1 mm in diameter, into the oil and observing their movement visually. A stable fluid flow was defined as a flow where the air bubbles moved in the expected direction consistently and at the rate expected based on the switching frequency. It was further required that the pump be left running long enough that the bubbles went all the way around the tracks several times with no signs of bulges forming.

Stable fluid flow was demonstrated with the short track pumps at the maximum switching frequency, and so the supply limited maximum flow rate of 15 cm/s was observed.

This same high flow rate was not observed with the long track pumps. Stable flows with the long track pumps were observed at a maximum switching frequency of 24 Hz, resulting in a flow rate of 3 cm/s. At higher switching frequencies, bulges would tend to form quickly. Since the long track pumps had relatively large volumes of oil, the bulges tended to lead to pump failure before even a single complete traversal of the path could be observed. As discussed above, the bulges seemed to be due to defects introduced by construction techniques associated with the large scale. Because of the scale, a solid spray adhesive and a relatively thick hydrophilic film (85 microns) were used. These materials meant that the gap between the electrodes and the water background was relatively large and therefore the interface deformation was very sensitive to variations in the gap thickness. It is expected that these problems could be overcome using an adhesive with a more uniform thickness on this large scale.

It should be noted that using small air bubbles in the oil to visualize the fluid flow was not ideal when transient bulges were observed. The air bubbles have a lower density than the oil, so they floated just below the oil-water interface. Once these bubbles entered a bulge, they would tend to get stuck at the top of the bulge even though there was still net oil flow. It was often obvious that there was still some oil flow because air bubbles could be inserted into the oil on either side of the bulge and they would move as expected. This, however, could not be classified as a stable flow, since without the air bubble moving everywhere along the track, it was not obvious what volume of oil was moving through the bulge. Better methods for flow visualization were not examined due to time constraints. Ideally flow could be visualized using particles with diameters less than 100 microns that could be suspended in the oil. That way buoyancy effects should not affect the observation of fluid flow.

3.2.3.2 – Heat measurements

Based on the relatively high flow rates that could be achieved, the thermal conductance expected from forced convection is calculated and compared to the expected conductance of a similarly dimensioned piece of copper in section 3.2.3.2.a. In section 3.2.3.2.b these estimates are compared to the measured thermal conductance of the long track pump.

3.2.3.2.a – Expected Conductance Measurements

As described in equation (3.5), the thermal conductance due to movement of oil is expected to depend on the mass flow rate of the oil. The track width was chosen to maximize the amount of oil on a given track while keeping gravitational effects negligible. Similarly, the no-field angle of contact oil drop on the heterogeneous surface was chosen to maximize the amount of oil while keeping the contact lines immobilized at all times.

For the thermal conductance measurements, one 2 mm wide track was used to transport heat. With this size, the oil drop was sufficiently small that distortions in the shape of the interface due to buoyancy were not visible. As described throughout this thesis, the tracks were oval shaped with the curved ends placed over the heat source and heat sink, as shown in Figure 3.23. The track path width was selected to be 2.2 cm wide, and the track path length was 23.2 cm long. As described above, this width was chosen to keep the local curvature of the track at all points small compared to the curvature of the oil-water interface. The length was chosen so that the separation between the heat source and heat sink could be kept relatively large, as discussed below. The separation between the heat source and heat sink, here termed the *transfer length*, was significantly shorter than the track path length so that the track would overlap the heat source and heat sink as shown in Figure 3.23.

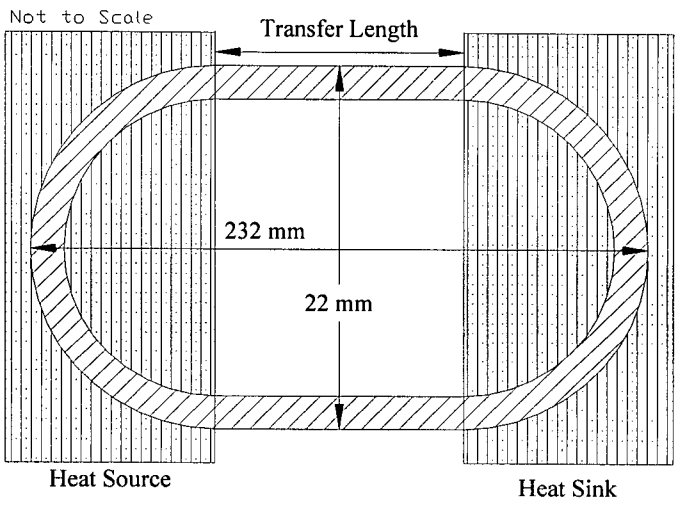

Figure 3.23 – Top view of track superimposed over heat source and sink

To judge the effectiveness of the pump for transporting heat, a uniform plate of copper with comparable dimensions to the pump was used as a reference. Since the track path width was set at 2.2 cm, the copper plate was also 2.2 cm wide. For convenience, the copper was selected to be 1.5 mm thick. This thickness was used since it tended to over-estimate of the minimum thickness of the liquid layer in the pump.

It should be noted that this choice for the reference tends to give a reference conductance which is too large since for the 2 mm wide track on a 2.2 cm wide pump, only 18% of the overall width of the system is being used to pump heat, whereas for copper, the entire width of the sample conducts heat. The cross-sectional area of the pump and the copper are shown in Figure 3.24. This meant that with this comparison, the pump could have up to five tracks pumping heat while the dimensions of the copper reference should remain the same. However, no correction factors are used to compensate in the work presented in this thesis.

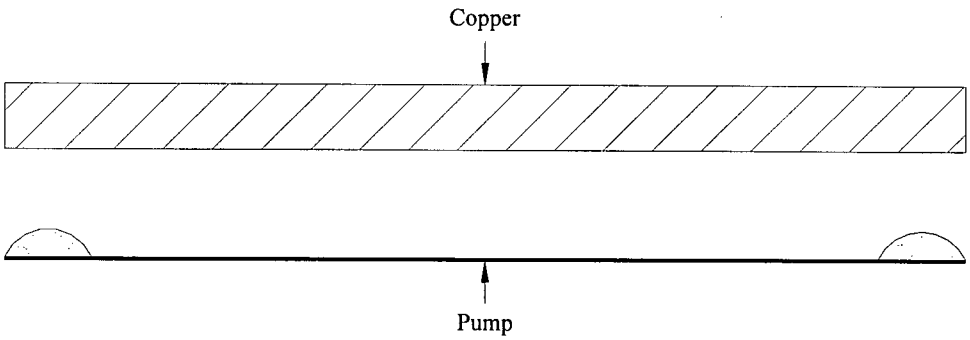

Figure 3.24 – Cross-sectional areas of pump and reference copper (to scale)

In the model for the conductance of the moving oil given by equation (3.6), the rate of heat transfer due to forced convection of the liquids is independent of the length over which the heat is being transferred. For simple conduction through copper, the conductance decreases inversely with the length of the sample, as shown in equation (3.4). The conduction length, l, of the copper sample was the separation between the heat source and sink in the thermal conductance tester. This length was shorter than the path length of the pump, since the pump needed to cover part of the heat source and heat sink. The length of the copper plate was chosen so the overlap area of the reference over the thermal reservoirs was the same as the oil's overlap area. The conduction length of the copper was the separation distance between the heat source and heat sink. The area of the copper above the source and sink was assumed to be at constant temperature. The relative arrangements of the pump and copper over the heat source and sink are shown in Figure 3.25.

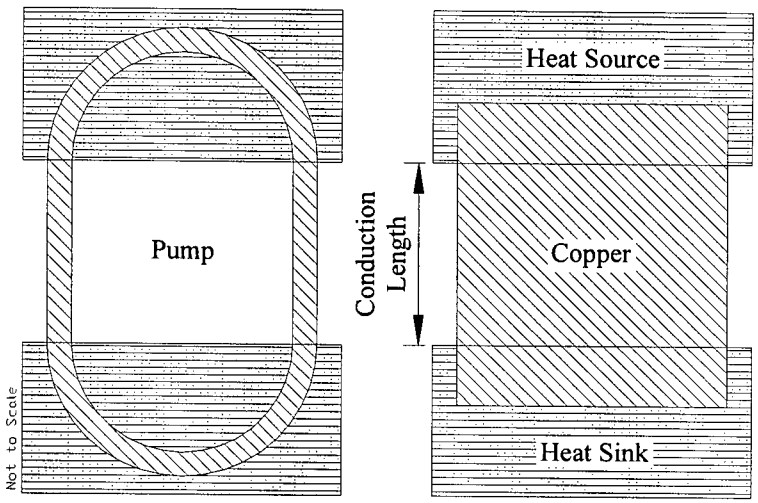

Figure 3.25 – Top view of oil drop and copper over heat source and sink

Although the model for the conductance of the moving oil is independent of the length of the system, it is sensitive to the flow rate and the undeformed angle of contact of the oil. The volume of OS-30 oil added to the track was controlled so the angle of contact with no fields was 30-45°. The thermal conductance due to the oil is expected to be proportional to the flow rate as shown in equation (3.6). Figure 3.26 shows the thermal conductance expected for the 2 mm wide track pumping OS-30 at various flow rates. As is shown by the two curves, by increasing the resting contact angle of the oil drop, the amount of heat transported can be increased since the amount of oil is increased. The expected conductance of two copper reference samples are also plotted; one with a transfer length of 10 cm and the other with a transfer length of 20 cm. The conductivity, K, of the copper was taken to be 401 W m^{-1} K^{-1} at 27°C.[54] The temperatures used in the experiment were sufficiently close to room temperature that any temperature dependence of the copper conductivity would be insignificant for the purposes of this discussion.

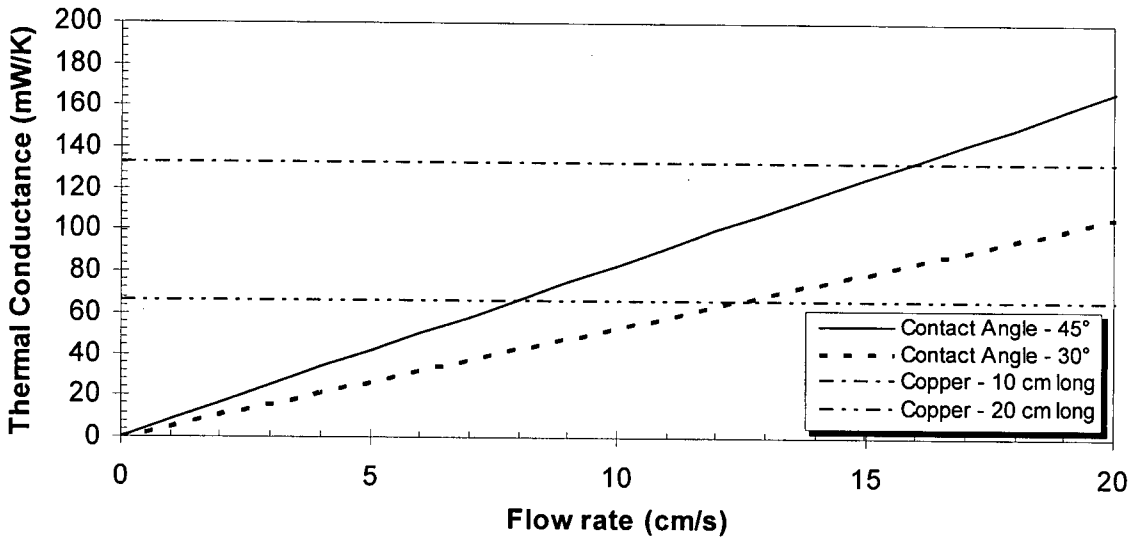

Figure 3.26 – Expected thermal conductance of oil as a function of flow rate (see text)

It is also useful to examine the expected thermal conductance of the piece of copper as a function of the length of the sample, as shown in Figure 3.27. The thermal conductances of oil rotating at two flow rates from Figure 3.26 are plotted as references.

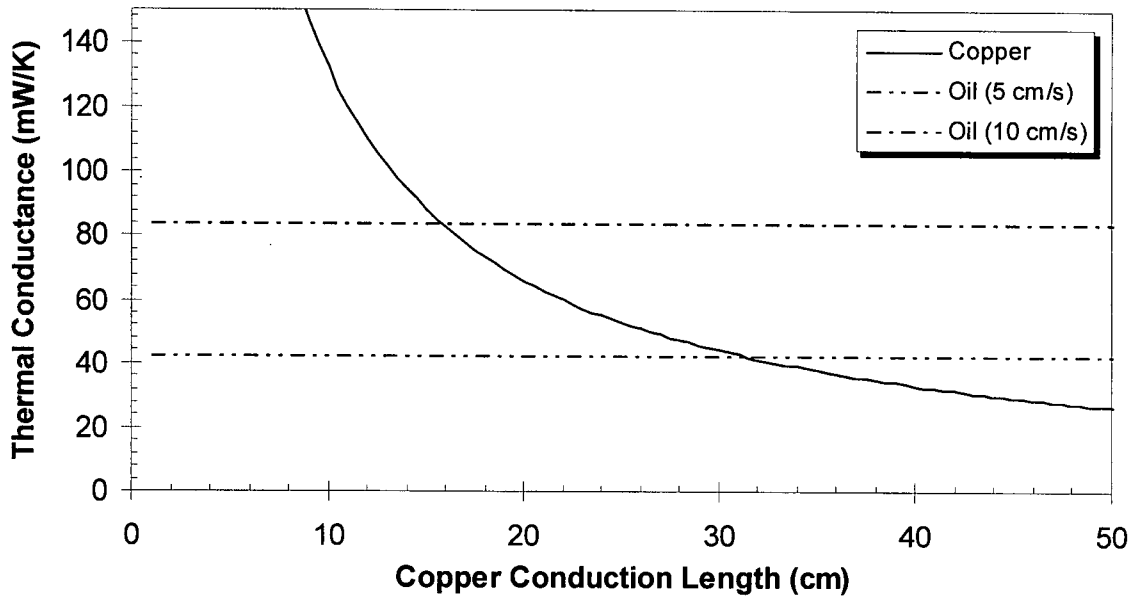

Figure 3.27 - Thermal conductance of copper sample as a function of length (see text)

Between Figure 3.26 and Figure 3.27, it is apparent that the moving oil has the potential to transport heat at a much higher rate than the copper over long distances. This suggested that the pump should be made as long as possible to highlight the difference in the two heat transport mechanisms. As stated above, the track path length was made to be 23.2 cm long. The separation between the heat source and sink was 16.7 cm.

As discussed in section 3.2.2.3, when measuring the thermal conductance of the actual pump, it was necessary to transport the heat through the pump substructure and the movement of water needed to be taken into account. This substructure was composed of many thermally insulating layers, as shown in Figure 3.18. A list of the thicknesses and estimated thermal conductivities of these layers is shown in Table 3-4. The manufacturers of the films used for some of the pump layers specified neither the thermal

conductivity nor the exact composition of their films. This meant that the thermal conductivities had to be estimated for the presented work. Derivations and justifications of the estimated values can be found in Appendix B.

Table 3-4 – Thicknesses and Estimated Thermal Conductivities of Layers of Pump

Layer	Measured Thickness (μm)	Estimated Thermal Conductivity ($W\ m^{-1}\ K^{-1}$)
Olive Oil (Gap 1)	80	0.17
PCB	1500	0.4
Electrodes (Copper)	20	401
Spray Adhesive (Gap 2)	100	0.06
Lee Optical Filter	84	0.2
Printed Wax	10	0.25

The pump substructure was treated as two thermal resistors in series with the moving liquid. Using equation (3.9), the conductances of these two thermal resistors were calculated and are shown in Table 3-5.

Table 3-5 – Thermal Conductances of Pump Substructure over Thermal Reservoirs

Thermal Resistor Near	Conductance (mW/K)
Source	31.7
Sink	52.4

As shown in Figure 3.28, by placing the thermal resistors in series with the moving oil, the measurable conductance tails off as the flow rate is increased. Alone, the model of the conductance due to fluid flow indicates that the conductance could be made arbitrarily large by choosing a large enough flow rate. When the substructure is

considered, the conductance of the entire pathway is limited by the conductance of the substructure at sufficiently high flow rates, as can be shown using equation (3.10). Setting the conductance due to the liquid motion to be infinite, by equation (3.10), the maximum measurable conductance is 19.8 mW/K. At flow rates under about 1 cm/s, the conductance of the moving oil is much smaller than those of the pump substructure, so there is a region at low flow rates where the measurable conductance is proportional to the flow rate.

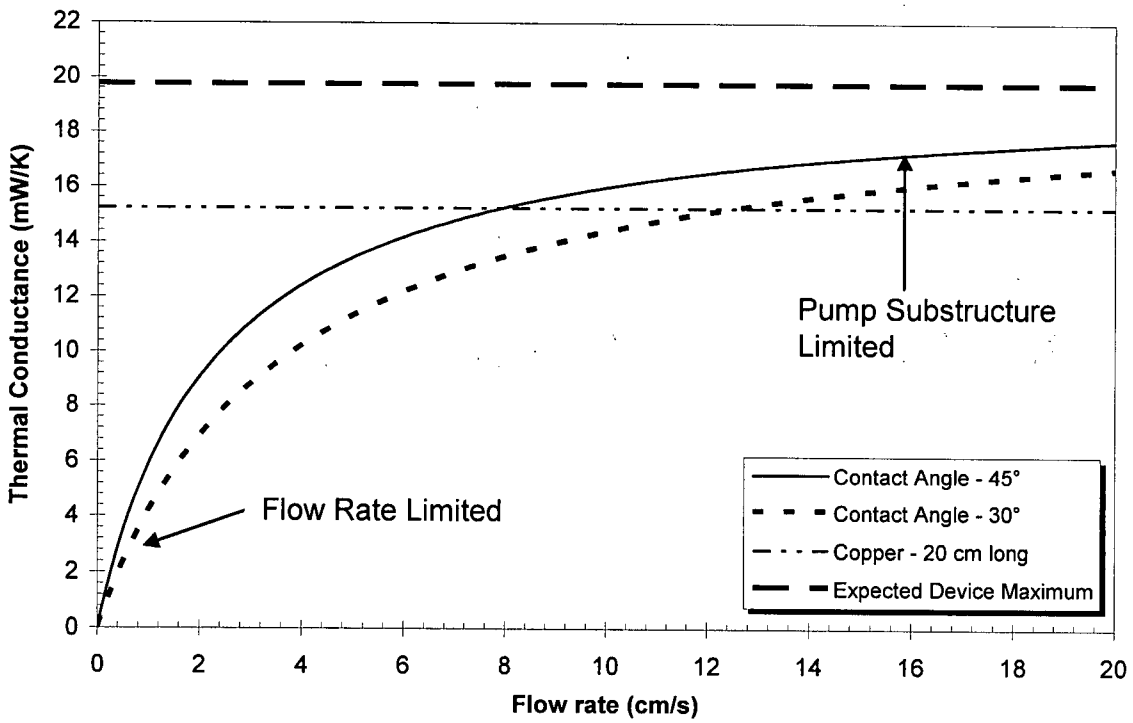

Figure 3.28 – Expected Thermal Conductance including Pump Substructure (see text)

As stated in section 3.2.2.3, since, in this work, the pump substructure was not optimized for thermal conductance, the copper reference needed to be similarly placed in series with

the pump substructure to make a fair comparison. To this end, the copper reference conductances are calculated using equation (3.11).

3.2.3.2.b – Measured Conductance

The conductance due to the movement of oil on one 2 mm wide track was measured at flow rates up to 2.5 cm/s. Figure 3.29 shows a plot of the measured conductances with the expected measurable conductance due to the moving oil. The expected conductance was calculated ignoring any motion of the water background.

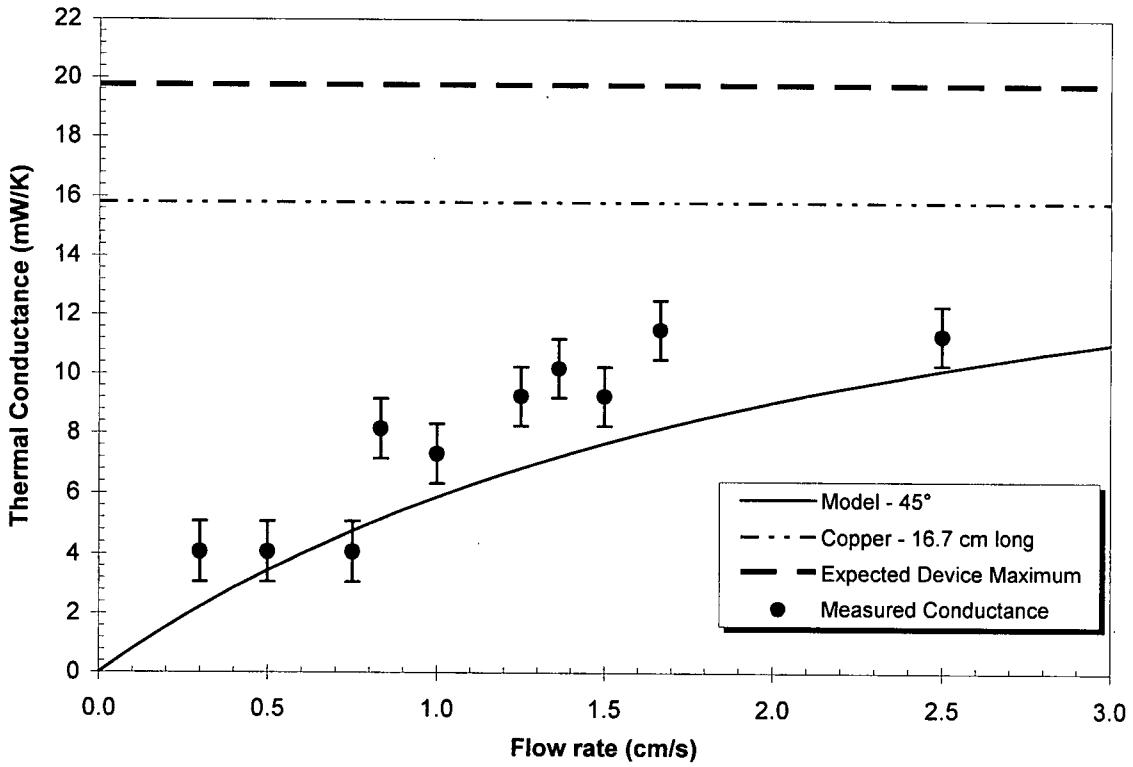

Figure 3.29 – Measured Thermal Conductance due to Moving Oil (see text)

From Figure 3.29 it is apparent that while the model gives a reasonable estimate, movement of the oil alone does not account completely for the measured conductance. The discrepancy can be accounted for by modelling heat transport by the movement of the entrained water. Bulk motion of the water was observed to occur at a slower rate than the pumped fluid by observing the motion of impurities, like dust, in the water. The motion of the impurities followed the direction of pumping, however, these observations lacked sufficient accuracy to characterize the flow profile of the water and how it related to the rate of pumping. It was assumed that, for the purposes of the conductance model, that the volume flow rate of the water was some fraction of the volume flow rate of the oil. Figure 3.30 was plotted using equation (3.7) to model the thermal conductance due to both the movement of the oil and the water. It was found that the model best fitted the data when the water's volume flow rate was 20% of the volume flow rate of the oil.

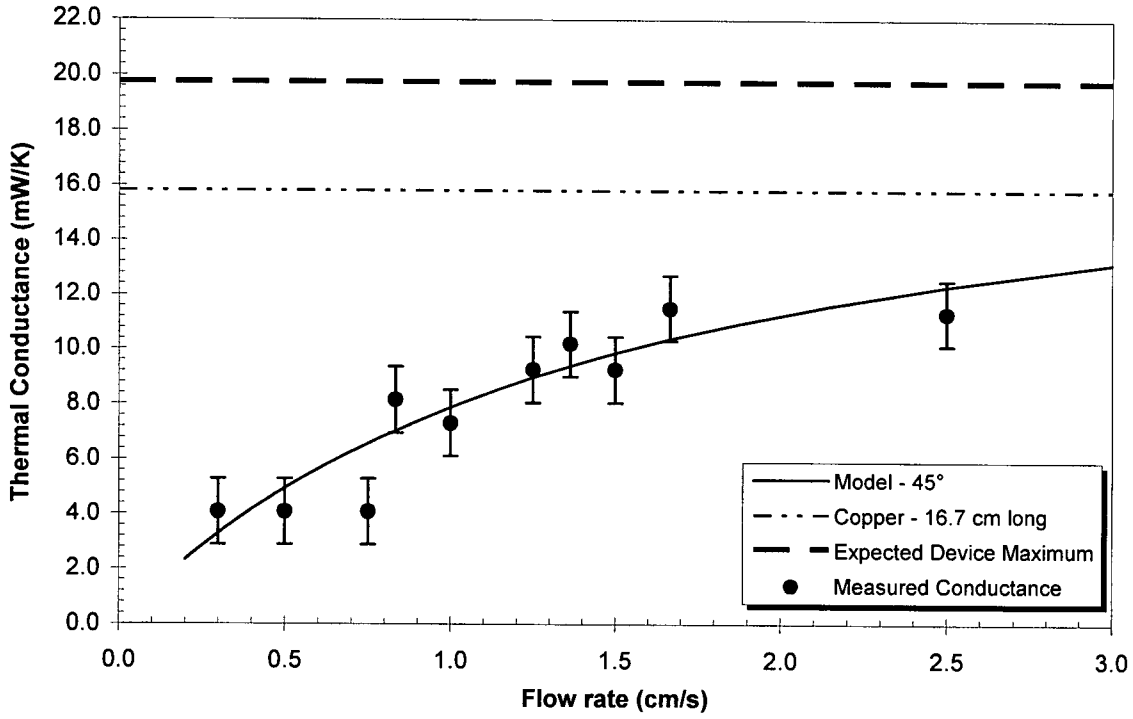

Figure 3.30 – Thermal conductance of pump with water modelled (see text)

As shown in Figure 3.30, by adding the effect of the entrained water into the model, the measured conductance due to the moving liquid can be well estimated with this relatively simple model.

Based on the success of the model in predicting the expected conductance, the conductance due to the pump can be extrapolated to higher flow rates and to cases where more tracks are moving liquid. It should be noted that as the number of tracks increases, the cross-sectional area of the pump substructure through which heat is transported also increases. To make a fair comparison, the copper references and the multiple track cases both take into account the change in area of the drop over the heat reservoirs as more tracks are added. The results are shown in Figure 3.31.

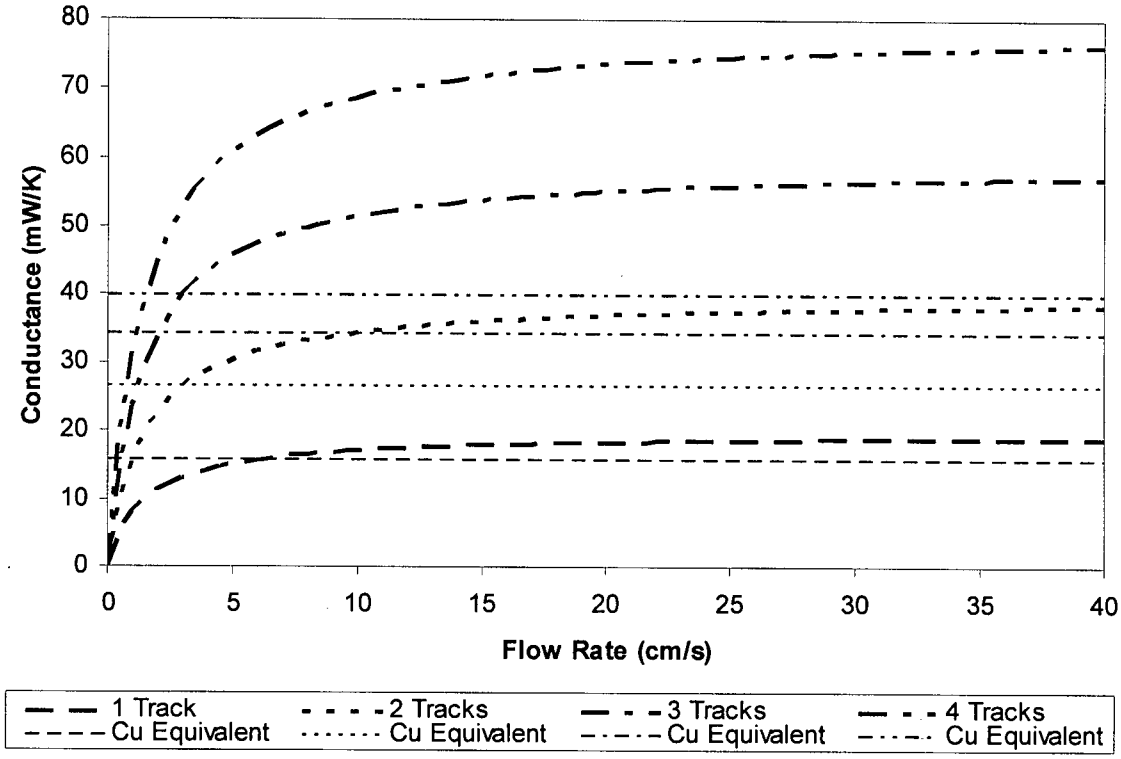

Figure 3.31 – Extrapolation of conductance for pumps with multiple tracks and high flow rates (see text)

As can be seen from Figure 3.31, as more tracks are added, the flow rate at which the conductance of the pumps is the same as the conductance of the copper equivalent occurs at lower flow rates. This suggests that by investigating heat transport with multiple tracks, it may be possible to run the system at relatively low flow rates while still getting significantly higher rates of heat transport compared to a uniform copper plate.

3.2.4 – Conclusions

A fluidic pump with no moving mechanical parts that was based on selectively deforming a liquid-liquid interface was designed, built and tested. It was shown that the pump could be used to transfer heat and a relatively simple model was derived to predict the measurable conductance.

The pump was designed such that an oil drop was confined to a specified area on a solid surface by patterning a hydrophobic material on a hydrophilic surface. It was found that a stable patterned surface could be made using Lee Optical filters and printing wax tracks onto the film using a Xerox® Phaser™ 8200DP wax printer. It was found that under water, Dow Corning® OS-30 silicone fluid had a low contact angle (0-10°) on the wax and a large contact angle (110-120°) on the filter material. In this way, the contact lines of an OS-30 drop could be immobilized at the borders between the two surfaces for a range of angles of contact. This range of angles was sufficiently large that no contact lines were formed or moved when the drop was deformed, thus minimizing friction and eliminating hysteresis.

A long track pump, 23.2 cm long, was built and run to make a reasonable comparison to a similarly dimensioned, uniform copper plate. The pump that was built could only pump the oil at relatively low flow rates since the construction techniques and materials used were not fully optimized. It was found with the short track pumps (3.6 cm long) that using thinner materials and construction techniques that reduced thickness variations

allowed the pump to be run at higher flow rates. The maximum flow rate demonstrated, 15 cm/s, was limited by the switching ability of the voltage supply being used.

A relatively simple electronically switchable voltage supply and an electronic controller were designed and built to run the pumps. The supply and controller were made to be flexible enough to allow for testing of different flow rates while demonstrating that the pumps can be run using potentially simple and inexpensive electrical systems.

Two primary electrode designs were designed, built and used to cause localized deformations of the oil-water interface. A design based on an ABCB' electrode repeat unit was used to allow the electrodes to be printed in a single layer of conductive material while having an arbitrary total number of electrodes and only three connections to the outside world. The long track pump, with 372 electrodes, was built using this scalable design.

Chapter 4 – Conclusions

In the course of the work presented, a novel technique for deforming fluid interfaces using electrostatic forces that avoids the hysteresis and friction associated with the motion of the bulk liquid has been investigated. The approach was examined in the context of two distinct applications; a proposed reflective information display and a new type of fluidic pump for use in surface heat transfer.

In both applications, the contact lines of a liquid drop were restricted to from a specific shape on the solid surface. The positions of these contact lines were immobilized on the solid surface to a degree which in turn constrained the drop shape in useful ways. This was accomplished using a solid with a surface that was patterned so the drop had different wetting behaviours in different regions. With an appropriate pattern on the solid surface, the contact lines were pinned at the border of a region where the liquid wetted the surface with a region where it did not. The positions of the contact lines were stable for a range of drop shapes. The drop was deformed by applying an inhomogeneous electric field to the fluid interface. Since the contact lines were stable, movement of the liquid in the drop was induced while no contact lines were formed or moved, thus minimizing friction and eliminating hysteresis.

For the information display application, a coloured liquid drop was moved through a thin, reflective solid substrate. The two surfaces of the substrate were patterned and small holes passed through the substrate to allow fluid transfer from one side to the other. Appropriate patterns were used so that a single drop was stable on both sides of the

substrate simultaneously. Light modulation was demonstrated by adjusting the height of a coloured liquid drop over the reflective surface. By arranging the system so that in the deformed state, the bulk of the drop was hidden from view, it was possible to switch between a reflective (white) state and an absorptive (dark) state. A simple estimate of the thickness of, and therefore the absorption due to, the liquid drop on the visible side in response to the applied field was derived using a simple energy perturbation argument. The change in height of a water drop in air was measured to give order of magnitude agreement with the estimate. Based on this agreement, a pixel was built and tested that showed that a visible colour change could be obtained. Motion in two additional systems was demonstrated; specifically motion of a water drop in oil and an oil drop in water were demonstrated. Both of these systems demonstrated that it was possible to avoid evaporation of the liquid drop, without using a sealed container. The oil drop in water system was also used to demonstrate that, in principle, relatively low voltages could be used to deform the oil-water interface. With the oil drop in water systems, the non-conductive phases were made relatively thin, so large electric fields could be applied using relatively low voltages. The work presented demonstrated the basic feasibility of this approach for an information display, and the results suggest that further research in this area is warranted. Further research pertaining to the proposed reflective information display should include further development of the materials used in the oil drop in water system to demonstrate a visible change in reflectivity. It would also be useful to accurately measure the change in the height of the drop so that more detailed models of the motion of the drop could be developed. Further research into materials may allow response times, grey-scale control and contrast to be measured and optimized.

Based on the investigation of the oil drop in water pixel, a new type of fluidic pump for surface heat transfer was designed and built. For the pump, the fluid in an oil drop, in a water background, was moved along the surface of a solid substrate. The solid substrate was patterned so that the drop was confined to tracks which form simple closed loops. The oil was deformed by applying a patterned electric field along the track. In turn, moving this pattern caused fluid motion; the oil was squeezed out of the high field regions and a net flow was produced by stepping the field pattern along the track. The heterogeneous surface required was patterned by printing wax tracks (using a Xerox® Phaser™ 8200DP printer) on Lee Filter optical filter film. With this surface, Dow Corning® OS-30 silicone fluid was found to wet the wax under water. The patterned electric field was applied using an AC voltage source and a novel scalable pattern of electrodes. With the materials used, the expected maximum flow rate, due to the viscosity of the oil, was estimated to be 40±20 cm/s. This was larger than the maximum flow rates (15 cm/s) that could be generated with the voltage supply used. The thermal conductance due to the pumping of oil was estimated using the mass flow rate. The measured conductance of the moving liquid was found to agree very well with the simple model. These results are very encouraging, and suggest many further avenues of study in this area. A modified power supply and corresponding electronic systems are needed to allow the viscosity limited flow rate to be observed. Research into suitable liquids may yield less viscous fluids which could allow higher flow rates to be achieved. It is expected that during this search, oils that are density matched with the water would be found. Such oils would allow construction of pumps that can be run over non-flat

surfaces. Further investigation of materials and techniques used for construction of the pump substructure may allow increased overall conductance and fewer irregularities which lead to bulges of the oil. Also, extrapolation of the simple model of conductance indicates that using multiple tracks can lead to large gains in the measurable conductance, thus making the pump very attractive for heat transport applications.

In brief, bulk motion of liquid by deforming a fluidic interface using patterned electric fields has been demonstrated in the context of two example applications that are presented in this thesis. While the work presented has focused on design and prototyping, the results are very encouraging and suggest that further research in this area is warranted.

References

[1] Shaw, D.J., *Colloid & Surface Chemistry,* 4th ed., p.64, Britain: Butterworth-Heinemann, 1992

[2] see Appendix A

[3] ibid 1, p.152

[4] ibid 1, p.125

[5] Kwong, V.H., *Electrostatic Manipulation of Fluidic Interfaces for Optical Control Purposes,* p.30, University of British Columbia: M.A.Sc. Thesis, December 2002

[6] ibid 1, p.5

[7] ibid 1, p.156

[8] ibid 1, p.67

[9] Griffiths, D.J., *Introduction to Electrodynamics,* 3rd ed., p.103, New Jersey: Prentice Hall, 1999

[10] Prins, M.W.J., Welters, W.J.J., Weekamp, J.W., 'Fluid Control in Multichannel Structures by Electrocapillary Pressure', *Science*, pp.277-279, Vol. 291, January 2001

[11] Fan, S.K., de Guzman, P.P., Kim, C.J. 'EWOD Driving of Droplet on NxM Grid Using Single-Layer Electrode Patterns', *Tech. Dig., Solid-State Sensor, Actuator, and Microsystems Workshop,* pp.134-137, Hilton Head Island, S.C., June 2002

[12] Hayes, R.A., Feenstra, B.J., 'Video-speed electronic paper based on electrowetting', *Nature,* Vol. 425, pp.383-385, 25 September 2003

[13] ibid 5

[14] see Appendix A

[15] Streeter, V.L., Wylie, E.B., *Fluid Mechanics,* 8th ed., p.199, U.S.A: McGraw-Hill, 1985

[16] see Appendix A

[17] ibid 5, pp.67-100

[18] ibid 12

[19] ibid 5, p.70

[20] ibid 5, pp.75-78

[21] ibid 5, pp.72-75

[22] Naphthol blue black, CAS #1064-48-8, manufactured by Aldrich Chemical Company Inc., Milwaukee, WI, 53233, USA

[23] Model 201 Ångstrom Resolver, manufactured by Opto Acoustic Sensors Inc., Raleigh, NC, 27607, USA

[24] *CRC Handbook of Chemistry and Physics,* 77th ed., s.v. 'Surface Tension of Common Liquids' (p.**6**-147)

[25] ibid 5, pp.75-78

[26] Type B Immersion Oil, Catalogue Number 16484, manufactured by Cargille Laboratories, Cedar Grove, NJ, 07009, USA

[27] 155 μm thick Glass Cover Slips, Catalogue Number 12-545D, manufactured by Fisher Scientific Co., Napean, ON, K2E 7L6, Canada

[28] DAG 154, manufactured by Acheson Colloids Canada Ltd., Brantford, ON, N3T 5P9, Canada

[29] Vikuiti™ Enhanced Diffusive Reflector, manufactured by 3M Company, St. Paul, MN, 55144-1000, USA

[30] 3.2 OD 48 g Double Metallized PET, manufactured by Celplast Metallized Products Limited, Toronto, Ontario, M1S 3M7, Canada

[31] 468MP Adhesive Transfer Tape, manufactured by 3M Company, St. Paul, MN, 55144-1000, USA

[32] 132 Medium Blue Colour Effects Lighting Filters, manufactured by Lee Filters, Andover, Hampshire, SP10 5AN, England

[33] ColorStix® 8200 Ink – Black, Xerox Part Number 016-2044-00, manufactured by Xerox Corporation – Office Group, Wilsonville, Oregon, 97070-1000, USA

[34] Mega-pure One Liter, manufactured by Corning Glass Works, Parkersburg, WV, USA

[35] OS-30, manufactured by Dow Corning Coporation, Midland, Michigan, 48686, USA

[36] *Material Safety Data Sheet: Dow Corning® OS-30,* p.1, Michigan, U.S.A: Dow Corning Corporation, 20 August 2001

[37] ibid 36, p.4

[38] ibid 36, p.4

[39] Bovin, Rhonda (Dow Corning Corporation Product and Services Specialist). E-mail exchange with Dow Corning Corporation Electronics Department, 3 through 10 September 2003.

[40] ibid 24, s.v. 'Physical Constants of Inorganic Compounds' (p.**4**-95)

[41] ibid 24, s.v. 'Viscosity of Liquids' (p.**6**-208)

[42] BD 30 Gauge General Use Needles, manufactured by Becton, Dickinson and Company, Franklin Lakes, NJ, 07417, USA

[43] ReMount™ Repositionable Adhesive 6091, manufactured by 3M Company, St. Paul, MN, 55144-1000, USA

[44] Ferrari, Dante (Celplast Metallized Products Product Development Engineer). E-mail exchange with Celplast Metallized Products Technical Information, 26 November 2003 through 4 December 2003.

[45] *Etching.* (n.d.) Retrieved 27 September 2004, from University of Pennsylvania, Electrical Engineering School, Microfabrication Laboratory website: http://www.ee.upenn.edu/~microfab/Etching.html

[46] GS-1525 Presensitized single-sided P.C.B., manufactured by Ever-Muse, Taiwan

[47] ibid 5, pp.72-75

[48] Lea, S.M., Burke, J.R., *Physics: The Nature of Things,* Annotated Instructor's ed., p.701-713, U.S.A.: West Publishing Company, 1997

[49] ibid 48, p.701

[50] ibid 48, p.705

[51] XKW 1kW 20-50, manufactured by Xantrex Technology Inc., Burnaby, BC, V5A 4B5, Canada

[52] ibid 1, pp.66-67

[53] ibid 36, p.4

[54] ibid 24, s.v. 'Thermal Conductivity of Metals and Semiconductors as a Function of Temperature' (p.**12**-174)

[55] ibid 54

[56] *Thermal conductivity and thermal properties theoretical background.* (n.d.) Retrieved 20 February 2004, from http://www.hukseflux.com/thermal%20conductivity/thermal.htm

[57] Kalogiannakis, G., Van Hemelrijck, D., Van Assche, G., 'Measurements of Thermal Properties of Carbon/Epoxy and Glass/Epoxy using Modulated Temperature Differential Scanning Calorimetry', *Journal of Composite Materials,* Vol. 38, no.2, pp.163-175, January 2004

[58] *RF Cafe – Thermal Conductivity.* (n.d.) Retrieved 24 November 2003, from http://www.rfcafe.com/references/general/thermal_conductivity.htm

[59] *Thermal Conductivity of some common Materials.* (n.d.) Retrieved 27 September 2004, from http://www.engineeringtoolbox.com/36_429.html

[60] ibid 57

[61] ibid 24, s.v. 'Thermal Conductivity of Gases' (p.**6**-214)

[62] Designed for use in undergraduate laboratory course, UBC Physics 319 – Electronics Laboratory, 2003-2004

[63] Chow, S., Kotlicki, A., *Programming the Analog to Digital Converter Module and the Seven Segment Display.* (University of British Columbia course laboratory materials - Physics 319), Retrieved 27 September 2004, from http://www.physics.ubc.ca/~kotlicki/Physics_319/ADC_programming.html

Appendix A – Liquid Drop Geometry

The work presented in this thesis examines the liquid-fluid interfaces of liquid drops in the context of two different example applications, a fluidic pump and a proposed reflective information display. The interfaces for the drops examined tended to form one of two basic shapes, either a spherical cap shape or a cylindrical cap shape. As shown in Figure A.1, both of these cap shapes are the portion of a sphere or cylinder "above" an intersecting plane. For the purposes of this discussion, the term "above" simply refers to the side of the plane where the smaller region of the curved solid can be found (for the examples in Figure A.1, this would be the part of the solids that are literally above the intersecting plane). For the sphere, any intersecting plane can be used to generate the spherical caps of interest. However, for the cylindrical caps in this work, the intersecting plane must be parallel to the longitudinal axis of the cylinder. A notable feature of these caps is their base areas (i.e. the area they cover on the intersecting plane). As shown in Figure A.1-(a), the spherical cap forms a circular base with a radius, a. The cylindrical cap's base forms a rectangle, with width, w, and length, L, as shown in Figure A.1-(b).

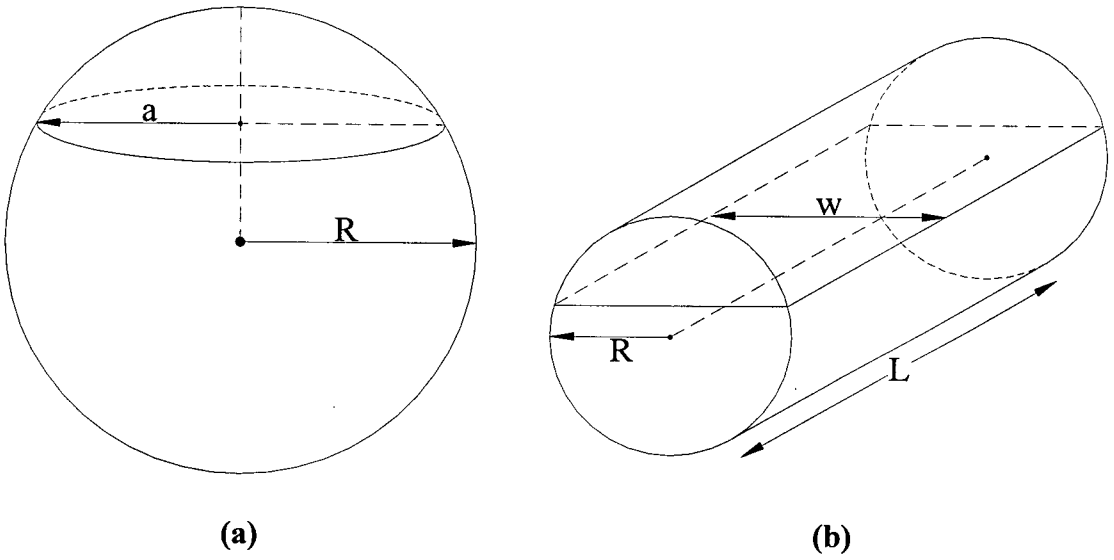

Figure A.1 – Drop shape construction for (a) Spherical and (b) Cylindrical caps

It is useful to find expressions for a few properties of these caps, like the contact angle, θ, and the maximum distance, h, between the top of the cap and the intersecting plane. To do so using elementary trigonometry, a cross-section of each shape is considered below. For the spherical cap, the cross-sectional plane to be considered is any plane that includes the center of the sphere and the center of the cap's base. For the cylindrical cap, the cross-section of interest is one that is perpendicular to the longitudinal axis. Given these definitions, the shape of the cross-section is a circular segment, shown by the shaded region in Figure A.2.

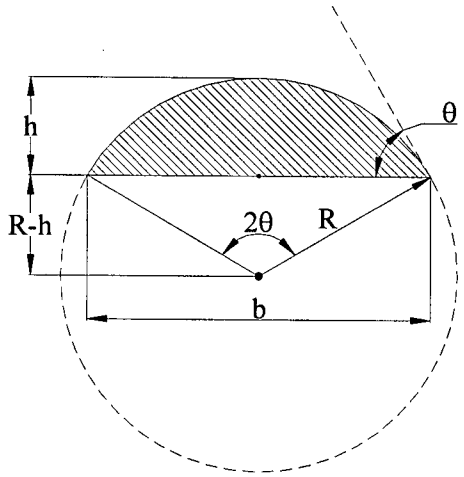

Figure A.2 – Circular cap with dimension definitions

The radius, R, can be expressed in terms of the contact angle, θ, and the cord length, b, as shown in equation (A.1). For the cylindrical cap, the cord length is just the cap base width, w, and for the spherical cap, it is the cap base diameter, $2a$.

$$R = \frac{b}{2\sin\theta} \tag{A.1}$$

The height, h, of the circular segment can be written in terms of the cord length and the contact angle,

$$h = \frac{b}{2}(\csc\theta - \cot\theta) \tag{A.2}$$

The height can also be written in terms of the radius and the chord length,

$$h = R - \sqrt{R^2 - \left(\frac{b}{2}\right)^2} \tag{A.3}$$

The area of the circular cap can be found by considering the area of the entire wedge-shaped region shown, and subtracting off the area of the extra triangular area.

$$A_{XS} = \frac{2\theta}{2\pi}\left(\pi R^2\right) - \frac{1}{2}b\left(R - h\right) \tag{A.4}$$

In terms of the contact angle and the cord length, the cross-sectional area given by equation (A.4) can be expressed,

$$A_{XS} = \left(\frac{b}{2}\right)^2 \left(\theta \csc^2 \theta - \cot\theta\right) \tag{A.5}$$

It should be noted that this area is proportion to the volumes of both solids, so by increasing the contact angle ($0 \le \theta < 180^\circ$), the volumes of the solids increase, as expected. However, looking at equation (A.1), the radius of curvature of the circular cap reaches a minimum at $\theta = 90^\circ$ and increases as the contact angle is moved away from this angle. This is an important consideration when discussing the drop and substrate arrangement used for the proposed information display.

Appendix B – Thermal Conductivity Estimates

In the work presented, a novel fluidic pump was built and used to transport heat along a surface. As discussed in section 3.2.2.3, when measuring the thermal conductance of the actual pump, it was necessary to transport the heat through the pump substructure and the movement of water needed to be taken into account. The manufacturers of the materials used for some of the pump layers specified neither the thermal conductivity nor the exact composition of their films. This meant that the thermal conductivities had to be estimated for the presented work. A summary of these estimates can be found in Table 3-4, which is duplicated here in Table B-1.

Table B-1 – Thicknesses and Estimated Thermal Conductivities of Layers of Pump

Layer	Measured Thickness (μm)	Estimated Thermal Conductivity ($W\ m^{-1}\ K^{-1}$)
Olive Oil (Gap 1)	80	0.17
PCB	1500	0.4
Electrodes (Copper)	20	401
Spray Adhesive (Gap 2)	100	0.06
Lee Optical Filter	84	0.2
Printed Wax	10	0.25

The two materials where rated conductivities are readily available in literature are copper (with a rated[55] conductivity of 401 $W\ m^{-1}\ K^{-1}$) and olive oil (with a rated[56] conductivity of 0.17 $W\ m^{-1}\ K^{-1}$).

The composition of the PCB, Lee optical filter and printed wax were proprietary and therefore not known exactly. In these cases, estimates were made by assuming that the

thermal conductivities of these materials could be estimated from the thermal conductivities of similar, but generic materials. It is known that the PCB is some glass-epoxy. Although there are many types of glass-epoxy, all with varying thermal conductivities, a typical value[57] of 0.4 W m^{-1} K^{-1} was used. It is known that the Lee Filter material is a polymer based film with a complex coating. It was assumed that the material could be approximated by Mylar with a conductivity[58] of 0.2 W m^{-1} K^{-1}. The wax ink was assumed to be similar to paraffin wax, so a conductivity[59] of 0.25 W m^{-1} K^{-1} was used.

In the case of the spray adhesive layer, the estimate was more complicated because the layer of adhesive was not continuous. The adhesive layer consisted of polymer droplets surrounded by air. The conductivity of this layer was determined by modelling the layer as two conductors in parallel. One of the two conductors was polymer, and the other air. The area of each was determined by the fraction of the layer that was polymer and the fraction which was air. It was found that the spraying the adhesive on the electrodes resulted in about 20% of the area covered in polymer and the remaining 80% of the area covered by air. For this estimate, the adhesive was assumed to be similar to a typical polymer like Mylar, which has a conductivity[60] of 0.2 W m^{-1} K^{-1}. Air has a conductivity[61] of 26.2 mW m^{-1} K^{-1}. So using equation (B.1), the spray adhesive layer was estimated to have a conductivity of 0.06 W m^{-1} K^{-1}.

$$k_{layer} = \left[\frac{1}{0.2 \times k_{polymer}} + \frac{1}{0.8 \times k_{air}} \right]^{-1} \qquad \textbf{(B.1)}$$

Appendix C – Fluidic Pump Power Supply

As discussed in section 3.2.1.3.e, a power supply was built that can output up to 320 V_{rms} at 60 Hz on three output channels relative to a common terminal. The supply was built so that the output channels can be switched between 320 V_{rms} or 0 V_{rms} electronically. The electronic interface uses simple digital logic circuitry (i.e. +5 V_{DC} or 0 V_{DC}), so a microprocessor based controller can be used (see Appendix D) to control the states of the power supply's outputs. Switching the outputs between states is limited to occur at the zero crossings of the AC voltage, so the maximum switching frequency is 120 Hz. A circuit diagram of this power supply is shown in Figure C.1.

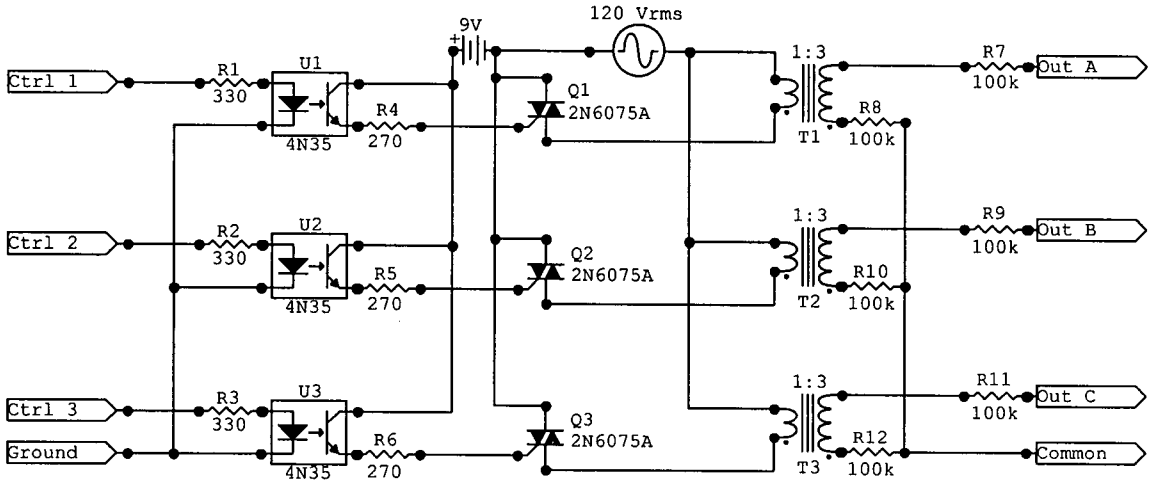

Figure C.1 – Circuit diagram for power supply used to run the fluidic pump

The power supply uses three independent transformers to step 120 Vrms up to 320 Vrms. The outputs of these three transformers are referenced to each other using a common line. To run a pump, this common line is connected to the water in the fluidic pump. The

other line from each of the transformers would be connected to one of the patterned electrode types (i.e. Out A would be connected to electrodes labelled A, etc.).

In series with each of the transformers and the 120 Vrms source is a triac (2N6075A) which is used as a switch. It should be noted that triacs will prevent disconnecting a flowing current and therefore can be useful for zero-crossing switching. However, when running the fluidic pump, the currents in the power supply are sufficiently small that the triacs can switch from being conducting to blocking at any point in the high voltage waveform, in response to a change in the control signal. The optoisolators are used to couple the controller input signals to the gates of the triacs. In this manner, electrical feedback (i.e. noise from the high voltage supply) to the controller can be minimized.

Appendix D – Electronic Controller for Fluidic Pump Power Supply

The power supply (described in Appendix C) used for the fluidic pump needs an electronic controller which can specify the appropriate time-dependent pattern of voltages to be applied to the electrodes in the fluidic pump. The controller that was built for this work is designed to output a set of logical high and low voltages on three independent channels, and is designed around the Motorola MC9S12DP256B microprocessor.

As discussed in section 3.2.1.3, the fluidic pumps require a set of patterned electrodes, placed under the solid substrate, which could be used to apply an inhomogeneous electric field in the oil. Fluid flow is induced by stepping this pattern along the pump's hydrophobic tracks. In the pumps used for this work, electrodes were placed as close together as possible all the way along the tracks, and connected in two simple repeating patterns that have three distinct electrode types; A, B, and C type electrodes. As discussed above, the two patterns used in this work were ABC and ABCB'. High field regions were generated by applying a non-zero AC voltage to only one electrode type (e.g. all the A electrodes) at a time. The oil is squeezed out of these high field regions by the water. Stepping the field pattern along the tracks is achieved by sequentially changing the electrode type to which this AC voltage is applied.

The power supply described in Appendix C can independently apply an AC voltage to each of the pump electrodes based on the states of three logical input channels. A logical

high on one input channel means that an AC voltage is applied a particular pump electrode. A logical low means that the corresponding pump electrode type is kept at the same voltage as the water in the pump. This means that there is a direct correspondence for the controller's outputs to the state of the pump. Fluid flow is induced by setting each logic channel sequentially to a logical high state while the other two are set to a logical low state. The time each channel is left in the logical high state is the same for all three channels. For convenience, this time is termed the *switching period* in this discussion. It is also convenient to define the *switching frequency* to be the reciprocal of the switching period.

As discussed above, with the arrangement of the patterned electrodes in the pump, a sustained fluid flow can be obtained by cyclically applying a voltage to each of the electrode types in turn. This means that the controller must also generate this cyclic sequence, where each output channel is placed in the logical high state in turn. There are two possible orders to this, the high channel could go from the A output to B to C before repeating, or it could go from the C output to B to A. The two sequences are equivalent; they just represent the two directions that the fluid can flow around the track. The controller was designed so the direction of fluid motion can be selected and changed while the pump is running.

The controller that was built has three major sections that can be considered independently; timing synchronization circuitry and input (section D.1), user input mechanisms and output for both display purposes and for controlling the power supply

(section D.2). These functions were obtained using a combination of external circuitry and features native to the microprocessor. The cross-assembler code for the microprocessor program written is shown in section D.3.

As described below in section D.1, the controller was designed so that the times at which the high state is switched from one channel to the next is determined by the output AC signal of the power supply. The controller was limited so it would only switch at the zero-crossings of that AC signal. Since the AC signal has a well defined waveform and frequency, the switching period can be timed in terms of the number of zero-crossings that occur between the controller's outputs changing states. The number of zero-crossings in a switching period can be set while the pump is running, thus allowing the pumping rate to be easily modified as necessary. A simple feedback circuit, described below in section D.1, was constructed which detects these zero-crossings and generates a timing signal. The microprocessor uses this timing signal to determine when switching is to occur, and to synchronize this switching to coincide with a zero-crossing.

The controller was designed so that the switching period and the pumping direction can be changed while the pump is running. The controller settings can be modified using simple mechanical switches that can be in either a logical high state, or a logical low state. For the switching period, two switches are used; one to increase the period, the other to decrease it. A change in state of these switches is detected on Port J of the microprocessor, at which point the appropriate settings in the software are changed. A third switch is used in a similar manner to allow the switching period to be quickly reset

to some convenient default value. The pumping direction input is also done using a simple switch, but in this case the switch's state is polled and used to determine order in which the controller output is switched. Details of how the microprocessor uses these inputs can be seen in the code listing found in section D.3.

As discussed in section D.2, the controller is designed primarily to output control signals that are used by the power supply. In addition, three simple visual displays were added to allow for simple monitoring of the controller's current state.

D.1 – Timing Synchronization and Control

As discussed above, the power supply output a high voltage AC (in this case 60 Hz) signal on three electronically switchable outputs. The controller was designed so that the timing with which switching occurs is set by zero-crossings of the AC voltage. This is done to guarantee that the high voltage waveforms applied to each electrode of the pump would have the same shape, and therefore the same root mean square (RMS) voltage. As discussed above, each of the power supply channels has an associated electrode type, so by ensuring that each channel has the same RMS voltage, it also ensures that the average deforming pressure is constant, regardless of which electrode type is being used. The constant RMS voltage condition can be met using any switching period which is an integer multiple of the AC half-period. Synchronization between the AC zero-crossings and switching is straightforward with the feedback circuit used. This synchronization has the benefit that any electrical noise due to switching of a high voltage signal can be minimized.

As described above, timing and synchronization of the controller output switching are achieved using a simple zero-crossing detection circuit which generates pulses (logical high and low) centered on the zero-crossings of the AC signal. These pulses are captured and counted by a pulse accumulator in the microprocessor. As discussed in Appendix C, the power supply transforms a 60 Hz AC signal from 120 V to 320 V. The detection circuit transforms the same 120V AC signal to a 17.6V AC signal. Using a bridge-rectifier and a simple voltage divider, the AC signal is converted to produce a positive waveform ranging from 0-5V. This low voltage analog signal is converted into digital logic pulses using two inverting triggers, made from NAND gates. This signal processing produces digital pulses that are centered on the zero-crossings of the original AC signal. These pulses are counted using pulse accumulator A on the microprocessor. A schematic of this circuit is shown in Figure D.1.

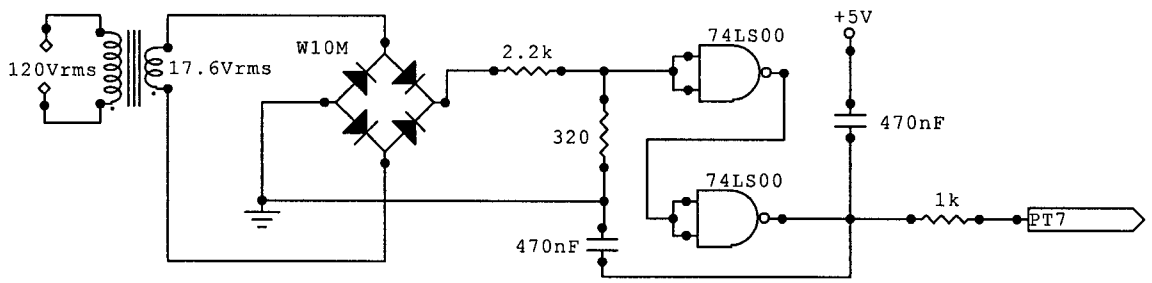

Figure D.1 – Zero-crossing detection circuit schematic for timing synchronization

Since counting the number of pulses coming out of the zero-crossing detection circuitry gives an integer number of half wavelengths, it is convenient to specify the switching period in terms of the number of zero-crossings. The pulse accumulator counts the

number of pulses, so timing can be controlled very easily by simply comparing the number of pulses counted to the switching period (specified in number of zero-crossings). When these two values are the same, the controller output can be switched. In the microprocessor, this comparison and code execution is quickly and easily achieved using the pulse accumulator overflow interrupt. The controller output is switched during this interrupt's service routine (PAOISR), and so switching accurately after an integer number of half periods of the AC signal is obtained very easily.

D.2 – Display and Control Output

The controller was designed primarily to output a timed logical signal which is used by the power supply to apply the selected patterns of electric fields across the oil drop. In addition to this control output, three basic pieces of information are displayed by the controller. The switching period (in units of zero-crossings) is displayed on a 4 digit display board.[62] The states of the control output channels are displayed using an LED attached to each channel. Finally, since interrupts are used extensively throughout the microprocessor program, a set of LEDs are flashed at 2 Hz during the main program loop as a crude indicator that the program execution is functioning as expected.

The microprocessor program listed in section D.3 uses a simple subroutine[63] to display a four digit decimal number on the board shown in Figure D.2. As stated above, the display board is used to display the period between switching the electrodes. For convenience, this time was specified in half periods of the power supply's AC signal.

The display board has 4 multiplexed 7-segment displays that each can display a single hexadecimal digit. Because the displays are multiplexed, a four digit hexadecimal number is transmitted to the board sequentially, one hexadecimal digit at a time, and can be controlled using Port B of the microprocessor. A circuit diagram for the display board is shown in Figure D.2. A simple loop used to convert the period to a decimal number and to transmit the digits sequentially to the display is listed in section D.3.

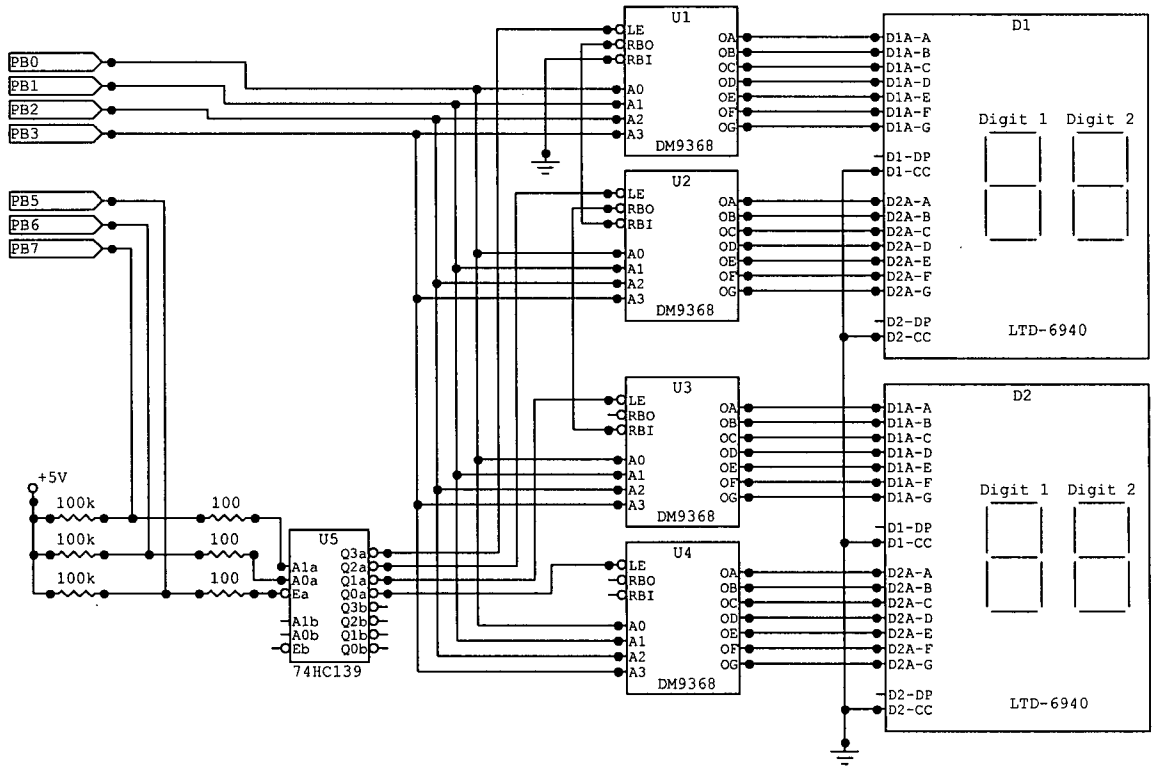

Figure D.2 – Circuit diagram and Port B pin mapping for hexadecimal display board with four 7-segment displays

The states of the controller output channels were controlled by three bits of Port A on the microprocessor. To prevent any significant current from being drawn directly through the microprocessor output pins, each of the three port A pins used are connected through

an inverting Schmitt trigger (74LS14) to a half-H driver (SN754410). The Schmitt trigger is used to provide the current necessary to drive the half-H driver. The half-H driver can supply significant currents on the controller outputs (a single driver chip with 4 half-H drivers can supply up to 2 amps of current) meaning that this design provides a large amount of flexibility in the loads that the controller can support. For this work, these outputs were used to drive two LEDs per channel; the channel status LED and the optoisolator LED in the power supply's input circuitry (see Appendix C). A logic ground must also be supplied by the controller to drive the optoisolator LEDs. The circuit diagram for the controller outputs are shown in Figure D.3.

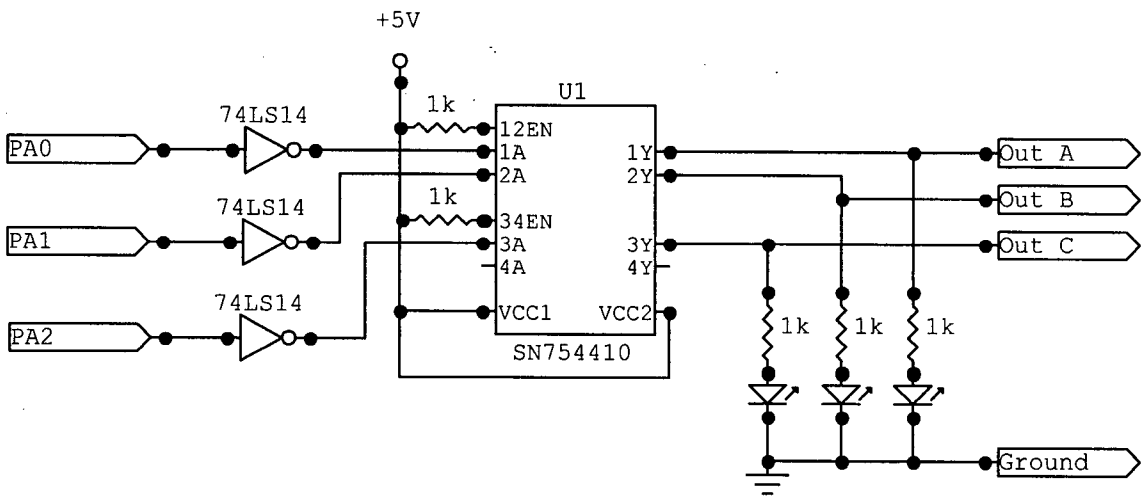

Figure D.3 – Circuit diagram and Port A pin mapping for logic output channels

During the main program loop execution, status LEDs connected to Port P are flashed at 2 Hz as a crude indicator that program execution is functioning as expected. Green and red dual LEDs are used as shown in Figure D.4.

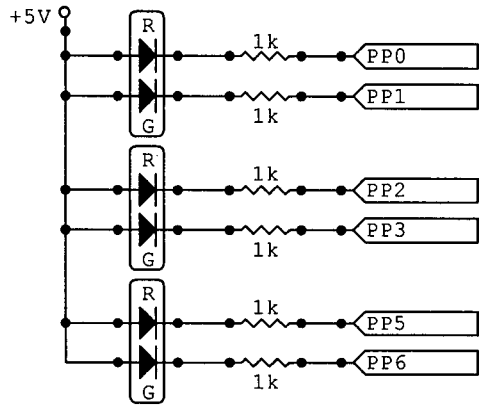

Figure D.4 – Circuit diagram for red and green program status LEDs

D.3 – MC9S12DP256B Microprocessor Program

Below is the assembler source code for the Motorola MC9S12DP256B microprocessor program which was used to control the rotation of the oil drop. This program was compiled using the ASM12 cross-assembler provided with MGTEK MiniIDE v.1.14 build 66.

```
;*****************************************************************
; rotate.asm
;    Program to control rotation of oil drop
;
;    Written April 18, 2003
;    Written by Januk Aggarwal
;
;    Last updated: July 7, 2003
;    Last updated by: Januk Aggarwal
;*****************************************************************

;-----------------------------------------------------------------
; Address Constant Definitions
;-----------------------------------------------------------------
porta       equ   $0000       ;-output port to control power supply
ddra        equ   porta+2     ;-port A data direction register

portb       equ   $0001       ;-output port to control speed display
ddrb        equ   portb+2     ;-port B data direction register
```

```
tcs         equ   $0040       ;-Timer control system
tscr1       equ   tcs+$06     ;-timer system control register 1
pactl       equ   tcs+$20     ;-pulse accumulator control register
paca        equ   tcs+$22     ;-pulse accumulator A count register
paoiva      equ   $3e5c       ;-vector address for pulse accumulator
                              ; A interrupt service routine


portp       equ   $0258       ;-port p
ddrp        equ   portp+2     ;-data direction register
ppsp        equ   portp+5     ;-polarity select register
piep        equ   portp+6     ;-interrupt enable register
pifp        equ   portp+7     ;-interrupt flag register
ppiva       equ   $3e0e       ;-vector address for port p interrupt
                              ; service routine

portj       equ   $0268       ;-port j
ddrj        equ   portj+2     ;-data direction register
ppsj        equ   portj+5     ;-polarity select register
piej        equ   portj+6     ;-interrupt enable register
pifj        equ   portj+7     ;-interrupt flag register
pjiva       equ   $3e4e       ;-vector address for port j interrupt
                              ; service routine


ram         equ   $1000       ;-first RAM address
stack       equ   $3C00       ;-last usable RAM address

speed       equ   500d        ;-constant for speed of incrementing
                              ; or decrementing delay

zerodel     equ   6d          ;-time between zero crossing and pulse
orgdel      equ   5d          ;-Default delay of 83 ms
msdel       equ   $1F40       ;-Value for y reg. to get 1ms delay

;---------------------------------------------------------------------
; Main Program
;     1. Initialize program
;     2. Main loop flashes onboard status LEDs at 2 Hz
;     3. Check pulse accumulator register to ensure that contents
;        are within expected range -> otherwise reset accumulator
;---------------------------------------------------------------------
      org   ram               ;-program starts at beginning of RAM
      lds   #stack            ;-stack pointer set to end of RAM
      jsr   init              ;-run initialization subroutine

mainlp:
      bset  portp,#$4f        ;-status lights on
      ldx   #250d             ;-setup 250 ms delay
      jsr   wait              ;-run delay loop
      bclr  portp,#$4f        ;-status lights off
      ldx   #250d             ;-setup 250 ms delay
      jsr   wait              ;-run delay loop

      ldd   #$FFFF            ;-maximum accumulator value
      subd  paca              ;-calculate how many pulses before
                              ; overflow
```

```
      cpd   delay             ;-check if there are fewer pulses
                              ; left than what the user selected
      bmi   mainlp            ;-Fewer pulses to go -> loop to start
                              ; otherwise reset pulse accumulator

      ldd   #$FFFF            ;-maximum accumulator value
      subd  delay             ;-set accumulator so only desired
      std   paca              ; no. of pulses occur before overflow

      bra   mainlp            ;-branch back to start of main loop

;---------------------------------------------------------------------
; Initialization subroutine
;---------------------------------------------------------------------
; Setup default number of zero crossings before switching pattern
init:
      ldy   #orgdel           ;-default switching delay
      sty   delay             ;-initialize working delay variable
      jsr   displ             ;-display delay

; Setup Pulse Accumulator A overflow
      bset  tscr1,#$10        ;-allow fast flag clearing
      movw  #orgdel,paca      ;-put delay into count register
      com   paca              ;-complement for overflow (high byte)
      com   paca+1            ;-16-bit complement (low byte)
      bset  pactl,#$42        ;-enable pulse acc. and set options
      movw  #paoisr,paoiva    ;-define PAO isr address

; Setup Port P for interrupt
      movb  #$4F,ddrp         ;-bit 7, 5 and 4 input, rest output
      bset  portp,#$4f        ;-Turn off onboard status LEDs
      bset  piep,#$80         ;-enable interrupt on pin 7
      movw  #ppisr,ppiva      ;-define port p isr address

; Setup Port J for interrupt
      bclr  ddrj,#$03         ;-set bit 1 and 0 to input
      bset  ppsj,#$03         ;-pull-down device attached, so
                              ;-interrupt on rising edge
      bset  piej,#$03         ;-enable interrupt on pins 0 and 1
      movw  #pjisr,pjiva      ;-define port j isr address

; Setup Ports A and B
      movb  #$F0,portb        ;-setup portb
      movb  #$FF,ddrb         ;-make all port B pins output
      movb  #$FF,ddra         ;-make all port A pins output
      movb  #$db,porta        ;-put electrode pattern into port A
                              ; the pattern is 11011011
      clc                     ;-clear carry bit for ROR command
                              ; effectively have 9-bit pattern
      tfr   CCR,A             ;-put CCR contents in acc. A
      staa  carry             ;-setup carry variable for CCR
                              ; this preserves carry bit's status
      cli                     ;-enable maskable interrupts
      rts                     ;-finished initialization


;---------------------------------------------------------------------
```

```
; Wait subroutine
;     - Simple waiting routine that burns processor cycles
;---------------------------------------------------------------------
wait:
      ldy   #msdel            ;-Chosen for 1 ms delay
wait2:
      dbne  y,wait2           ;-decrement y until y = 0 (1ms)
      dbne  x,wait            ;-repeat 1ms delay x times
      rts                     ;-finished waiting

;---------------------------------------------------------------------
; 7 segment display subroutine
;      Displays value in index register Y - Courtesy Sing Chow
;---------------------------------------------------------------------
displ:
      movb  #$F0,portb        ;-set port b so display doesn't change
      movb  #$FF,ddrb         ;-ensure all port b pins set to output

; put a 0 byte onto the stack (used for display addressing)
      clrb                    ;-clear one byte
      pshb                    ;-store it on the stack

; do calculation so numbers displayed in decimal
dloop:
      tfr   y,d               ;-transfer contents of y to D
      ldy   #$0000            ;-clear y since ediv uses Y:D
      ldx   #$000A            ;-dividing by decimal 10
      ediv                    ;-(Y:D)/(X) -> Y, Remainder -> D (A:B)
      aba                     ;-put remainder (R <= 9) into acc. A

; setup addressing for display digit of interest
      pulb                    ;-extract address from stack
      aba                     ;-add address to accumulator A

; display digit
      adda  #$20              ;-set strobe bit (prevent display)
      staa  portb             ;-put digit and addressing on port
      bclr  portb,#$20        ;-clear strobe to let digit change
      nop                     ;-give display time to change
      bset  portb,#$20        ;-set strobe to freeze digit

; update address for next digit and loop if not done
      addb  #$40              ;-calculate address of next digit
      pshb                    ;-store addressing on stack
      bcc   dloop             ;-branch if no address overflow
                              ; (ie stop after 4 digits shown)

; clean up and finish subroutine
      pulb                    ;-cleanup stack pointer
      rts                     ;-finished displaying

;---------------------------------------------------------------------
; Port P interrupt service routine
;    - If PP7 is hit, then reset delay time for rotation
;---------------------------------------------------------------------
ppisr:
pp7:  ldy   #orgdel           ;-Load original delay
```

```
      sty   delay             ;-reset active switching delay
      jsr   displ             ;-Display new delay

      movw  delay,3,sp        ;-reset x for main loop delay
      movw  #msdel,5,sp       ;-reset y for main loop delay

      ldx   #speed            ;-introduce a bit of a delay
      jsr   wait              ; for debouncing

      bclr  pifp,#$7F         ;-clear interrupt flag
      rti                     ;-finished resetting switching delay

;---------------------------------------------------------------------
; Port J interrupt service routine
;    - If PJ0 is high, then increase delay time for rotation
;    - If PJ1 is high, then decrease delay time for rotation
;---------------------------------------------------------------------
pjisr:
      movw  #1D,incspd        ;-step delay by 1 zero crossing (83ms)
chck0:
      brclr pifj,#$01,chck1   ;-Check if flag bit 0 is set
                              ; skip next part if increase
                              ; switch was not selected

; increase button hit
dlinc:
      ldd   delay             ;-get current switching delay
      addd  incspd            ;-increase it
      tfr   d,y               ;-put new delay in y
      sty   delay             ;-save new delay
      jsr   displ             ;-display new delay
      ldx   #speed            ;-waste some time (slow incrementing)
      jsr   wait              ;-run time wasting subroutine
      brset portj,$01,dlinc   ;-check if switch is held on and loop
                              ; back to repeat increment if it is
      bclr  pifj,#$fe         ;-clear port j interrupt flag (bit 0)
      bra   deldsp            ;-jump to delay processing commands

chck1:
      brclr pifj,#$02,jend    ;-Check that flag bit 1 is set
                              ; make sure this is a valid
                              ; interrupt, otherwise abort
; decrease button hit
dldec:
      ldd   delay             ;-load current delay time
      subd  incspd            ;-decrease current delay
      tfr   d,y               ;-transfer new delay to y
      sty   delay             ;-save new delay
      jsr   displ             ;-update display with new delay
      ldx   #speed            ;-waste some time (slow decrementing)
      jsr   wait              ;-run time wasting subroutine
      brset portj,$02,dldec   ;-check if switch is held on and loop
                              ; back to repeat decrement if it is
      bclr  pifj,#$fd         ;-clear port j interrupt flag (bit 1)

; setup pulse accumulator with new delay
deldsp:
```

```
      ldd   #$FFFF            ;-load max. accumulator value
      subd  delay             ;-calculate complement of delay
                              ; for overflow
      std   paca              ;-store delay in pulse accumulator
                              ; count register
      ldy   delay             ;-reload newest delay
      jsr   displ             ;-update display

jend: rti                     ;-finished changing delay time

;---------------------------------------------------------------------
; Pulse Accumulator A overflow interrupt service routine
;    - If PP4 is set (switch high), rotate right, otherwise left
;---------------------------------------------------------------------
paoisr:
      ldaa  carry             ;-get stored CCR value for saved carry
      exg   A,CCR             ;-exchange stored CCR with current CCR
      sei                     ;-prevent maskable interrupts
      ldx   #2000d            ;-short delay between overflow and
      dbne  x,*               ; true zero crossing
      brclr portp,#$10,rotl   ;-switch grounded => rotate left else
                              ; rotate right

rotr: ror   porta             ;-rotate right (shift pattern to right)
      bra   rotend            ;-skip rotate left
rotl: rol   porta             ;-rotate left (shift pattern to left)

rotend:
      tfr   CCR,A             ;-get updated CCR to save carry bit
      staa  carry             ;-save CCR values (ie carry bit)
      ldd   paca              ;-load pulse accumulator count, should
                              ; be small, but not necessarily zero
      subd  delay             ;-subtract delay for overflow
      std   paca              ;-store back in count register
      cli                     ;-enable maskable interrupts
      rti                     ;-finished changing pattern

;---------------------------------------------------------------------
; Variables
;     - reserve memory for program to use
;---------------------------------------------------------------------
delay       rmb   2           ;-16-bits for working delay time
incspd      rmb   2           ;-16-bits for delay step size
carry       rmb   1           ;- 8-bits for CCR preservation
```